RHODES UNIVERSITY

Thermoluminescence of Natural Quartz

by

Aaron Joel Lontsi Sob

supervised by

Professor Makaiko L. Chithambo

A thesis submitted in fulfilment for the degree of

Master of Science

in the

Faculty of Science

Department of Physics and Electronics

March 2014

Abstract

The kinetic and dosimetric features of the main thermoluminescence peak of quartz have been investigated in unannealed as well in quartz annealed at 500 °C for 10 minutes. The main peak is found at 92 and 86 °C respectively for aliquots of unannealed and annealed samples irradiated to 10 Gy and heated at 5.0 °C/s. For each sample, the intensity of the main peak is enhanced with repetitive measurement whereas its maximum temperature is unaffected. The peak position of the main peak in each sample is independent of the irradiation dose and this, together with its fading characteristics are consistent with first-order kinetics. For low doses, typically between 2 and 10 Gy, the dose response of the main peak in each sample is linear. In the intermediate dose range from 10 to 60 Gy, the growth of the main peak in each sample is sub-linear and for greater doses, in the range from 60 Gy to 151 Gy, it is linear again. The half-life of the main peak of the unannealed sample is about 1.3 h whereas that of the annealed sample is about 1.2 h. The main peak in each sample can be approximated to a first-order glow peak. As the heating rate increases, the intensity of the main peak in each sample decreases. This is evidence of thermal quenching. The main peak in each sample is the only peak regenerated by phototransfer. The resulting phototransferred peak occurs at the same temperature as the original peak and has similar kinetic and dosimetric features. For a preheat temperature of 120 °C, the intensity of the phototransferred peak in each sample increases with illumination time up to a maximum and decreases afterwards. At longer illumination times (such as 30 min up to 1 h), no further decrease in the intensity of the phototransferred peak is observed. The traps associated with the 325 °C peak are the main source of the electrons responsible for the regenerated peak. Radioluminescence emission spectra were also measured for quartz annealed at various temperatures. Emission bands in quartz are affected by annealing and irradiation. A strong enhancement of the 3.4 eV ($\sim$ 366 nm) emission band is observed in quartz annealed at 500 °C. A new emission band which grows with annealing up to 1000 °C is observed at 3.7 eV ($\sim$ 330 nm) for quartz annealed at 600 °C. An attempt has been made to correlate the changes in radioluminescence emission spectra due to annealing with the influence of annealing on luminescence lifetimes in quartz.

Acknowledgements

"Knowledge is marvelous, but wisdom is even better."

– Kay Redfield Jamison

I would like to express my gratitude to the Almighty God for the gift of life, friendship and family. To Professor Chithambo my supervisor, I would like to express my deepest gratitude. It has been a privilege to work with you Prof. Your kindness, patience and devotion shaped me. Out of the lab, you also taught me how to be generous. I would also like to thank Prof Martini and Dr Fasoli for the warm welcome at Università degli Studi di Milano Bicocca in Italy and for their assistance with the radioluminescence measurements. To my family and friends, I say thank you for your many support. Without your love and encouragement none of this would have been possible. To my fellow mates, I say thank you for the sleepless nights we spent together in the lab. Thank you also for the fun we had out of the lab. To the members of the Physics Department at Rhodes University, I would also like to extend my deep gratitude. During the course of my studies, I benefited from funding from Rhodes University in the form of scholarship, merit award and travel grant to conferences. Thank you Rhodes! you are indeed "A Small University with a Big Heart". I am and will always be a proud Rhodian. I am also grateful to the National Research Foundation of South Africa for funding my research visit to Italy.

I dedicate this work to my Grandfather. Thank you GrandPa for believing in me...

Contents

List of Figures

List of Tables

Chapter 1

Introduction

1.1 Luminescence

For the material of interest, luminescence can be defined as a process through which some previously irradiated materials emit light of a given wavelength upon stimulation. However, luminescence may also be observed without prior irradiation (photoluminescence). Depending on their electronic structure, materials can be classified into insulators, semiconductors and metals [1]. Only insulators and semiconductors exhibit luminescent properties. Such materials are also known as phosphors. Luminescence differs from the spontaneous emission of light which is observed when a material is heated to incandescence [2].

The type of luminescence phenomenon dealt with in this work consists of two main steps namely, excitation and irradiation [3]. In the excitation step, the material is exposed to an external energy source. Nuclear radiation such as γ-rays, β-particles and X-rays are common sources of excitation. However, the excitation source may also be optical (e.g., ultra-violet light) [2, 3]. The excitation creates electron-hole pairs which may later on recombine radiatively. After excitation, the luminescence is thermally or optically stimulated from the material. This is the second main step of the luminescence process. Thermal stimulation is accomplished by gradually increasing the temperature of the material from a specific temperature T_0 to a final temperature T at a controlled heating rate. The process results in thermally stimulated luminescence also known as thermoluminescence [4]. If the sample is rather exposed to light (470 nm blue light for example), the resulting luminescence is known as optically stimulated luminescence.

Luminescence can primarily be classified into two types, namely; fluorescence and phosphorescence. If the emission of light occurs some time $\tau < 10^{-8}$ s after stimulation, the luminescence is known as fluorescence. Figure 1.1 shows the basic process of fluorescence emission. After absorption of energy from the external source, the electron moves from the ground state g to an excited energy level e. From e, it relaxes back to the ground state g with emission of light.

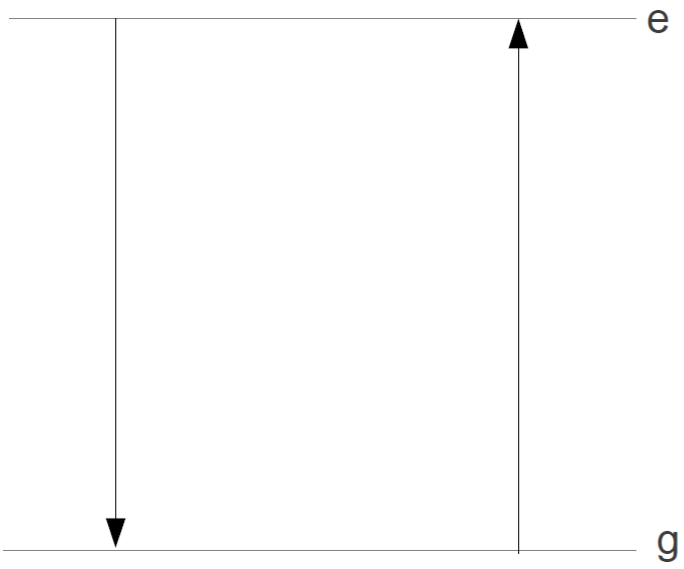

FIGURE 1.1: Energy level diagram showing the fluorescence process. The up and down arrows correspond to absorption and emission of energy respectively (reproduced from McKeever [2])

If the luminescence is emitted with $\tau > 10^{-8}$ s, it is referred to as phosphorescence. Figure 1.2 shows the steps involved in phosphorescence. The energy level diagram of phosphorescence differs from that of fluorescence by the inclusion of an additional state labelled m. An electron at energy level e transits into and out of level m before decaying to the ground state g. The time spent at level m accounts mostly for the long delay between stimulation and emission of light. Fluorescence is temperature independent whereas phosphorescence depends strongly on temperature [4]. The thermal energy in phosphorescence assists in freeing the electron from the metastable state m. The energy provided by heating should therefore be at least equal to the energy difference between level e and level m.

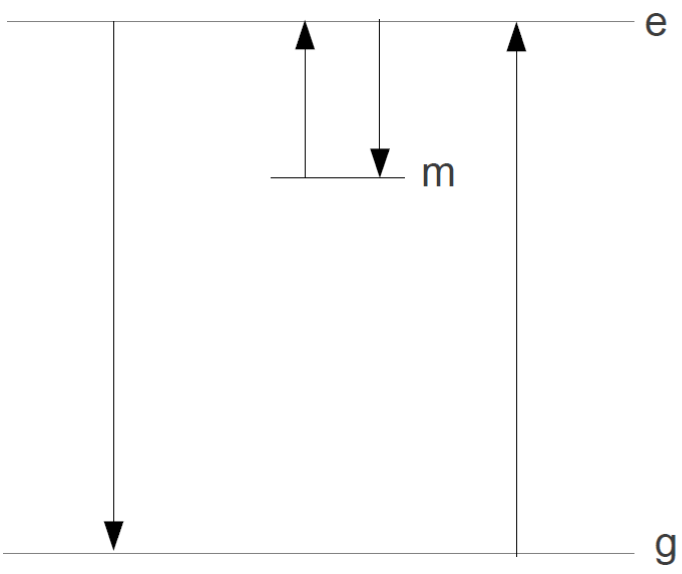

FIGURE 1.2: Energy level diagram showing the phosphorescence process. The electron may be trapped at level m before decaying to the ground state g. The up and down arrows correspond to absorption and emission of energy respectively (reproduced from McKeever [2]).

1.1.1 Thermoluminescence

Thermoluminescence (TL) is the thermally stimulated emission of light from materials which have been previously irradiated [2, 4]. As mentioned before, only insulators and semiconductors are suitable luminescent materials. According to the energy band model of solids, electrons in crystals occupy a set of allowed energy bands. These allowed energy bands are separated by a forbidden gap for which no Schrödinger eigenfunction exists [1]. Hence, in a perfect crystal there should not be localised energy levels within the forbidden gap. In reality, crystals have defects or impurities which result in additional energy levels within the crystal. It therefore becomes possible for electrons to be at energy levels which lie within the forbidden gap. Insulators and semiconductors are materials with wide and narrow band gaps respectively and this makes them suitable for luminescence studies. For example in quartz, a natural mineral, the forbidden gap is about 9 electron volts (eV) wide [5].

Figure 1.3 shows a basic energy band model which explains the transfer of charges leading to luminescence.

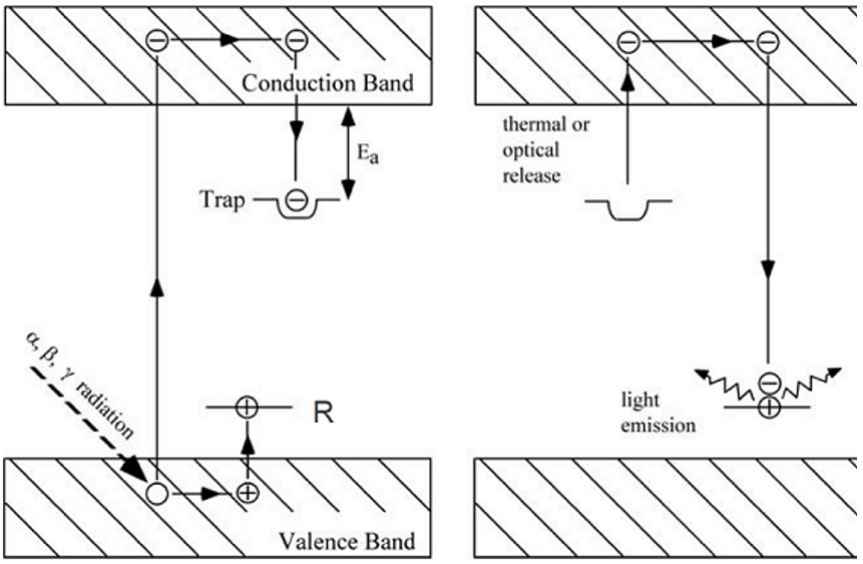

FIGURE 1.3: Basic energy band model used to explain luminescence phenomena.

In Figure 1.3, the valence band is the lowest allowed energy band that electrons can occupy. The next available energy band is the conduction band. When the material is exposed to ionising radiation, valence electrons gain energy and become free to move within the crystal. This results in the creation of electron-hole pairs. A hole, positively charged, corresponds to the absence of an electron in the valence band. The free electrons transit through the conduction band and some of them eventually get trapped at localised energy levels. Localised energy levels at which electrons can be trapped are known as electron traps. Similarly, holes may also be trapped at hole centres. If the energy from thermal stimulation is at least equal to E_a, the energy depth of the trap below the conduction band, the trapped electrons will be evicted from the trap to the conduction band. After detrapping, some of these electrons recombine with holes. The recombination process may be radiative in which case luminescence is emitted. In the case of a non-radiative recombination, the energy from the recombination process is dissipated as phonons. In the model shown in Figure 1.3, the recombination centre R and the hole centre mentioned above refer to the same centre.

1.2 Mathematical treatment of TL

1.2.1 TL intensity

Let us consider the one trap - one recombination centre model (OTOR) shown in Figure 1.4. Let n and n_c denote the concentration of electrons in the trap T and conduction

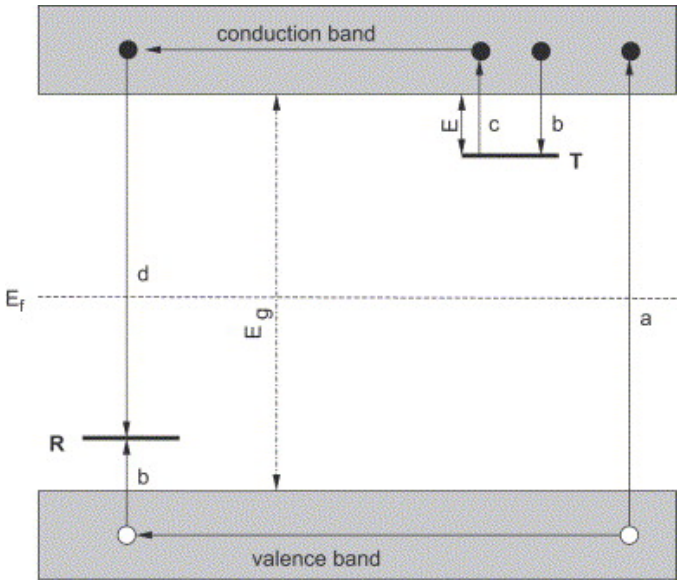

FIGURE 1.4: Energy band model showing electronic transitions in a TL material. (a) generation of electrons and holes; (b) electron and hole trapping; (c) electron release due to thermal stimulation; (d) recombination. Solid circles represent electrons and open circles are holes. Level T is an electron trap, level R is a recombination centre, E_f is the Fermi level, E_g is the energy band gap. Diagram reproduced from Bos [6].

band respectively at time t. We also denote by m the concentration of holes at the recombination centre R. During thermal stimulation, the trap T is progressively emptied as electrons move to the conduction band (transition c). The probability p per unit time of release of an electron from the trap, is proportional to a Boltzmann factor and is given by the Arrhenius equation

$$p = s \exp(-\frac{E}{kT}), \tag{1.1}$$

where s is the frequency factor or attempt-to-escape factor [4, 6]. For this simple model, s is considered to be a constant independent of temperature. Its value is of the order of the lattice vibration frequency namely 10^{12} - 10^{14} s^{-1} [7]. The trap depth E is the energy needed to evict a trapped electron into the conduction band (transition c), k is Boltzmann's constant and T is the absolute temperature. Equation (1.1) shows that if $E \gg kT_0$, where T_0 is the temperature at the time of irradiation, then p is very small and the electron remains indefinitely trapped. The probability p increases with increasing temperature thereby enabling the release of trapped electrons into the conduction band. Light is emitted as a result of the recombination of conduction electrons with holes at the centre R. The intensity of the emitted light is proportional to the rate at which electrons and holes recombine and may be stated as

$$I(t) = -\frac{dm}{dt}, \tag{1.2}$$

where the negative sign indicates the reduction in the concentration of holes due to recombination. In equation (1.2), it is assumed that all recombinations are radiative. In addition, the recombination rate is proportional to the concentration of electrons in the conduction band and the concentration m of holes. Henceforth, equation (1.2) becomes

$$I(t) = -\frac{dm}{dt} = n_c m A_m, \tag{1.3}$$

where A_m, the recombination probability, has units of volume per unit time and is assumed to be temperature independent. The rate of change in the concentration of trapped electrons with respect to time is

$$\frac{dn}{dt} = -np + n_c(N-n)A_n, \tag{1.4}$$

with N being the concentration of electron traps and A_n, the probability of re-trapping is also expressed in units of volume per unit time. The rate of change in the concentration of free electrons is therefore defined as

$$\frac{dn_c}{dt} = np - n_c(N-n)A_n - n_c m A_m = -\frac{dn}{dt} + \frac{dm}{dt}. \tag{1.5}$$

Furthermore, for charge to be conserved,

$$n_c + n = m. \tag{1.6}$$

Equations (1.1) to (1.5) describe the transfer of charges leading to TL. These equations do not each have an analytical solution. However, with simplifying assumptions, one may develop a general solution. At this point of the derivation, it is assumed that charges do not accumulate in the conduction band. In other words, the concentration of electrons in the conduction band is almost constant. This assumption is referred to as the quasi-equilibrium (QE) assumption [4]. Mathematically, the QE assumption translates to

$$|\frac{dn_c}{dt}| \ll |\frac{dn}{dt}| \,; |\frac{dn_c}{dt}| \ll |\frac{dm}{dt}|. \tag{1.7}$$

This further implies that $n_c \approx 0$ which then leads to $n \approx m$ hence equation (1.5) reduces to

$$-\frac{dm}{dt} \approx -\frac{dn}{dt} = I(t). \tag{1.8}$$

With the QE assumption, equation (1.3) and equation (1.5) lead to

$$I(t) = \frac{m A_m np}{(N-m)A_n + mA_m} = \frac{mA_m}{(N-n)A_n + mA_m} ns \exp(-\frac{E}{kT}). \tag{1.9}$$

Equation (1.9) is known as the general one trap (GOT) equation. Equations describing first-, second- and general- order kinetics can be derived from the GOT equation under specific assumptions.

1.2.2 First-order kinetics

First-order kinetics was derived by Randall and Wilkins [8, 9]. They assumed that once electrons are detrapped, the probability of re-trapping is negligible i.e., $mA_m \gg (N-n)A_n$. Under this assumption, the GOT equation reduces to

$$I(t) = -\frac{dn}{dt} = sp = ns\exp(-\frac{E}{kT}). \tag{1.10}$$

Equation (1.10) shows that the intensity I is proportional to n and for that reason, it is referred to as the first-order kinetics equation. If the TL readout is done at constant temperature, in which case p is constant, the intensity follows an exponential decay of the form

$$I(t) = I_0\exp(-tp), \tag{1.11}$$

where I_0 is the initial intensity and t is the time. If the measurement temperature changes during the readout process, and if we assume a linear heating profile then the temperature of the sample at time t is

$$T(t) = T_0 + \beta t, \tag{1.12}$$

where β is the heating rate. The concentration of trapped electrons at time t will be obtained by integrating equation (1.10) as

$$n(t) = n_0\exp[-\int_{T_0}^{T}\frac{s}{\beta}e^{-E/kT'}dT'], \tag{1.13}$$

where n_0 is the concentration of trapped electrons at time $t = 0$ i.e., prior to stimulation and T', the variable of integration, represents the temperature. The luminescence intensity, $I(T)$, will then be obtained by deriving equation (1.13) with respect to T.

$$I(T) = n_0 s e^{-E/kT}\exp[-\int_{T_0}^{T}\frac{s}{\beta}e^{-E/kT'}dT']. \tag{1.14}$$

The temperature T_m corresponding to the maximum intensity of a first-order glow curve (a plot of the luminescence intensity as a function of temperature) is obtained from $dI/dT = 0$ where I is defined by equation (1.14). T_m is related to the other parameters by

$$\frac{\beta E}{kT_m^2} = s\exp(-\frac{E}{kT_m}). \tag{1.15}$$

From equation (1.15), we note that for first-order kinetics, T_m does not depend on n_0 i.e., T_m is independent of dose. This is a characteristic of first-order kinetics [4, 10].

1.2.3 Second-order kinetics

Garlick and Gibson [11] discussed the case when re-trapping dominates i.e, $mA_m \ll (N-n)A_n$. This leads to

$$I(t) = -\frac{dn}{dt} = m\frac{A_m}{(N-n)A_n}ns\exp(-\frac{E}{kT}). \tag{1.16}$$

Furthermore if we assume that the trap is far from saturation, i.e., $N \gg n$ and $n = m$, we obtain

$$I(t) = -\frac{dn}{dt} = s\frac{A_m}{NA_n}n^2\exp(-\frac{E}{kT}). \tag{1.17}$$

In equation (1.17), the intensity $I(t)$ is proportional to n^2 and hence the equation is referred to as the second-order kinetics equation. Assuming $A_m = A_n$, and a linear heating profile, the luminescence intensity can be obtained as a function of temperature by integrating (1.17) to find

$$I(T) = \frac{n_0^2}{N}\frac{s}{\beta}\exp(-\frac{E}{kT})[1 + \frac{n_0 s}{N\beta}\int_{T0}^{T}\exp(-\frac{E}{kT'})dT']^{-2}. \tag{1.18}$$

If the glow curve is recorded at constant temperature, the phosphorescence in second-order kinetics follows a Becquerel's decay law of the form

$$I(t) = \frac{I_0}{(1+n_0\alpha t)^2}, \tag{1.19}$$

where $\alpha = s/N\ \exp(-E/kT)$. For second-order kinetics, the temperature T_m associated with the maximum intensity of a TL glow peak can be obtained by taking the derivative with respect to temperature of equation (1.18) and setting it to zero. The relationship between T_m and the other parameters is given by

$$\frac{\beta E}{kT_m^2} = s(1 + \frac{2kT_m}{E})\exp(-\frac{E}{kT_m}). \tag{1.20}$$

1.2.4 General-order kinetics

May and Partridge [12] considered the case in which none of the assumptions used in deriving the first- and second-order kinetics hold. They developed the following expression for general-order kinetics:

$$I(t) = -\frac{dn}{dt} = n^b s^a \exp(-\frac{E}{kT}), \tag{1.21}$$

where s^a has the dimension of $m^{3(b-1)}s^{-1}$ and b is the order of kinetics. An equation similar to equation (1.13) can be derived for the intensity as

$$I(T) = \frac{s^*}{\beta} n_0 \exp(-\frac{E}{kT})[1 + (b-1)\frac{s^*}{\beta}\int_{T_0}^{T} \exp(-E/kT')dT']^{-b/b-1}, \tag{1.22}$$

where $s^* = s^a n_0^{(b-1)}$. All the other parameters are as defined previously. We note that when b approaches 1 or 2, equation (1.22) reduces to the appropriate equation for first- or second-order kinetics. Taking $dI/dt = 0$ for the general order-kinetics, we get

$$\frac{\beta E}{kT_m^2} = s(1 + \frac{2kT_m(b-1)}{E}) \exp(-\frac{E}{kT_m}). \tag{1.23}$$

1.3 Quartz

Natural quartz is the subject of our investigation. As such, this section gives a brief discussion of natural quartz and highlights some of its characteristics which are relevant to luminescence.

1.3.1 Physical properties of quartz

Natural quartz is a silicate mineral whose crystalline structure consists of a three-dimensional repetition of SiO_4 tetrahedrons. Each oxygen atom is shared between two silicon atoms and each Si atom is connected to four O atoms. Quartz is an abundant mineral in the earth's crust and it is found in most rocks [13]. Natural quartz is affected by many factors such as the conditions at the time of formation. Quartz has phases which occur at specific temperatures. $\alpha-$quartz has a rhombohedral crystal structure and it is stable at temperatures below 573 °C. At temperatures greater than 573 °C, $\alpha-$quartz changes to $\beta-$quartz. $\beta-$quartz has a hexagonal crystal structure and exists at temperatures greater than 573 °C and is stable between 573 and 870 °C. These two temperatures correspond to phase changes in quartz. During the $\alpha - \beta$ phase transition, atomic positions are readjusted [2, 13]. The phase change in quartz is a reversible process. Quartz is an insulator with a band gap of about 9 eV [5]. The fact that quartz is the most occurring silica in nature and its having a large band gap have made it an important luminescent material. Under mechanical stress, and in the presence of an external electric field, the quartz crystal develops opposite charges at both ends. This property is referred to as piezoelectricity [1]. Apart from its use as a luminescence dosimeter, quartz in synthetic form is manufactured for electronics devices and many other applications which require quartz of high purity.

1.3.2 Defects and impurities in quartz

Defects in quartz can be intrinsic or extrinsic. Intrinsic defects are due to Si or/and O vacancies or interstitials. A vacancy refers to the absence of an atom from its position in the lattice. An interstitial atom occupies a position not allowed in the perfect crystal structure. Extrinsic defects are due to impurities or foreign atoms. These types of defects may vary with the conditions and the geological environment of the quartz at the time of formation. Some of the impurity atoms reported in quartz are Al, Fe, Ti, Ge, P, Li, and Na. From these atoms, more defects can be formed. Intrinsic defects result in O- and Si- related centres. Among impurities related centres, $[AlO_4]^o$ and $[H_3O_4]^o$ have been identified as possible recombination centres for the 110 °C TL peak in quartz [14]. Martini et al. [15] studied the role played by $[AlO_4]^o$ recombination centres in the optically stimulated luminescence of quartz while de Lima et al. [16] investigated the role played by $[H_3O_4]^o$ recombination centres in the 110 °C TL emission of quartz. A more detailed discussion on quartz defects and reasons as to why quartz is used in luminescence has been given by Preusser et al. [13].

1.4 Aim of the thesis

The goal of this thesis is threefold. To start with, we will study the kinetic and dosimetric features of the main TL peak in natural quartz. Secondly, the kinetic and dosimetric features of peaks resulting from phototransfer will be studied. At last, the effect of annealing on radioluminescence emission spectra from quartz will be investigated. The main objective is to contribute to the understanding of mechanisms responsible for luminescence in quartz.

1.5 Thesis plan

The rest of the thesis is organised as follows: Chapter 2 describes phototransferred thermoluminescence and models which have been proposed to explain its dynamics. Models of luminescence in quartz which may be relevant to this study are also mentioned. Chapter 3 deals with the various methods of analysis used to determine the kinetic parameters of glow peaks during this work. In Chapter 4, we describe the experimental setup and the procedure for thermoluminescence measurements. Chapter 5 presents and discusses the results of this study. The summary of the results and suggestions for future studies are given in Chapter 6.

Chapter 2

Phototransferred thermoluminescence

This chapter describes phototransferred thermoluminescence (PTTL) and models which have been proposed to explain its dynamics. TL models for quartz which may be relevant to this study are also discussed. In order to describe PTTL and the stages involved in PTTL emission, we need to define some terms first. Each trap is associated with an energy depth E and a temperature T at which electrons can escape from that trap as was shown in Figure 1.3. The trap depth E is the energy required to free electrons from a given trap. A shallow trap is a trap with a low energy depth. Electrons from a shallow trap have a short half-life and can be evicted from their trap at room temperature. In comparison, traps with larger depths are known as deep traps. To remove electrons from a deep trap, the energy provided by heating or illumination should be at least equal to the depth of the trap. Having dealt with these basic concepts, we are now in a position to give a formal definition of PTTL and to discuss the steps associated with its emission.

PTTL is the thermal stimulation of luminescence due to electrons which have been optically transferred from deep traps to shallow traps [2, 4]. The PTTL process consists of four main steps namely, irradiation, depletion of electrons in shallow traps, illumination and thermal stimulation. To start with, the sample being studied is irradiated at temperature T_0. The irradiation leads to the creation of electron-hole pairs. Electrons are trapped at the various traps while holes are trapped at recombination centres. Some defects which capture holes can also act as traps while the electrons are captured at defects acting as recombination centre. In both cases, the mathematical descriptions lead to the same result.

In order to enable the emission of PTTL from the sample, it is necessary to first remove electrons from shallow traps or to at least reduce their concentration to a minimal level. This removal of electrons from shallow traps can be accomplished in two ways. The first method is by heating the sample to a temperature just sufficient to excite electrons from shallow traps but not deeper ones. At this stage, any TL is due to the recombination of holes with electrons from shallow traps. The other way of removing electrons from shallow traps simply consists in allowing the concentration of electrons to decrease spontaneously at room temperature i.e by phosphorescence.

In the next step of the PTTL procedure, the sample is cooled back to temperature T_0 (the irradiation temperature) and then exposed to monochromatic light for some time t. The light source is chosen in such a way that the energy it provides is enough to excite electrons from deep traps into the conduction band. In the case of quartz for example, Santos et al. [17] exposed their sample to ultra-violet light after cooling it to -100 °C. Other researchers have reported PTTL glow curves resulting from exposure to blue light at the temperature of irradiation (e.g., Bertucci et al. [18]). During illumination, electrons from deep traps are evicted into the conduction band from where some of them are trapped at shallow traps. In addition to getting trapped at shallow traps, some of the electrons recombine with holes to give optically stimulated luminescence (OSL) while others are re-trapped at deep traps. Shallow traps may also lose electrons during illumination.

Having exposed the sample to light, the luminescence from shallow traps is then stimulated by heating. The glow curve which is recorded during heating is known as a PTTL glow curve. The regeneration of the low temperature peaks associated with the shallow traps is evidence of phototransfer of electrons from deep traps to shallow ones. From this discussion, it is evident that the description of PTTL requires a model with at least two traps and one recombination centre. In section 2.1, such a model is described and in section 2.2, a more complex model is discussed.

2.1 Simple model of PTTL

The simplest energy model which can be used to explain the movement of charges leading to PTTL is shown in Figure 2.1. This model consists of one shallow trap (level 1), one deep trap (level 2) and one radiative recombination centre (level 3).

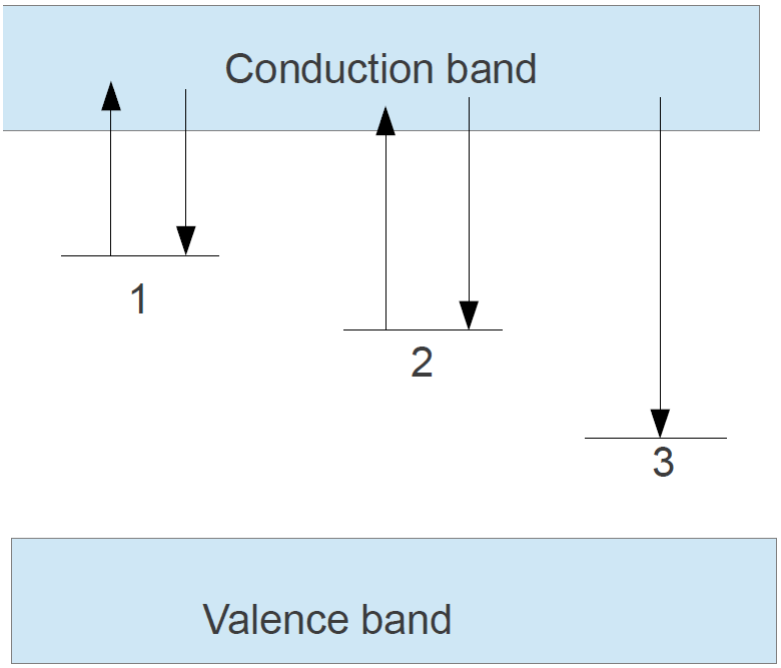

FIGURE 2.1: Simple energy band model showing the flow of charges during PTTL in the shallow trap (level 1), deep trap (level 2) and radiative recombination centre (level 3).

In the mathematical description to follow, traps will be indexed by numbers from 1 to k with k being the total number of traps. Recombination centres will be labelled by numbers from $k+1$ to j where j is the total number of traps and recombination centres in the model. However, for the model with a single recombination centre, the index will be omitted. For example the concentration of traps for the trap labelled 1 will be N_1 and n_1 will be that of trapped electrons. The probability of re-trapping for trap 1 will be denoted by A_1 whereas A_1^* will be that of detrapping. The total concentration of holes for the recombination centre will be denoted by M while m will denote the concentration of trapped holes at the recombination centre. In addition, n_c and n_v will denote the concentration of electrons and holes in the conduction and valence bands respectively.

The first stage of the PTTL process is the irradiation. During irradiation, there is creation of electron-hole pairs with electrons being trapped at the shallow and deep traps respectively while holes are trapped at the recombination centre. The equations describing the flow of charges during irradiation are:

$$\frac{dn_1}{dt} = A_1(N_1 - n_1)n_c, \tag{2.1}$$

$$\frac{dn_2}{dt} = A_2(N_2 - n_2)n_c, \tag{2.2}$$

$$\frac{dn_v}{dt} = R - A_m^*(M - m)n_v, \tag{2.3}$$

where R is the rate of electron-hole pairs creation and A_m^* is the probability of hole trapping at the recombination centre. For charge neutrality, the total number of trapped electrons should be equal to the number of holes at the recombination centre. Mathematically, this condition is written as

$$n_1 + n_2 = m. \tag{2.4}$$

After the removal of electrons from the shallow trap via heating or natural decay, it is assumed that the new concentration of electrons at level 1 is $n_{10} = 0$, and that of electrons at level 2 is n_{20}. Charge conservation then requires $n_{20} = m_0$ with m_0 being the new concentration of holes. If the electrons are removed by heating (preheat), a TL glow peak associated with the shallow trap is obtained. Subsequent heating does not produce a peak due to the shallow trap because the electrons from this trap are removed during preheating.

Now let f_1 and f_2 be the rates at which electrons are optically excited from the shallow trap (level 1) and deep trap respectively (level 2). The equations governing the flow of charges during illumination are:

$$\frac{dn_2}{dt} = -n_2 f_2 + A_2(N_2 - n_2)n_c, \tag{2.5}$$

$$\frac{dn_1}{dt} = -n_1 f_1 + A_1(N_1 - n_1)n_c, \tag{2.6}$$

$$\frac{dm}{dt} = -A_m m n_c, \tag{2.7}$$

$$\frac{dn_v}{dt} = 0, \tag{2.8}$$

the charge neutrality condition leads to

$$\frac{dn_c}{dt} = -\frac{dn_1}{dt} - \frac{dn_2}{dt} + \frac{dm}{dt}. \tag{2.9}$$

The quasi-equilibrium (QE) approximation is assumed during illumination i.e., $dn_c/dt \approx 0$. If we further assume that re-trapping into the deep trap is negligible, then the solutions to equations (2.5) to (2.7) are respectively:

$$n_2(t) = n_{20} \exp(-tf_2), \tag{2.10}$$

$$n_1(t) = N_1[1 - \exp(-Bt)], \tag{2.11}$$

$$m(t) = m_0 \exp(-t/\tau), \tag{2.12}$$

where $B = n_c A_1$. As a result of the illumination, there is now a non-negligible concentration of trapped electrons in the shallow trap. Equation (2.10), which is an exponential function with parameters t and f_2, describes the loss of electrons from the deep trap during illumination. Equation (2.11) on the other hand describes the filling of the shallow trap during illumination. The OSL observed during illumination contributes to the reduction in the concentration of holes at the recombination centre. This loss of holes is describes by equation (2.12).

PTTL emission is then stimulated by heating the sample. The equations describing the flow of charge during thermal release of charges are:

$$\frac{dn_1}{dt} = -n_1 p_1 + A_1(N_1 - n_1)n_c, \tag{2.13}$$

$$\frac{dn_2}{dt} = A_2(N_2 - n_2)n_c, \tag{2.14}$$

$$\frac{dm}{dt} = -A_m m n_c, \tag{2.15}$$

where p_1 and p_2 are the probabilities of thermal release of electrons from the shallow trap and the deep trap respectively. Again, the QE approximation is assumed to hold during this stage. Since the range of preheat temperatures is restricted in such a way that the deep trap remains stable, $p_2 \approx 0$ as such, the term -$n_2 p_2$ does not appear in equation (2.14). Electrons that are evicted from the shallow trap during heating can either be re-trapped in the shallow trap; recombine with holes to give PTTL or be trapped at the deep trap. In addition to the QE assumption, Chen and McKeever [4]

assumed that at the beginning of the heating step, i.e. immediately after illumination, $n_1(t^*) << N_2 - n_2(t^*)$. This assumption implies that re-trapping into the deep trap will be negligible if the deep trap is close to saturation. Under these assumptions, they found the phototransferred signal to be

$$S(t^*) = \frac{C_s \exp(-t^*/\tau) N_1 [1 - \exp(-Bt^*)]}{N_2/n_{20} - \exp(-t^* f_2)} \tag{2.16}$$

where C_s is a constant and S describes the variation of the intensity of the phototransferred peak as a function of illumination time. For long illumination times, the population of electrons in the deep trap becomes negligible i.e., n_2 approaches 0 whereas m approaches n_1 and $S(t^*)$ increases towards a maximum. This simple model of PTTL therefore predicts a PTTL signal which increases with illumination time up to a maximum value. Figure 2.2 is a simulated example showing the growth in the population of electrons in the shallow trap during the illumination phase of a PTTL sequence.

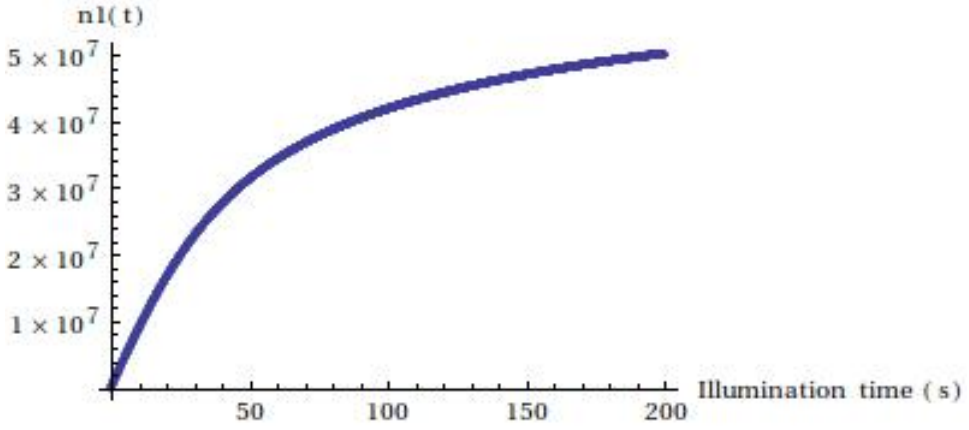

FIGURE 2.2: Growth in the population of shallow trap electrons during illumination. The values used in the simulation are: $N_1 = 10^{10}\,cm^{-3}$, $N_2 = 10^{12}\,cm^{-3}$, $M = 10^{12}\,cm^{-3}$, $s_1 = 5 \times 10^{11}\,s^{-1}$, $E_1 = 0.9\,eV$, $k = 8.617 \times 10^{-5}\,eVK^{-1}$, $R = 10^{11}\,cm^{-3}\,s^{-1}$, $A_1 = 10^{-10}\,cm^3\,s^{-1}$, $A_2 = 10^{-9}\,cm^3\,s^{-1}$, $A_m = 10^{-7}\,cm^3\,s^{-1}$, $A_m^* = 10^{-9}\,cm^3\,s^{-1}$, $f_1 = 0$ and $f_2 = 0.1\,s^{-1}$. These values were taken from page 123 of Chen and Pagonis [19].

Simulations performed with the parameters shown in the caption of Figure 2.2 show that the concentration n_1 of electrons in the shallow trap increases with illumination time to a maximum value. As expected, the PTTL will grow as n_1 increases since there will be enough holes for the electrons to recombine with. If we allowed the loss of electrons from the shallow trap during illumination step of the simulation by setting f_1 to a value greater than 0 but less than f_2, n_1 will increase up to a maximum value and then start to decrease with further illumination. Figure 2.3 shows the corresponding change in n_1 with illumination time in this case.

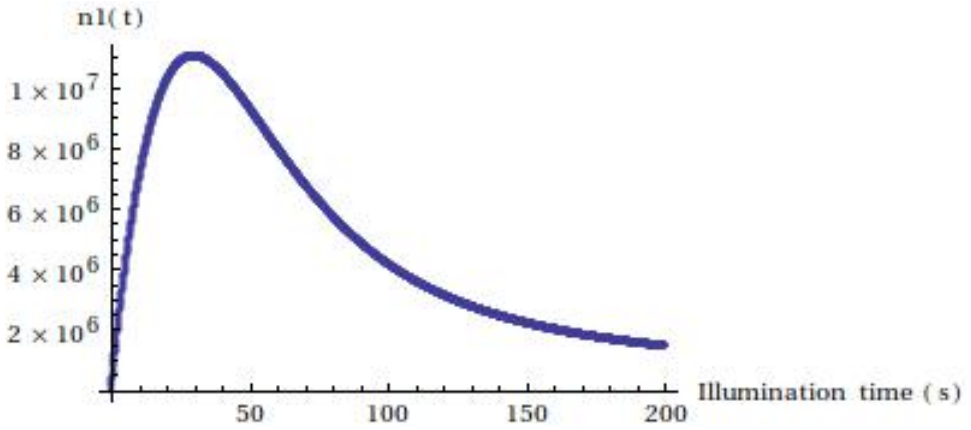

FIGURE 2.3: Variation in the population of shallow trap electrons during illumination. The parameters used in the simulation are: $N_1 = 10^{10}\,cm^{-3}$, $N_2 = 10^{12}\,cm^{-3}$, $M = 10^{12}\,cm^{-3}$, $s_1 = 5{\times}10^{11}\,s^{-1}$, $E_1 = 0.9\,eV$, $k = 8.617{\times}10^{-5}\,eVK^{-1}$, $R = 10^{11}\,cm^{-3}\,s^{-1}$, $A_1 = 10^{-10}\,cm^3\,s^{-1}$, $A_2 = 10^{-9}\,cm^3\,s^{-1}$, $A_m = 10^{-7}\,cm^3\,s^{-1}$, $A_m^* = 10^{-9}\,cm^3\,s^{-1}$, $f_1 = 0.05\,s^{-1}$ and $f_2 = 0.1\,s^{-1}$. These parameters were taken from page 123 of Chen and Pagonis [19].

However, some experiments have shown PTTL signals which increase with illumination up to a maximum and then decrease towards a steady value [4, 18]. Milanovitch-Reichhalter and Vana [20] reported examples of such PTTL from quartz.

We earlier assumed no loss of electrons from the shallow trap during illumination (i.e., $f_1 = 0$) however, this is not necessarily always the case. Walker et al. [21] found that in the case of $\alpha{-}Al_2O_3$:C, electrons are optically bleached from shallow traps during illumination. If electrons are lost from the shallow trap during illumination, then this simple model can explain the decreasing part of most PTTL curves. However, the PTTL intensity will decrease to zero and not necessarily to a non-zero constant value as shown by Alexander et al. [22, 23]. In section 2.2, we present a qualitative model which leads to an initial increase in PTTL intensity followed by a decrease to a constant level without the requirement of optical bleaching of electrons from the shallow trap during illumination.

2.2 A more complex model of PTTL

An alternative model of PTTL is shown in Figure 2.4.

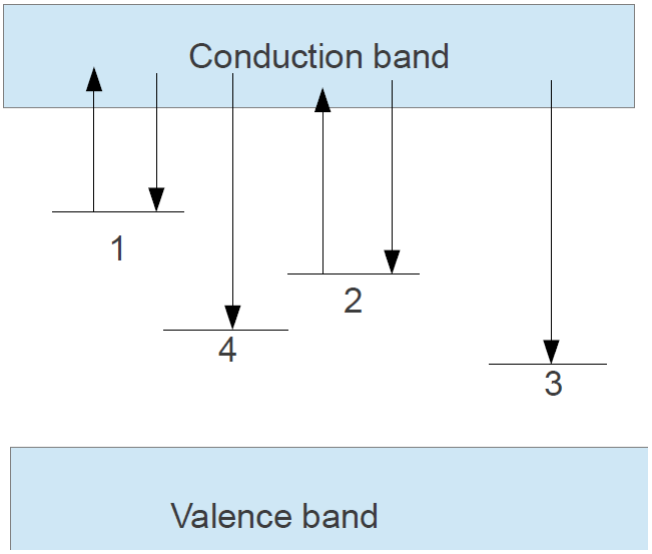

FIGURE 2.4: An energy band model showing the flow of charges during PTTL in the shallow trap (level 1), deep trap (level 2), radiative recombination centre (level 3) and non-radiative recombination centre (level 4).

This model consists of one shallow trap (level 1), one deep trap (level 2), one radiative recombination centre (level 3) and a non-radiative recombination centre (level 4). The charge neutrality condition becomes

$$n_1 + n_2 = m_3 + m_4 \tag{2.17}$$

where m_3 and m_4 are the population of holes at the radiative and non-radiative recombination centres respectively. All the other parameters are as previously defined. The mathematical description of the transfer of charges during each stage of the PTTL process is similar to that of the simple model of section 2.1. The important point here is that during the heating process, some holes can be transferred from the radiative to the non-radiative recombination centre. This implies that the loss of holes is not just due to the OSL observed during illumination. As a consequence of the competition between the two centres, the PTTL signal depends on n_1 and m_3. In the simple model of section 2.1, the concentration of electrons n_1 at the shallow trap cannot be greater than that of holes (charge conservation). But in this model, it is possible for n_1 to be greater than m_3 at some time t. If we assume that at the start of the heating $n_1 < m_3$ then as the illumination time increases, the PTTL signal will grow until the deep trap is depleted or there are no longer enough holes at m_3 for electrons to recombine with. When one of the two situations mentioned occurs, the PTTL will start decreasing with further increase in illumination time. The behaviour of the PTTL intensity can be summarised with [4]

$$S \propto min(n_1, m_3). \tag{2.18}$$

The inclusion of a non-radiative recombination centre in the model of PTTL shown Figure 2.4 leads to a PTTL signal which increases to a maximum and then decreases with further illumination. However, as shown by Alexander et al. [22, 23], the dependence of the PTTL signal on illumination is affected by factors such as the wavelength of the simulating light, its intensity and the photoionisation cross-section σ from the deep trap (σ is related to the rate f_2 at which electrons are optically removed from the deep trap). Simulations such as those presented here only show the behaviour of a PTTL curve for a particular set of parameters; in practice, an experimental PTTL curve will depend on the factors mentioned above and the electronic structure of the material in question.

2.3 TL model for quartz by Bøtter-Jensen et al. [24]

The model of Bøtter-Jensen et al. [24] for quartz has all the essential features of a PTTL model and could be relevant to this study. For this reason, the model is described in some detail below.

In order to explain sensitivity changes in quartz as a result of annealing, Bøtter-Jensen et al. [24] proposed the energy band model shown in Figure 2.5. The model in Figure 2.5 is similar to the complex model of PTTL presented in section 2.2 with the exception of the additional deep inactive trap. Thermal or optical stimulation of electrons from the deep inactive trap does not occur. The deep inactive trap is not necessary for PTTL to occur, however, it is useful in explaining non linear dose dependence effects [4]. The study of Bøtter-Jensen et al. [24] showed that the changes in luminescence sensitivity observed in PTTL and OSL as a result of annealing are due to changes at the recombination centres during annealing. As in the Zimmermann [25] model, Bøtter-Jensen et al. assumed a transfer of holes from the non-radiative to the radiative centre during annealing. By monitoring the TL emission spectra for annealed and unannealed samples of synthetic quartz, they found enhancements in both the 380 and 470 nm emission bands of the annealed sample. In addition to explaining changes in luminescence sensitivity and features of dose dependence in quartz, the model in Figure 2.5 may be valid for PTTL.

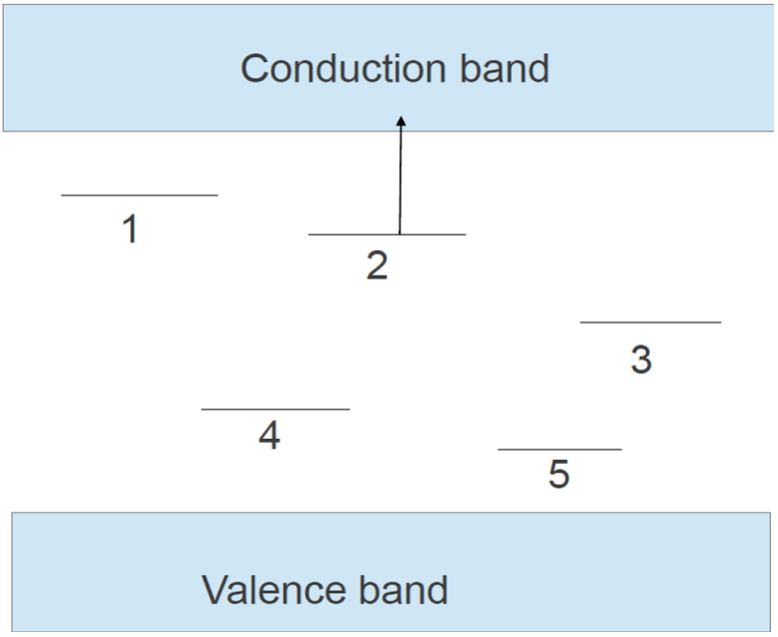

,

FIGURE 2.5: Energy band model of quartz consisting of shallow traps (level 1), optically active traps (level 2), deep inactive traps (level 3), a radiative recombination centre (level 4) and a non-radiative recombination centre (level 5) (reproduced from Bøtter-Jensen et al. [24])

Chapter 3

Methods of kinetics analysis

In this chapter, we describe the methods used in this work to evaluate trapping parameters. The trapping parameters are associated with the transfer of charges between point defects which leads to luminescence. Among the trapping parameters, the most important are the activation energy or trap depth E, the order of kinetics b and the frequency factor s. The methods discussed in this chapter fall into two categories namely partial and whole curve methods.

3.1 Initial rise method

The initial rise (IR) method of analysis is used to calculate the activation energy E of a TL glow peak. The IR method relies on the assumption that the concentration of trapped charges in the low temperature part of a glow peak is nearly constant [2]. As a rule of thumb, the low temperature part of the glow curve with intensities between 5% to 15% of the maximum TL intensity I_M is used [10]. To gain a better understanding as to why the concentration n of trapped charges is approximately constant at low temperature, let us revisit the solution to the first-order kinetics case. As discussed in Chapter 1, first-order kinetics yields a TL intensity of the form

$$I(T) = n_0 s e^{-E/kT} \exp[-\frac{s}{\beta}\int_{T_0}^{T} e^{-E/kT'}dT']. \tag{3.1}$$

It is evident from equation (3.1) that if the change in temperature from T_0 to T is small enough, then $\exp[-\frac{s}{\beta}\int_{T_0}^{T} e^{-E/kT'}dT']$ is close to 1 and the TL intensity can be written as

$$I(T) = C\exp(-E/kT), \tag{3.2}$$

where C is a constant and all the other parameters are as defined previously. Equation (3.2) is also valid for second- and general-order kinetics. Applying the natural logarithm to both sides of equation (3.2) gives

$$\ln(I) = \ln(C) - E/kT. \tag{3.3}$$

Equation (3.3) describes a straight line with intercept $\ln(C)$ on the y-axis and slope $-E/k$. The activation energy E is deduced from the plot of $\ln(I)$ versus $1/T$. The IR method of analysis is suitable for well isolated peaks. Methods of peak separation have been devised to deal with the case of overlapping peaks (e.g., Nahum and Halperin [26]). However, as pointed out by Haake [27], the value of E obtained after the application of such a method for a given peak may be inaccurate since there is a possibility that the preceding peak may only have been partially removed.

The frequency factor s can be obtained by substituting E in the equation giving the maximum TL intensity. For first-order kinetics,

$$s = \frac{\beta E}{kT_M^2} \exp(\frac{E}{kT_M}), \tag{3.4}$$

for second-order kinetics,

$$s = \frac{\beta E}{kT_M^2(1 + \frac{2kT_M}{E})} \exp(\frac{E}{kT_M}), \tag{3.5}$$

and for general-order kinetics,

$$s = \frac{\beta E}{kT_M^2(1 + \frac{2kT_M(b-1)}{E})} \exp(\frac{E}{kT_M}). \tag{3.6}$$

3.2 Various heating rates methods

As can be deduced from equations (3.4) to (3.6), the position T_M of the TL peak depends on the heating rate β at which the glow curve is recorded. The peak position shifts to higher temperatures when the heating rate is progressively increased. As suggested by Booth [28], Bohum (see Pagonis et al. [10] and references therein) and Parfianovitch (see Pagonis et al. [10] and references therein), this shift in peak position with heating rate can be exploited to evaluate the kinetic parameters E and s. If two glow curves are measured at two different heating rates β_1 and β_2 for example, and if in addition

first-order kinetics apply, equation (1.15) can be written for the two heating rates as

$$\frac{\beta_1 E}{kT_{M_1}^2} = s\exp(-\frac{E}{kT_{M_1}}), \tag{3.7}$$

and

$$\frac{\beta_2 E}{kT_{M_2}^2} = s\exp(-\frac{E}{kT_{M_2}}). \tag{3.8}$$

Dividing equation (3.7) by equation (3.8) and rearranging, we obtain

$$E = k\frac{T_{M_1}T_{M_2}}{T_{M_1}-T_{M_2}}\ln[\frac{\beta_1}{\beta_2}(\frac{T_{M_2}}{T_{M_1}})^2]. \tag{3.9}$$

The value of E can then be substituted into equation (3.4) to get the frequency factor s. The various heating rates method described above requires only two glow curves measured at two different heating rates. If we record multiple glow curves at different heating rates, the method suggested by Hoogenstraaten [29] can be used to determine E and s. Following Hoogenstraaten [29], equation (1.15) is rewritten into the form

$$\ln(T_M^2/\beta) = E/kT_M + \ln(E/sk). \tag{3.10}$$

A plot of $\ln(T_M^2/\beta)$ as a function of $1/kT_M$ yields a straight line with slope E. By extrapolating the line to $1/kT_M \to 0$, the value of s can be found from $\ln(E/sk)$. The various heating rates methods described so far are only applicable to first-order kinetics. Chen and Winer [30] used the condition of maximum emission for general-order kinetics and derived a method similar to that of Hoogenstraaten. As discussed earlier, general-order kinetics is described by equation (1.22) and as shown by Chen and Winer [30], the integral in equation (1.22) approximates to

$$\int_{T_0}^{T}\exp(-E/kT')dT' = (\frac{kT^2}{E})\exp(\frac{-E}{kT})(1-\Delta) \tag{3.11}$$

where $\Delta = 2kT/E$ will be of order 0.01 to 0.1 since k and T are of order 10^{-5} and 10^2 respectively. The integral approximation can then be inserted in equation (1.22) to derive equation (1.23) which gives the condition for maximum emission. Equation (1.23) can therefore be rewritten as

$$\beta/T_M^2 = (sk/E)[1+(b-1)\Delta_M]\exp(-E/kT_M). \tag{3.12}$$

Following Chen and Winer [30], the term $[1+(b-1)\Delta_M]$ can be regarded as a constant whose value is close to unity. Hence a plot of $\ln(\beta/T_M^2)$ as a function of $1/kT_M$ should yield a straight line with slope $-E$. Chen and Winer [30] derivation therefore shows that in general, Hoogenstraaten method (equation (3.10)) still yields a good approximation

of E for a non first-order peak.

3.3 Thermal cleaning techniques

As stated in section 3.1, the IR method applies only to single isolated peaks. In the presence of overlapping peaks, peak resolution techniques such as those described in this section are used. A thermal cleaning procedure consists of heating a sample to a specific temperature T_h and cooling it back to room temperature before recording the complete TL glow curve [2]. The choice of T_h depends on the position of peaks in the glow curve. For example to apply the IR method to the second peak in a glow curve, the sample has to be heated to a temperature T_h greater than the maximum temperature T_M of the first peak but less than that of the second peak.

3.3.1 T_M - T_{stop} method

McKeever [31] proposed a thermal cleaning method in which the temperature T_M of the peak intensity is monitored as the T_{stop} temperature of thermal cleaning is increased. T_{stop}, which refers to the temperature at which the sample is preheated before recording the complete TL glow curve, is increased in small steps (2 or 3 °C) and the heating is done at the same linear rate. The temperatures T_M are then plotted with respect to the temperatures T_{stop}. For first-order kinetics, the concentration n_0 of trapped electrons is constant in the initial rise part of the curve and hence T_M does not depend on it. For second- and general-order peaks, T_M does not remain constant with the increase in T_{stop}. In the presence of overlapping peaks, more complex curves of T_M versus T_{stop} are obtained.

3.4 Peak shape methods

Peak shape methods make use of the geometrical parameters associated with a glow peak to determine the trapping parameters E and b. Instead of using part or the whole glow curve, peak shape methods rely on a few points on the glow curve. Figure 3.1 illustrates the parameters used in peak shape methods to obtain E and b.

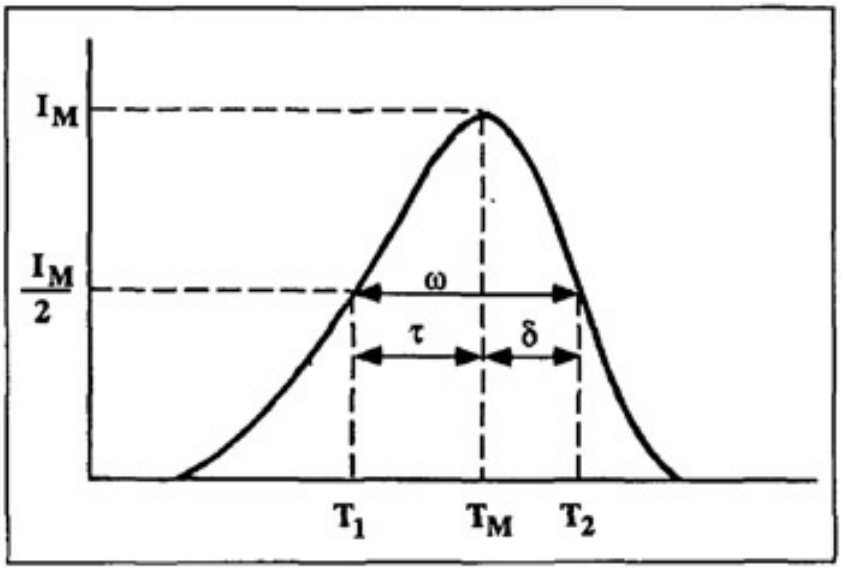

FIGURE 3.1: A glow peak showing the geometrical parameters used in the peak shape method (reproduced from Furetta [32]).

In Figure 3.1, I_M denotes the maximum TL intensity and T_M the corresponding temperature. The half maximum intensity $I_M/2$ occur at temperatures T_1 and T_2. The full width of the peak at half maximum is given by

$$\omega = T_2 - T_1. \tag{3.13}$$

The low and high temperature half-widths are obtained from

$$\tau = T_M - T_1 \tag{3.14}$$

and

$$\delta = T_2 - T_M. \tag{3.15}$$

Halperin and Braner [33] defined the geometrical factor $\mu_g = \delta/\omega$ which gives an indication of the symmetry of the peak. Chen [34] showed that a first-order glow peak is asymmetric and has a value of $\mu_g \approx 0.42$ whereas a second-order glow peaks is nearly symmetric and has a value of $\mu_g \approx 0.52$. For general-order kinetics, μ_g takes intermediate values between 0.42 and 0.52. In the general order case, μ_g can also take values below 0.42 and above 0.52. Chen [34] also developed a general formula for evaluating the activation energy E namely,

$$E_\gamma = c_\gamma(kT_M^2/\gamma) - b_\gamma(2kT_M) \tag{3.16}$$

where γ is δ, τ or ω. The constants c_γ and b_γ are defined by

$$c_\tau = 1.51 + 3(\mu_g - 0.42) \qquad b_\tau = 1.58 + 4.2(\mu_g - 0.42), \tag{3.17}$$

$$c_\delta = 0.976 + 7.3(\mu_g - 0.42) \qquad b_\delta = 0, \tag{3.18}$$

$$c_\omega = 2.52 + 10.2(\mu_g - 0.42) \qquad b_\omega = 1.0. \tag{3.19}$$

3.5 Whole curve method

The whole curve method (WCM) uses the area, $n(T)$, under a TL peak to determine its activation energy E and its order of kinetics b. The area $n(T)$ under the glow peak is computed as

$$n = \frac{1}{\beta} \int_{T_0}^{T_f} I dT, \tag{3.20}$$

where T_0 is a temperature in the initial rise region of the peak, T_f is the temperature at the tail of the peak and β is the heating rate [10]. Equation 3.20 leads to

$$\ln(\frac{I}{n^b}) = \ln(\frac{s}{\beta}) - \frac{E}{kT}. \tag{3.21}$$

Several lines of $\ln(I/n^b)$ versus $1/kT$ are then plotted for a range of b values and the correct values of E and b are retained from the best straight line.

3.6 Isothermal decay methods

An isothermal or phosphorescence decay curve is a plot of luminescence intensity measured at constant temperature as a function of time [4]. The irradiated sample is held at a constant temperature for time t during which the luminescence is recorded. For first-order kinetics, the TL intensity is described by an exponential decay function of the form

$$I = I_0 \exp(-mt), \tag{3.22}$$

where I_0 is the initial TL intensity and

$$m = s \exp(-E/kT_i), \tag{3.23}$$

is the decay constant. The temperature T_i is the temperature at which the sample is held at during TL readout. A plot of $\ln(I)$ as a function of time is a straight line with

slope $-m$. The frequency factor s and the activation energy E can be determined by taking two different isothermal decay curves at temperatures T_1 and T_2. For these two isotherms, the respective decay constants are

$$m_1 = s\exp(-E/kT_1), \tag{3.24}$$

and

$$m_2 = s\exp(-E/kT_2). \tag{3.25}$$

From equation (3.24) and equation (3.25), the following equation can be derived

$$\ln\left(\frac{m_1}{m_2}\right) = \frac{E}{k}\left(\frac{1}{T_2} - \frac{1}{T_1}\right). \tag{3.26}$$

Having determined m_1 and m_2 from plots of the corresponding TL intensity I_1 and I_2 against t on a semi-log scale, that is, $\ln(I) = -mt + \ln(I_0)$, the activation energy E is then computed from equation (3.26). The value of E thus found is reinserted into equation (3.24) to determine the frequency factor s. Another way of determining E and s consists of recording several isotherms at different temperatures thereby getting a set of $m(T_i)$ values. Plotting $\ln(m)$ as a function of $1/kT_i$ yields a straight line with slope $-E$ and y-intercept $\ln(s)$ from which s is readily found. The application of the isothermal decay method to general-order kinetics was suggested by May and Partridge [12]. For a general-order TL glow peak measured at constant temperature, equation (1.21) integrated with respect to time can be written as

$$I = I_0\left[1 + s'n_0^{(b-1)}(b-1)t\exp(-E/kT)\right]^{\frac{b}{1-b}}, \tag{3.27}$$

where

$$I_0 = s'n_0^b\exp\left(-\frac{E}{kT}\right). \tag{3.28}$$

I_0 is the initial TL intensity and and n_0 is the initial concentration of trapped electrons. Equation (3.27) can be rearranged into the form

$$\left(\frac{I}{I_0}\right)^{\frac{1-b}{b}} = \left[1 + s'n_0^{(b-1)}(b-1)t\exp(-E/kT)\right]. \tag{3.29}$$

Provided that the order of kinetics b is known, a plot of $\left(\frac{I}{I_0}\right)^{\frac{1-b}{b}}$ versus time t should yield a straight line with slope m where m is given by

$$m = s'n_0^{(b-1)}(b-1)\exp(-E/kT). \tag{3.30}$$

In practice, the value of b is not known beforehand so a set of lines with slopes given by equation (3.30) are plotted for different values of b. The order of kinetics b then corresponds to the b which gives the best straight line. Hence for a general order peak, the isothermal decay method can be used to estimate the order of kinetics b.

3.7 Curve fitting

Curve fitting is aimed at extracting kinetic parameters from a glow curve. In contrast to most methods of analysis, curve fitting uses the whole glow curve and hence provides an independent way of checking the parameters obtained with the other methods. Mohan and Chen [35] developed a curve fitting method for first- and second-order glow peaks and the method was extended to general-order peaks by Shenker and Chen [36]. The first stage of curve fitting usually consists of guessing the initial values of the parameters that are sought. For each glow peak, initial guesses of the kinetic parameters E, s and b are required. In practice, trapping parameters obtained with one or a combination of methods described earlier can be used as initial values. In the next stage of the fitting process, a function $y(T)$ is used to generate a theoretical curve. Kitis et al. [37] developed appropriate functions for first-order kinetics:

$$I(T) = I_M \exp\left[1 + \frac{E}{kT}\frac{T-T_M}{T_M} - \frac{T^2}{T_M^2}\left(1 - \frac{2kT_M}{E}\right)\exp\left(\frac{E}{kT}\frac{T-T_M}{T_M}\right) - \frac{2kT_M}{E}\right], \quad (3.31)$$

second-order kinetics:

$$I(T) = 4I_M \exp\left(\frac{E}{kT}\frac{T-T_M}{T_M}\right)\left[1 + \frac{T^2}{T_M^2}\left(1 - \frac{2kT}{E}\right)\exp\left(\frac{E}{kT}\frac{T-T_M}{T_M}\right) - \frac{2kT_M}{E}\right]^{-2}, \quad (3.32)$$

and general-order kinetics:

$$\begin{aligned} I(T) = I_M b^{\frac{b}{b-1}} \exp\left(\frac{E}{kT}\frac{T-T_M}{T_M}\right)\Big[1 + (b-1)\frac{2kT_M}{E} + (b-1)\times \\ \left(1 - \frac{2kT}{E}\right)\left(\frac{T^2}{T_M^2}\exp\left(\frac{E}{kT}\frac{T-T_M}{T_M}\right)\right)\Big]^{\frac{-b}{b-1}}. \end{aligned} \quad (3.33)$$

For a glow curve consisting of say j peaks, the function $y(T)$ is a linear combination of functions of the form given by equations (3.31) to (3.33) depending on the order of kinetics that applies. The fitting algorithm then iterates in search of the parameters E, s and b which minimises the difference between the experimental curve and the computer-generated curve. The Marquardt nonlinear least-squares fitting algorithm [38] is commonly used for this purpose. As suggested by Horowitz and Yossian [39], the figure

of merit (FOM) defined as

$$FOM = \frac{\sum_j |y_{experimental} - y_{fit}|}{\sum_j y_{fit}} \tag{3.34}$$

can then be used to evaluate the goodness of the fit. In equation (3.34), $y_{experimental}$ is the intensity of the TL at a specific temperature and y_{fit} is the value obtained from fitting. A fit is deemed to be acceptable if the value of FOM is less than 10% [37].

Chapter 4

Experimental details

This chapter gives a brief description of the luminescence system used for experiments and describes the quartz samples used in this work.

4.1 Instrumentation

The Risø TL/OSL Reader (model TL/OSL-DA-20) was used to irradiate, stimulate and detect luminescence from samples of natural quartz. The Risø TL/OSL Reader consists of two separate units namely the reader and the controller. The Reader comprises of the luminescence detection system, the luminescence stimulation system and the irradiation source. Figure 4.1 shows the essential components of the Reader. The controller houses the electronics used to control the Reader and also displays the instruction currently being executed. The controller may be connected to a computer via an RS-232 serial cable or a USB port.

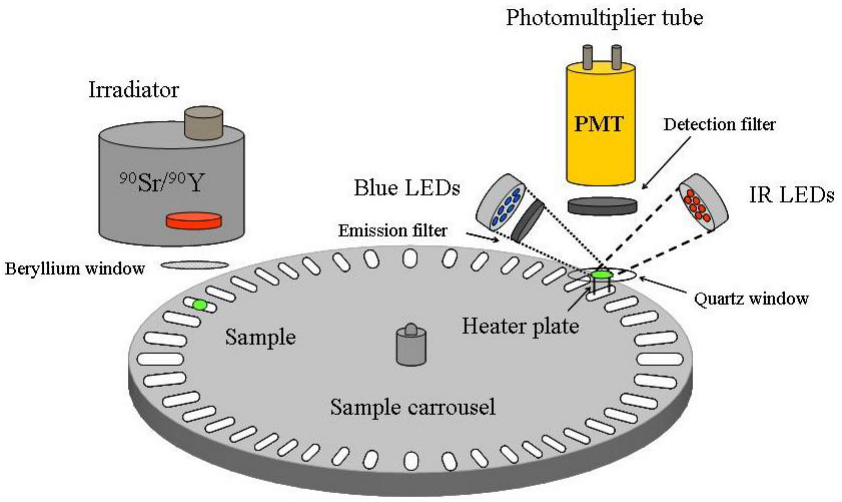

FIGURE 4.1: Schematic diagram of the Risø TL/OSL Reader (taken from the Risø manual [40])

4.1.1 The luminescence detection system

The luminescence detection system consists of a bialkali EMI 9235QB photomultiplier tube (PMT) and a set of transmission filters. The photomultiplier tube has a maximum detection efficiency between 200 and 400 nm which is suitable for luminescence detection in quartz. The luminescence was measured through a 7.5 mm thick Hoya U-340 filter (transmission band 270 - 380 nm) was used for measurements involving OSL.

4.1.2 The luminescence stimulation system

The Reader has a heating system for TL stimulation and an optical system for OSL stimulation. The heating system consists of a heater strip and a lift mechanism. The Reader also has a carousel with 48 positions at which sample holders can be loaded. Before thermal stimulation, the carousel is rotated to position a holder containing the sample above the heater. The heating strip is then raised to ensure contact between the heater and the sample holder. The Risø Reader allows the use of heating rates in the range from 0.1 to 10 °C/s. Samples can be heated at a constant rate from room temperature to a maximum temperature of 700 °C. The heating is done in a nitrogen atmosphere. Nitrogen is used to facilitate the cooling of the heating strip and

to improve thermal contact between the sample holder and the heater strip [41]. The optical stimulation system consists of two separate sets of blue and infrared light emitting diodes (LEDS). For quartz samples, blue LEDS are used for optical stimulation. The set of blue LEDS is made up of 28 LEDS arranged in 4 clusters each with 7 LEDS. The blue LEDS (NICHIA type NSPB-500AS) emit at 470 nm (FWHM = 20 nm). The LEDS have an emission angle of 15 degrees and a total power of 80 mW/cm^2. The switching of the LEDS is controlled by software and the power at which they operate can be adjusted.

4.1.3 The irradiation source

Sample irradiation is done *in-situ* with the ^{90}Sr/^{90}Y beta source attached to the Risø TL/OSL Reader. The beta source emits beta particles with a maximum energy of 2.27 MeV. The activity of the source is about 1.48 GBq which corresponds to a dose rate of 0.1028 Gy/s. The beta source has a half life of 30 years. The irradiation is software controlled. Before the start of the irradiation, the carousel is rotated to position the sample holder directly below the irradiation source.

4.2 Sample preparation

Natural quartz samples with grain size between 90 - 500 μm from BDH Ltd.(UK) were used. The quartz samples used in the present work are the same samples used previously by Chithambo and Galloway [42] for the studies of luminescence lifetimes. The samples consisted of unannealed and samples annealed at 500 °C for 10 minutes. Annealing is a thermal treatment which enhances the sensitivity of the luminescent material and erases previous irradiation effects [32]. For each measurement, a few grains of quartz were affixed to a stainless steel sample holder with the aid of silicon spray and then placed at a given position on the carousel. Once the sample is placed on the carousel, the irradiation, stimulation and detection of the luminescence signal are software controlled.

Chapter 5

Results and discussions

This chapter reports and discusses the results obtained from thermoluminescence (TL) studies conducted on natural quartz. The kinetics analysis of TL glow curves from unannealed and annealed samples is the subject of sections 5.1 and 5.2 respectively. Section 5.3 deals with the study of phototransferred effects in both samples and radioluminescence emission spectra from the same quartz annealed at various temperatures are discussed in section 5.4.

5.1 Kinetic and dosimetric features of the unannealed sample

5.1.1 General features

5.1.1.1 Natural TL signal

To start with, the natural TL signal was recorded from the unannealed sample of natural quartz prior to laboratory irradiation. Figure 5.1 shows the TL glow curve obtained from the sample at a heating rate of 5.0 °C/s.

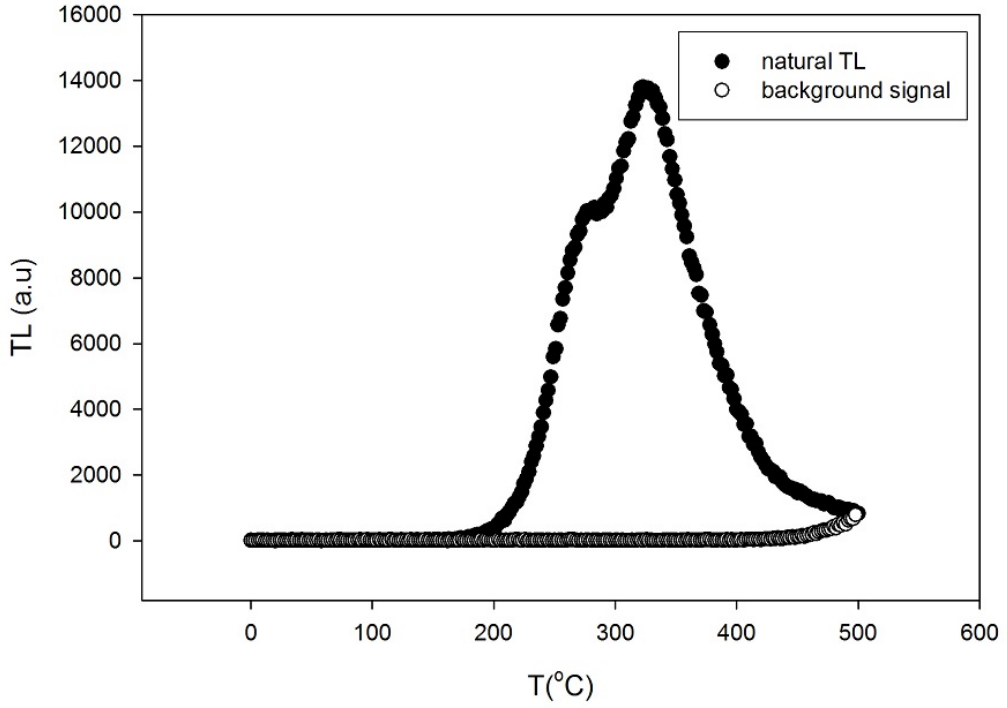

FIGURE 5.1: TL signal measured from unannealed natural quartz at a heating rate of 5.0 °C/s prior to irradiation. The background signal (open circles) is shown for comparison.

The TL glow curve shown in Figure 5.1 consists of two peaks at 280 and 325 °C respectively. These two peaks are due to the recombination of deep-trap electrons with holes. Deep traps in this case refer to all traps from which electrons cannot be evicted at temperatures less than 200 °C. The background signal (open circles), which was recorded at the same heating rate after the natural TL yielded no TL as expected. Similarly, the natural TL measured from a fresh aliquot of the same sample at a heating rate of 1.0 °C/s gave peaks at 250 and 300 °C respectively. The shift in peak temperatures is a consequence of the lower heating rate used. The mass of the two samples from which the glow curves were recorded at 5.0 °C/s and 1.0 °C/s respectively were not identical. Figure 5.2 shows the TL glow curve obtained at a heating rate of 1.0 °C/s.

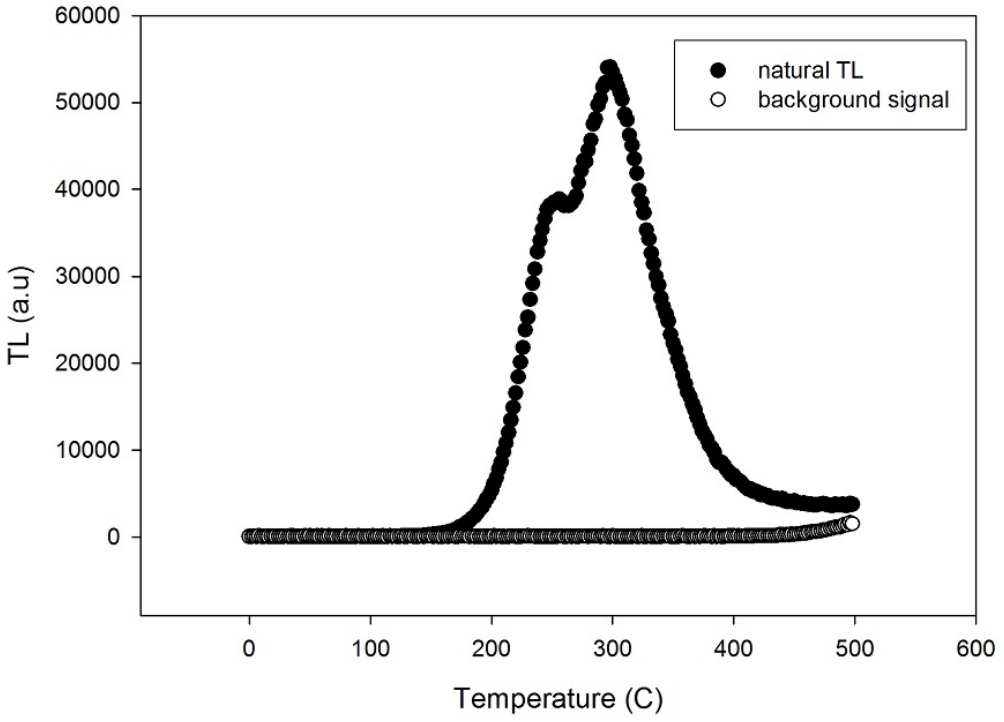

FIGURE 5.2: TL signal measured from unannealed natural quartz at a heating rate of 1.0 °C/s before irradiation. The background signal, represented by open circles, is shown for comparison.

The same aliquot from which the natural TL was measured at 1.0 °C/s was then irradiated to 10 Gy and heated at the same rate of 1.0 °C/s to observe the induced TL signal. The resulting glow curve is shown in Figure 5.3 and has a dominant peak at 72 °C. This dominant peak is the so called "110 °C" TL peak which appears here at a lower temperature because of the heating rate used. A change in scale from linear to semi-log reveals the presence of other peaks as shown in the inset. Hence the glow curve has peaks at 72 °C (peak I), 124 °C (peak II), 180 °C (peak III), 248 °C (peak IV) and 318 °C (peak V). Peak I, II and III which occur at relatively low temperatures compared with the other two peaks are absent in the natural TL glow curve in Figure 5.2. These low temperature peaks are attributed to the recombination of shallow trap electrons with holes. Electrons from such traps have short half-lives and hence their corresponding peaks are absent in the natural

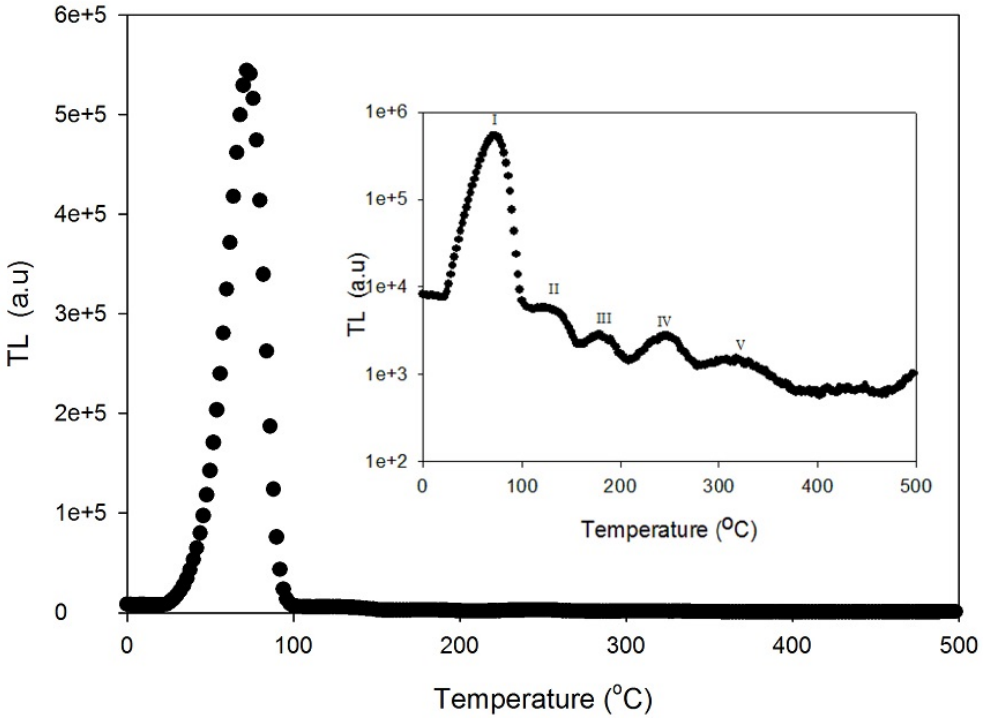

FIGURE 5.3: TL glow curve taken from unannealed natural quartz at a heating rate of 1.0 °C/s after irradiation to 10 Gy. The low intensity peaks at higher temperatures are revealed on the semi-log plot shown in the inset.

TL glow curve. A TL glow curve obtained from a sample freshly irradiated to 10 Gy and measured at a heating rate of 5.0 °C/s after the natural TL signal was recorded is shown in Figure 5.4. In contrast to the TL glow curve taken at the heating rate of 1.0 °C/s (Figure 5.2), this TL glow curve shows only three clear peaks and a weak-intensity overlapping peak at 110 °C. These peaks occur at 92 °C (peak I), 200 °C and 280 °C. For the heating rate of 5.0 °C/s, peak I remains the most intense peak in the glow curve. The complex structure of the TL glow curve, as shown in the inset to Figure 5.4, is probably due to the shift in peak temperature with heating rate. Peaks in a TL glow curve are not necessarily affected by heating rate in the same way. As such, increasing the heating rate might cause large shifts in temperature for some peaks and smaller shifts for others.

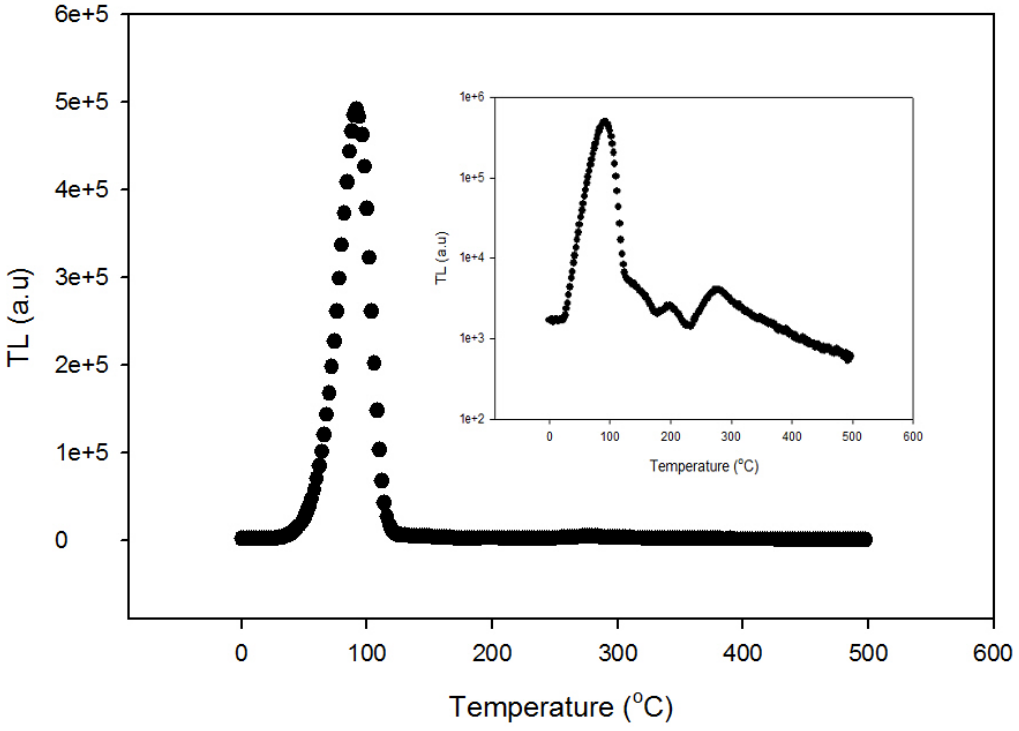

FIGURE 5.4: TL glow curve obtained from unannealed natural quartz at a heating rate of 5.0 °C/s after irradiation to 10 Gy.

5.1.1.2 Influence of repetitive measurements

The influence of repetitive measurement on the position of the main TL peak was investigated by taking a sequence of TL measurements from a single aliquot under the same experimental conditions. In other words, after recording the natural TL signal from the sample, it was cooled to room temperature and irradiated to measure the induced TL signal. This process of irradiation and TL read out was repeated a given number of times. The experiment was carried out on two separate aliquots irradiated to 10 Gy for each measurement and heated at either 1.0 or 5.0 °C/s respectively. The intensity and temperature of each peak were noted each time. However, we will only focus on the main TL peak here. Figure 5.5 shows the effect of repetitive measurement on the temperature of peak I. The position of peak I, as shown in Figure 5.5, is unaffected by re-use.

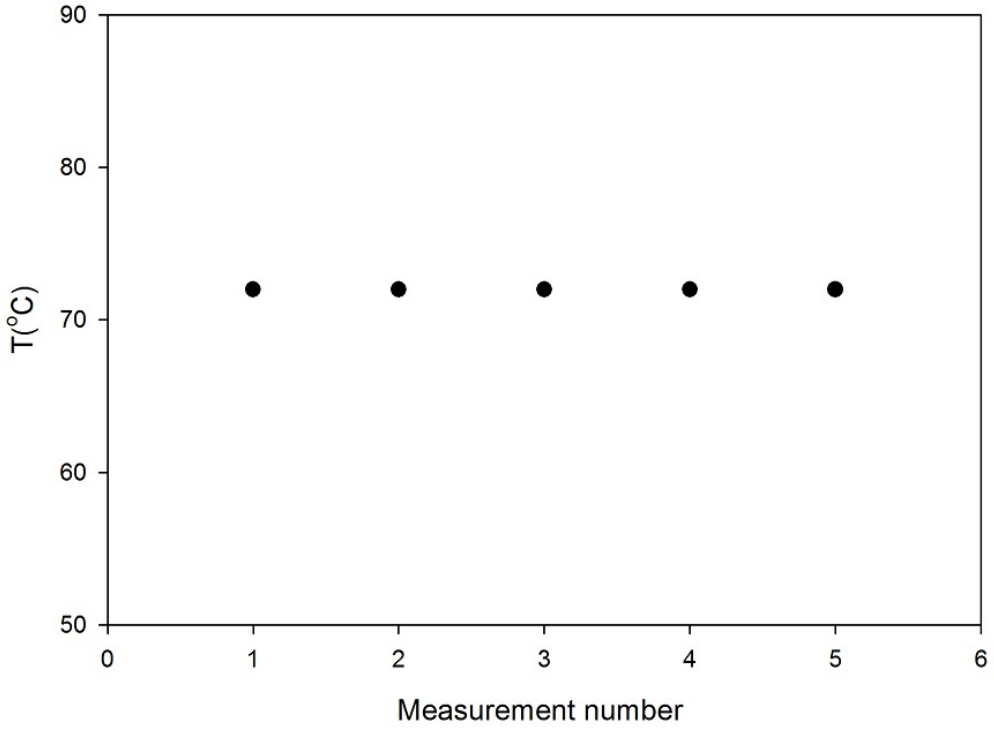

FIGURE 5.5: Influence of sample re-use on the position of peak I. The sample was irradiated to 10 Gy and heated at 1.0 °C/s.

Similarly; Figure 5.6, a plot of maximum TL intensity versus measurement number for TL from peak I, shows that the intensity of peak I grows linearly with the measurement number.

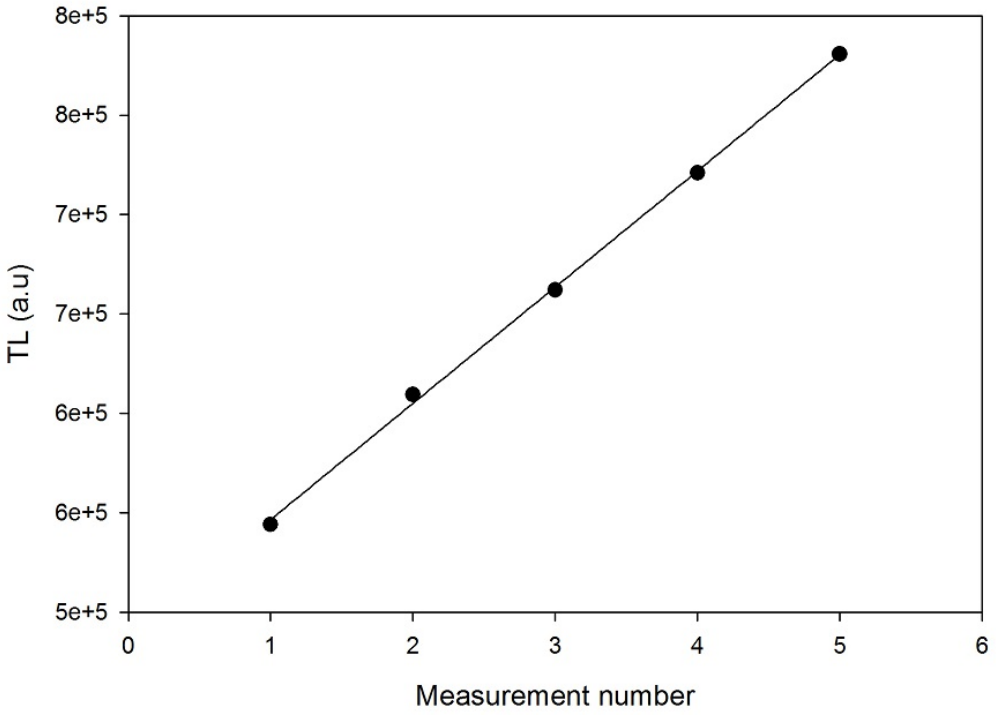

FIGURE 5.6: Growth in TL intensity with sample re-use for peak I (irradiation dose 10 Gy and heating rate of 1.0 °C/s). The solid line, of the form y = mx + c, shows the linear increase of the peak intensity.

The effect of repeated measurements studied on a second aliquot with a heating of 5.0 °C/s and a sequence of ten TL measurements instead of six yielded results similar to those found for a heating rate of 1.0 °C/s. As evident in Figure 5.7, the main TL peak appeared at 92 °C and its peak temperature remained unaffected by repeated measurement.

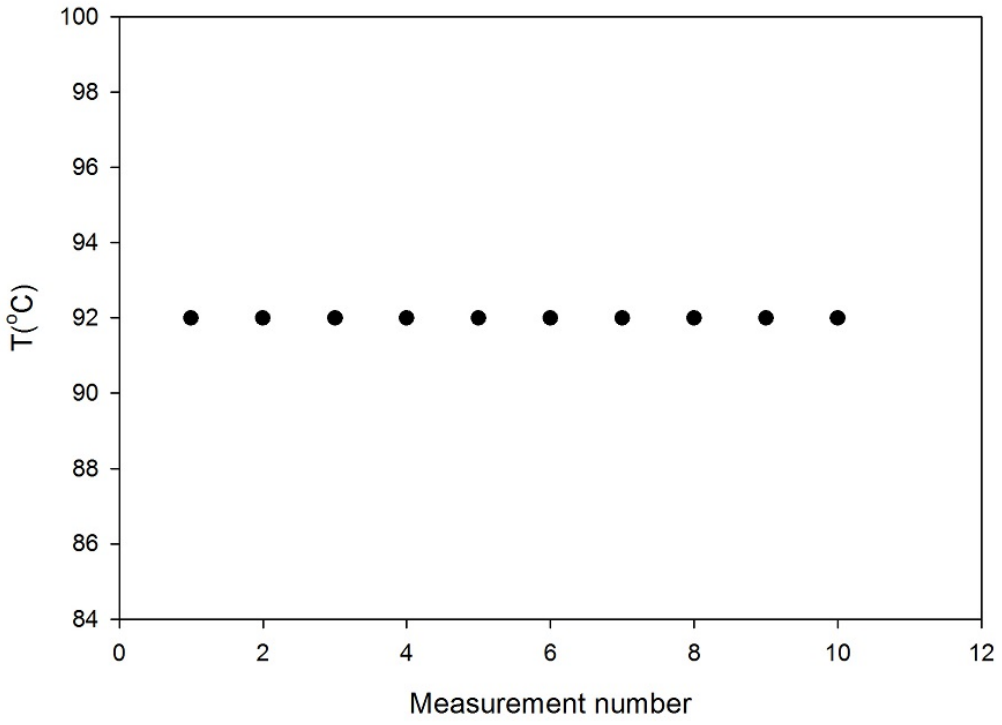

FIGURE 5.7: Influence of repeated measurement on the maximum temperature of peak I (irradiation dose 10 Gy, heating rate 5.0 °C/s).

In comparison with the result found for a heating rate of 1.0 °C/s, the intensity of the main TL peak was also found to increase with sample re-use. However, the increase was not linear as noted earlier (Figure 5.6).

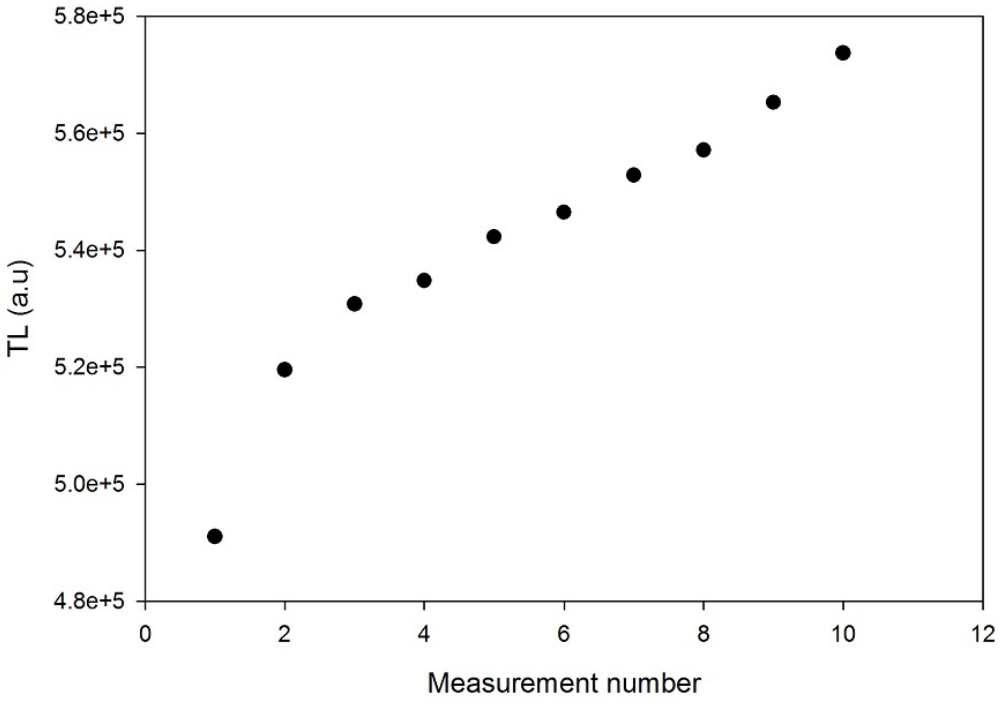

FIGURE 5.8: Growth in the TL intensity of peak I with repeated runs for an irradiation dose 10 Gy and a heating rate 5.0 °C/s.

We believe that this increase in TL intensity with repeated measurements is due to changes in the sensitivity of the sample due to repeated irradiation and heating. The increase in TL sensitivity as a result of irradiation and thermal treatments is also known as the predose effect [14, 43]. This effect has been reported by many other authors (e.g., Koul [43] and references therein) for the main TL peak in quartz. One of the first theoretical models to account for the sensitisation effect was proposed by Zimmerman [25]. For this thesis, an experiment was conducted to check if this increase in TL intensity with repeated measurements was indeed a consequence of the predose effect. This is described next.

5.1.1.3 Thermal activation and sensitisation

The experiment performed to test for sensitisation effects consisted of three main steps. In the first step, a fresh unannealed sample was irradiated to 10 Gy and then heated to 150 °C at a rate of 5.0 °C/s. The sample was irradiated to 10 Gy before heating to reproduce the "110 °C" peak which is not present in unannealed samples because of its short half-life. Heating the sample to 150 °C removes the induced "110 °C" TL peak. Secondly, the sample was given a test dose of 1 Gy and heated to 150 °C at the same

rate of 5.0 °C/s. The TL recorded at this stage, as shown in Figure 5.9, has a weak peak around 80 °C. The sample was then activated by heating from room temperature to 500 °C. During the activation step, the population of holes at the recombination centres is increased [4, 25]. Following the activation step, the sample was given the same test dose and heated to 150 °C at the same rate of 5.0 °C/s to measure the new TL glow peak. As shown in Figure 5.10, the intensity of the new TL glow peak is greater than that of the TL peak in Figure 5.9 by a factor of at least 5.

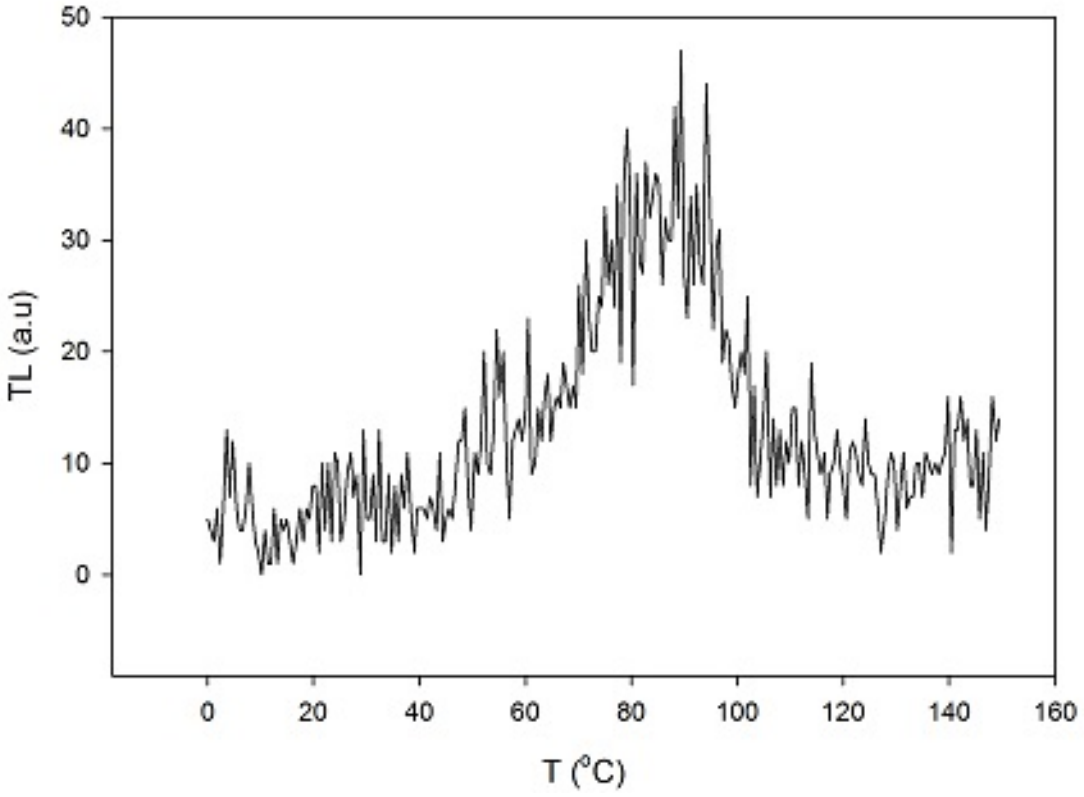

FIGURE 5.9: TL glow curve measured from a fresh sample irradiated to 1 Gy and heated at 5.0 °C/s. The sample was not subjected to any thermal treatment before this measurement.

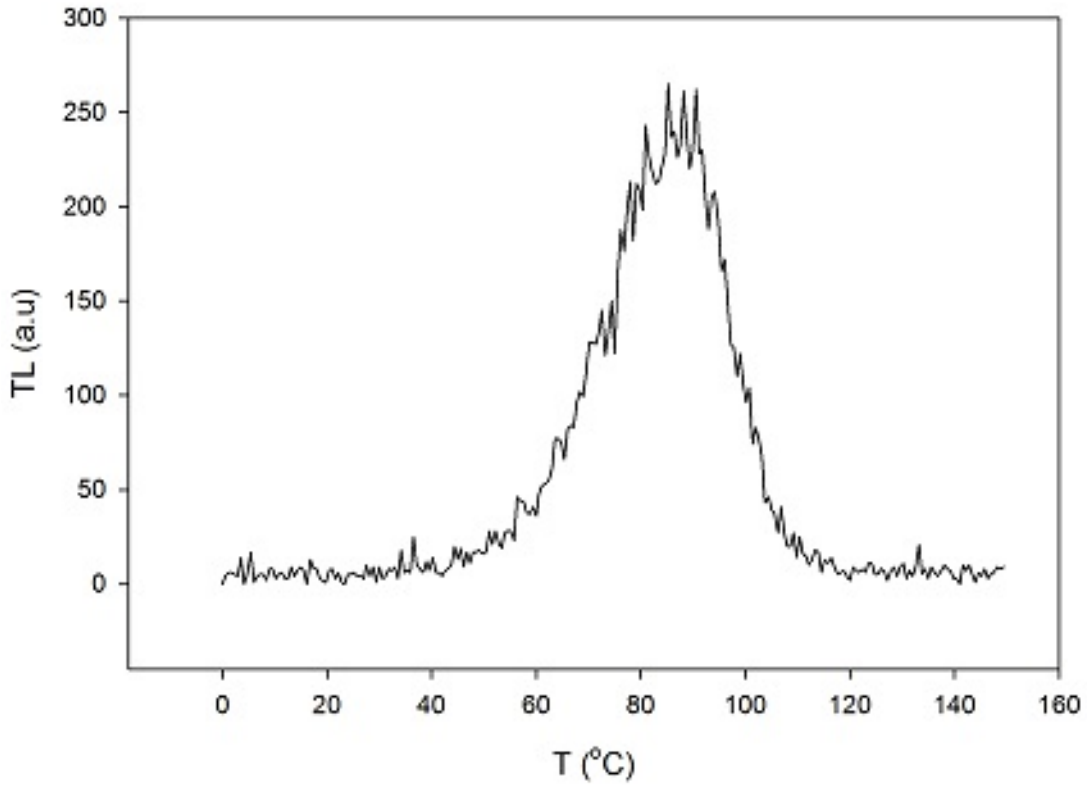

FIGURE 5.10: TL glow curve measured at a heating rate of 5.0 °C/s after thermal activation and irradiation to 1 Gy.

A new heating to 500 °C followed by the same test dose did not yield a noticeable increase in the intensity of the new TL glow peak; this observation shows that, as suggested by Chen and McKeever [4], the increase in sensitivity is not just due to thermal activation but is a combined effect of heating and irradiation. The sensitisation test therefore shows that sample re-use leads to changes in the TL sensitivity of the main peak for our sample. These changes in TL sensitivity account for the increase in the TL intensity of the main peak.

5.1.2 Peak resolution methods

5.1.2.1 Thermal cleaning analysis

In subsubsection 5.1.1.2, when discussing the preliminary TL measurements performed on the two aliquots at heating rates of 1.0 °C/s and 5.0 °C/s respectively, we pointed out the fact that in comparison to the TL glow curve obtained at 1.0 °C/s (Figure 5.3), that recorded at 5.0 °C/s had a rather complex structure (Figure 5.4). Even though our

primary focus was the main TL peak, it was important to resolve glow curves (especially those measured at 5.0 °C/s) into their component peaks. Therefore, the aim of thermal cleaning [2] as employed here was to determine the various position of peaks in a given glow curve. Knowledge of the position of peaks in the glow curve was essential to the investigation of phototransferred effects. Figure 5.11 shows a TL glow curve measured at a heating rate of 5.0 °C/s after irradiation to 123 Gy. The main TL peak in this glow curve is at 117 °C which is somewhat higher than expected.

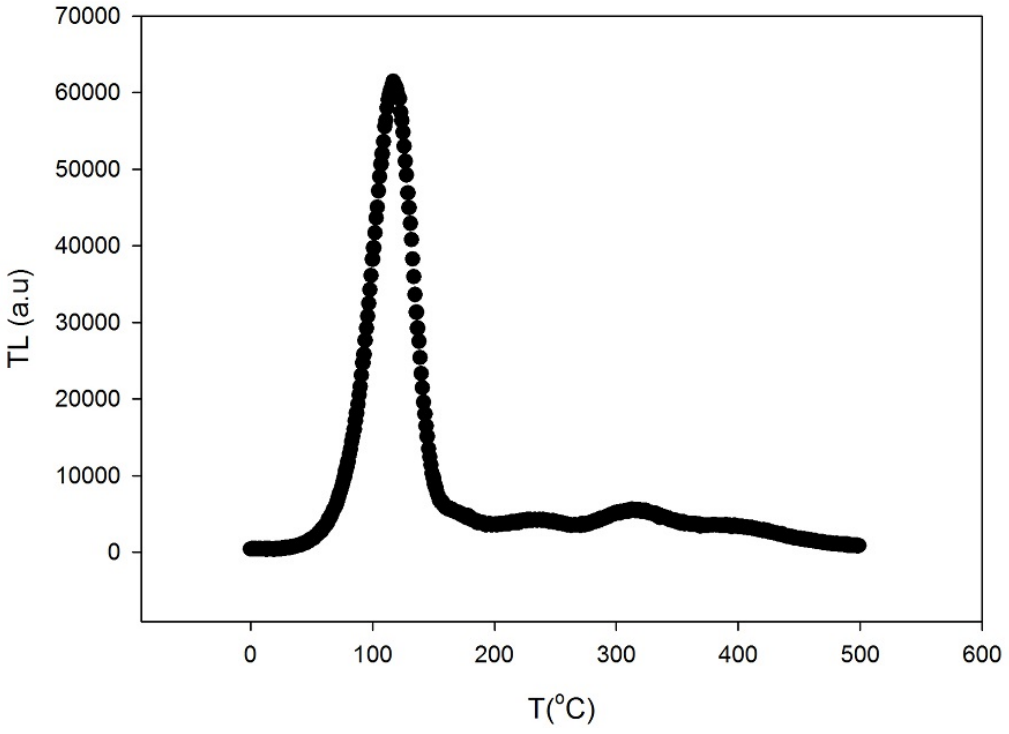

FIGURE 5.11: TL glow curve measured at a heating rate of 5.0 °C/s from a sample of unannealed quartz irradiated to 123 Gy.

Having an idea of the position of the prominent peaks allowed us to choose the temperature T at which the sample could be preheated to remove a given peak before taking the full TL glow curve as described in section 3.3. The main TL peak was removed by heating the sample to 140 °C after irradiation before taking the new TL glow curve. As evident in Figure 5.12, the new TL glow curve consisted of peaks at 170, 235, 315 and 390 °C.

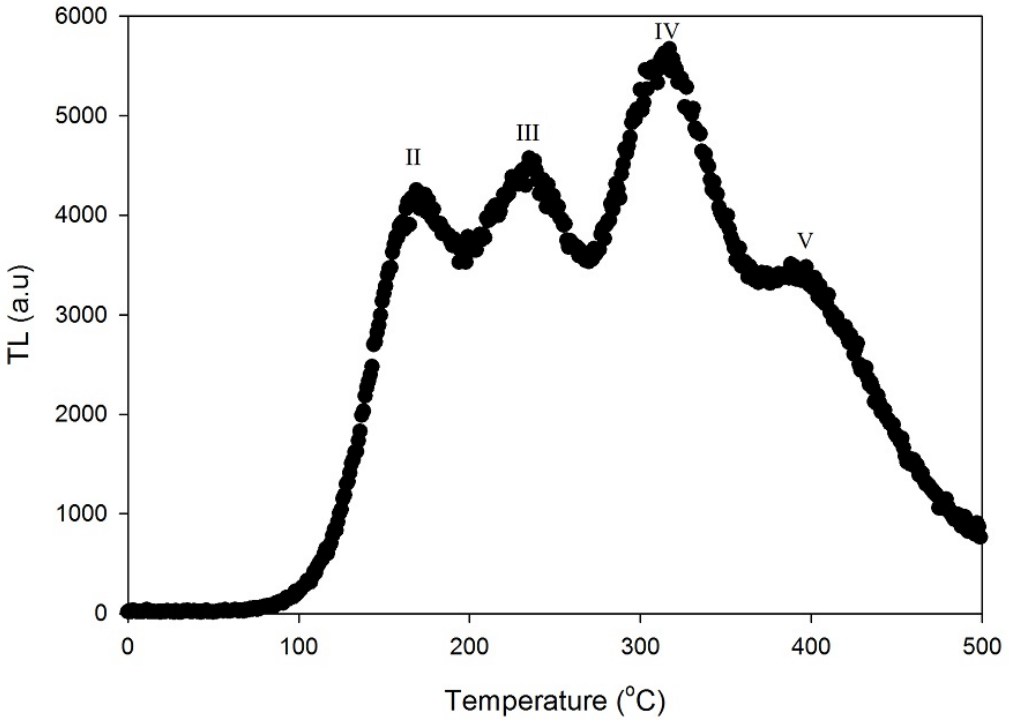

FIGURE 5.12: TL glow curve recorded after the removal of the main TL peak by a preheat to 140 °C (heating rate of 5.0 °C/s, irradiation dose 123 Gy).

By progressively increasing the preheat temperature used before TL read out, the glow curve in Figure 5.11 was resolved into peaks at 117, 170, 235 - 240, 315, 390 and 452 °C respectively. These peak temperatures are similar to those reported elsewhere for a heating rate of 5.0 °C/s (e.g., de Lima et al. [16], Ankama Rao et al. [44]).

5.1.2.2 T_M - T_{stop} method

The T_M - T_{stop} method [2, 4] was used to determine whether the main TL peak had any peaks on its rising edge. The experiment was performed on a fresh sample. As such, the natural TL signal was measured before irradiation. The TL glow curve recorded at a heating rate of 5.0 °C/s after irradiation to 93 Gy had the main TL peak at 84 °C. Following a fresh irradiation to 93 Gy, the sample was heated to a T_{stop} temperature of 40 °C at the same rate of 5.0 °C/s and cooled to room temperature before measuring the full TL glow curve. The sequence consisting of irradiation, heating to T_{stop} and TL read out was repeated for T_{stop} temperatures ranging from 43 to 77 °C in steps of 3 °C. The temperature T_M of the main peak was noted for each measurement. Figure 5.13 shows the dependence of the peak temperature T_M on the T_{stop} temperature.

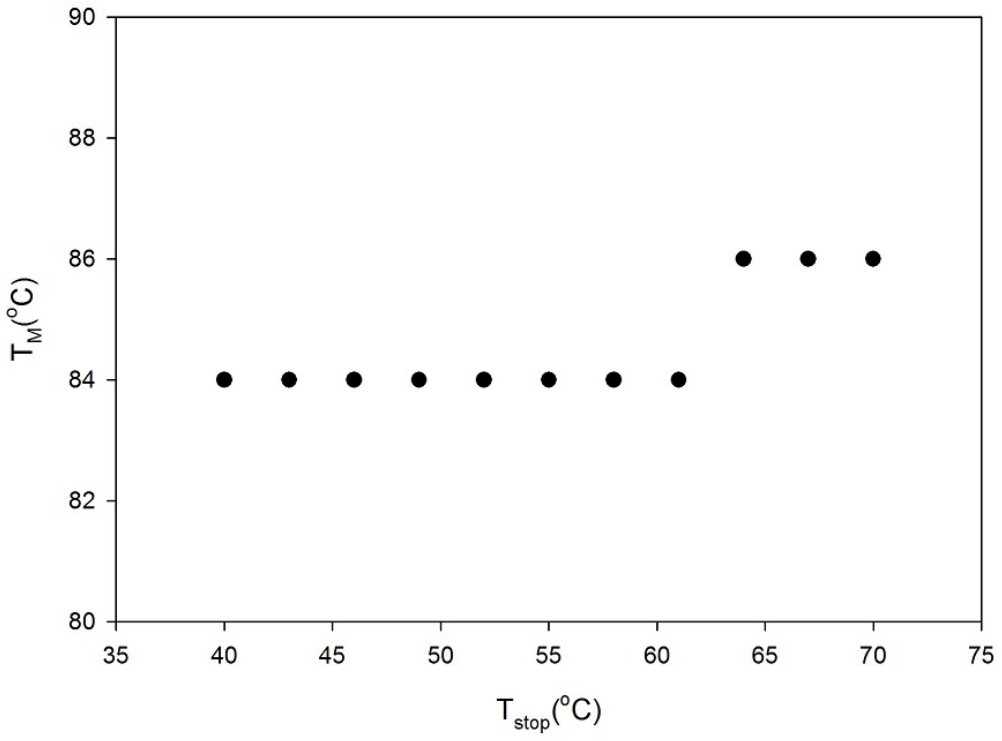

FIGURE 5.13: Dependence of the peak temperature T_M on the T_{stop} temperature. The sample was irradiated to 93 Gy and heated at a rate of 5.0 °C/s for each measurement.

As seen in Figure 5.13, the temperature of the main TL peak remains at 84 °C with T_{stop} up to 63 °C. For T_{stop} higher than 63 °C, the peak temperature is constant at 86 °C. The last 3 points are within the magnitude of statistical scatter for this type of measurement. The peak temperature is therefore essentially independent of the T_{stop} temperature. This suggests that the main TL peak follows first-order kinetics since the peak temperature is not affected by the change in the initial concentration of trapped charges [32]. The traps associated with the main TL peak are partially depleted each time the sample is heated to T_{stop}. Hence, the intensity of the main TL peak decreases progressively with the increase in the T_{stop} temperature (Figure 5.14).

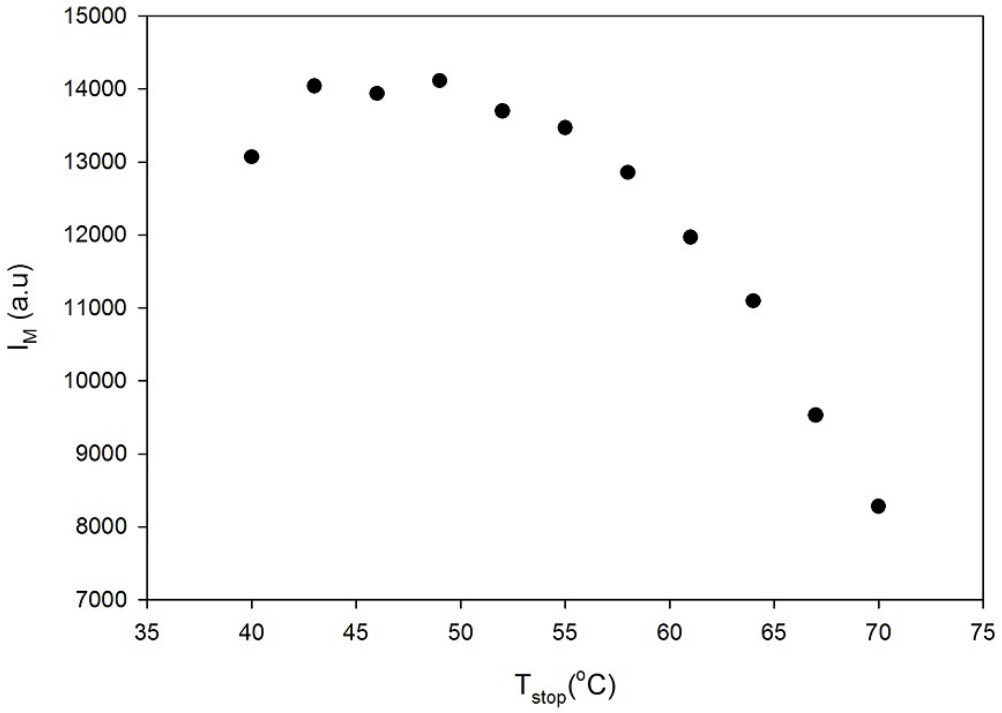

FIGURE 5.14: Dependence of the peak intensity I_M on the T_{stop} temperature. The sample was irradiated to 93 Gy and heated at a rate of 5.0 °C/s for each measurement.

5.1.3 Evaluation of the kinetic parameters

5.1.3.1 Curve fitting

The aim of curve fitting is to obtain the best set of parameters which minimises the difference or residuals between the experimental and the predicted data. Thermal cleaning revealed the presence of six peak in glow curves measured from the unannealed sample. The equation used for fitting was therefore a sum of six terms where each term is given by the general-order TL equation (i.e., equation (3.33)) derived by Kitis et al. [37]. Figure 5.15 shows a glow curve measured at a heating rate of 5.0 °C/s after irradiating the sample to 123 Gy and the fit obtained. The fit is the solid line through the data points. For the glow curve shown in Figure 5.15, the trapping parameters generated for the main peak were $E = 0.93 \pm 0.02$ eV and $b = 1.08 \pm 0.01$. Given E and b, the frequency factor s was computed from equation (3.6) to be 2.3×10^{12} s^{-1}. The figure of merit (FOM) and the coefficient of regression R^2 were 1.10% and 0.9993 respectively. For a good fit, the FOM is expected to be less than 10% and R^2 close to unity. Unless stated otherwise, we assumed the frequency factor to be temperature independent in applying the various methods of analysis.

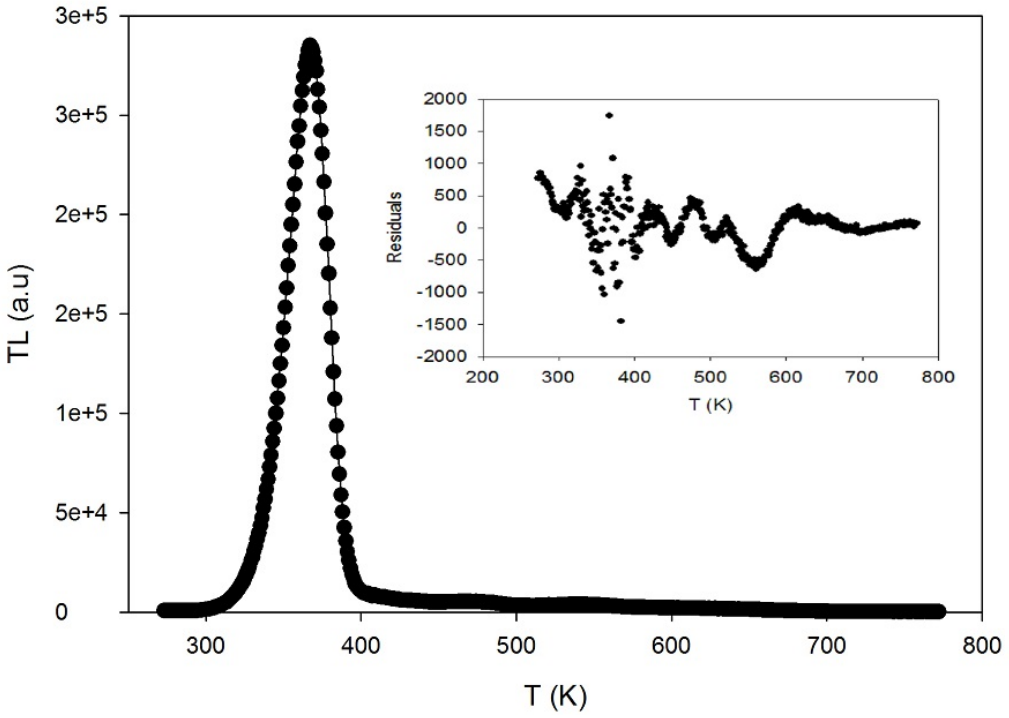

FIGURE 5.15: Experimental TL glow curve and best fit. The equation used to fit the glow curve was a sum of six general-order terms (i.e., equation (3.33)). The glow curve was measured at 5.0 °C/s after irradiation to 123 Gy.

As shown in the inset of Figure 5.15, the residuals oscillate closely about the origin. The resulting fit is fairly satisfactory. The results found for glow curves measured at various heating rates are summarised in table 5.1. $T_{M_{fit}}$ denotes the peak temperature obtained from fitting. The frequency factor s was evaluated from equation (3.6).

TABLE 5.1: Kinetic parameters obtained from fitting for the main TL peak. The sample was irradiated to 123 Gy for each measurement.

HR (°C/s)	T_M (K)	$T_{M_{fit}}$ (K)	E (eV)	b	s $(\times 10^{12} s^{-1})$	FOM	R^2
0.2	331.15	330.77 ± 0.12	0.91 ± 0.01	1.00 ± 0.01	1.42	3.30%	0.9982
0.4	338.15	338.17 ± 0.07	0.90 ± 0.01	1.00 ± 0.01	0.95	2.22%	0.9983
0.6	342.15	341.87 ± 0.26	0.91 ± 0.02	1.01 ± 0.02	1.41	2.68%	0.9988
0.8	345.15	344.93 ± 0.12	0.91 ± 0.01	1.05 ± 0.01	1.40	1.24%	0.9990
1.0	347.15	347.26 ± 0.02	0.91 ± 0.01	1.01 ± 0.01	1.41	1.83%	0.9992
2.0	355.15	354.80 ± 0.01	0.90 ± 0.01	1.01 ± 0.01	1.01	1.20%	0.9994
3.0	360.15	360.01 ± 0.12	0.92 ± 0.01	1.03 ± 0.01	1.87	1.05%	0.9997
4.0	364.15	364.19 ± 0.17	0.92 ± 0.01	1.06 ± 0.01	1.73	1.12%	0.9996
5.0	367.15	367.17 ± 0.24	0.93 ± 0.02	1.08 ± 0.01	2.32	1.10%	0.9993

5.1.3.2 Peak shape method

The peak shape (PS) method uses the geometrical features of the TL glow curve to determine the trapping parameters E and b. The application of the peak shape method requires the knowledge of the glow intensity at peak maximum (T_M, I_M) as well as the temperatures T_1 and T_2 corresponding half maximum intensity. The same data onto which curve fitting was applied were used to compute the geometric and trapping parameters. As reported in Table 5.1, the order of kinetics b was found to be nearly constant with heating rate. The PS method also revealed that Halperin and Braner's [33] geometrical factor only increases slightly with heating rate. Such a result was expected because of the relationship between the order of kinetics b and the geometrical factor μ_g. Figure 5.16 shows a plot of the order of kinetics b as a function of the heating rate. An inset also shows the influence of the heating rate on the geometrical factor μ_g.

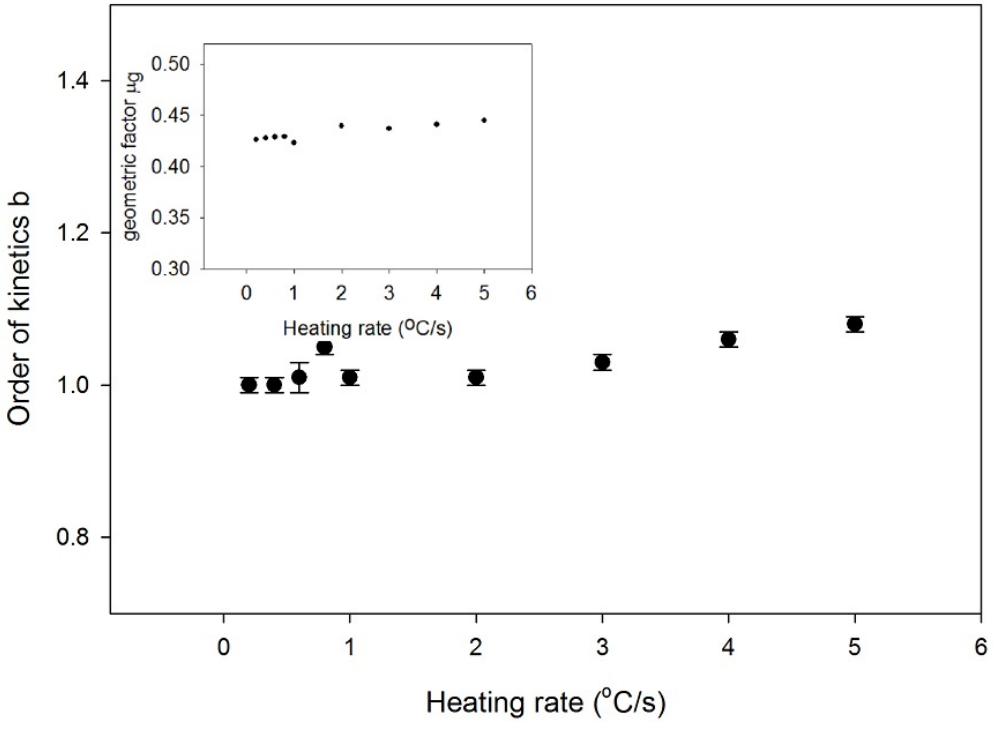

FIGURE 5.16: Influence of the heating rate on the order of kinetics b. These results were obtained from a sample irradiated to 123 Gy for each measurement.

The inset in Figure 5.16 shows that the geometric factor μ_g increases with heating rate from 0.42 to 0.44. These values of μ_g correspond to values of b between 1.0 and 1.2 on Chen's graph [2]. The values of b predicted from Chen's graph are therefore consistent with the values of b found from curve fitting (see Table 5.1, Figure 5.16). Having obtained

the values of μ_g, Chen's equations which relate the geometric factors to the activation energy E_γ [34] were then use to evaluate E. The subscript γ stands for τ, δ or ω. The values of E computed from Chen's equations are shown in Table 5.2. To compare the

TABLE 5.2: Activation energy E of the main TL peak computed from Chen's [34] equations

HR(°C/s)	E_τ(eV)	E_δ(eV)	E_ω(eV)
0.2	0.92	0.91	0.93
0.4	0.92	0.92	0.93
0.6	0.93	0.93	0.94
0.8	0.93	0.93	0.94
1.0	0.91	0.91	0.91
2.0	0.96	0.96	0.96
3.0	0.94	0.95	0.95
4.0	0.95	0.96	0.96
5.0	0.96	0.97	0.97

values of activation energy obtained from curve fitting and the PS method, we plotted them against the heating rate as shown in Figure 5.17.

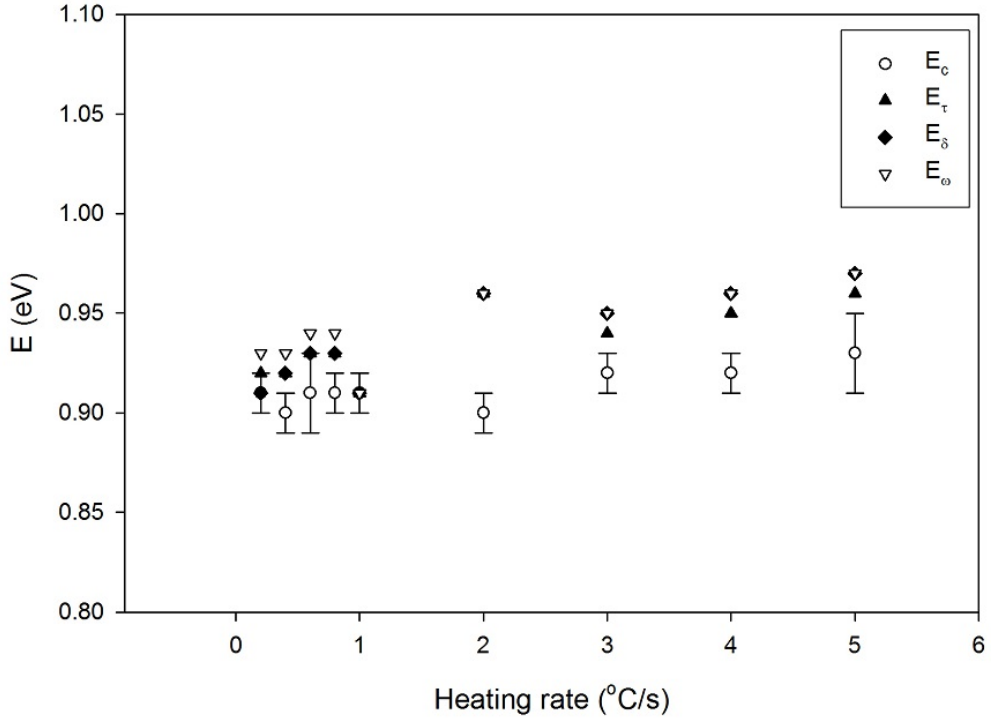

FIGURE 5.17: Dependence of the activation energy E on the heating rate. E_c is the activation energy found from curve fitting. These results were obtained from a sample irradiated to 123 Gy for each measurement.

The values of the activation energy E obtained from curve fitting varie from 0.91 ± 0.01 to 0.93 ± 0.02 eV (see Table 5.1). As shown in Figure 5.17, the values of activation energy given by E_τ, E_δ and E_ω are in good agreement with the values of the activation energy generated by curve fitting. The PS method is susceptible to error because of subjectivity in choosing the points to use.

5.1.3.3 The whole curve method

The whole curve method (WCM) was also used to determine the activation energy E and the order of kinetics b of the main peak. As described in section 3.5, a series of lines of $\ln(TL/n^b)$ versus $1/kT$ were plotted for a range of b values and the desired values of E and b were retained from the best straight line. Figure 5.18 shows the lines obtained for the main peak for b taking values 0.9, 1.0, 1.1, 1.2 and 1.3 respectively.

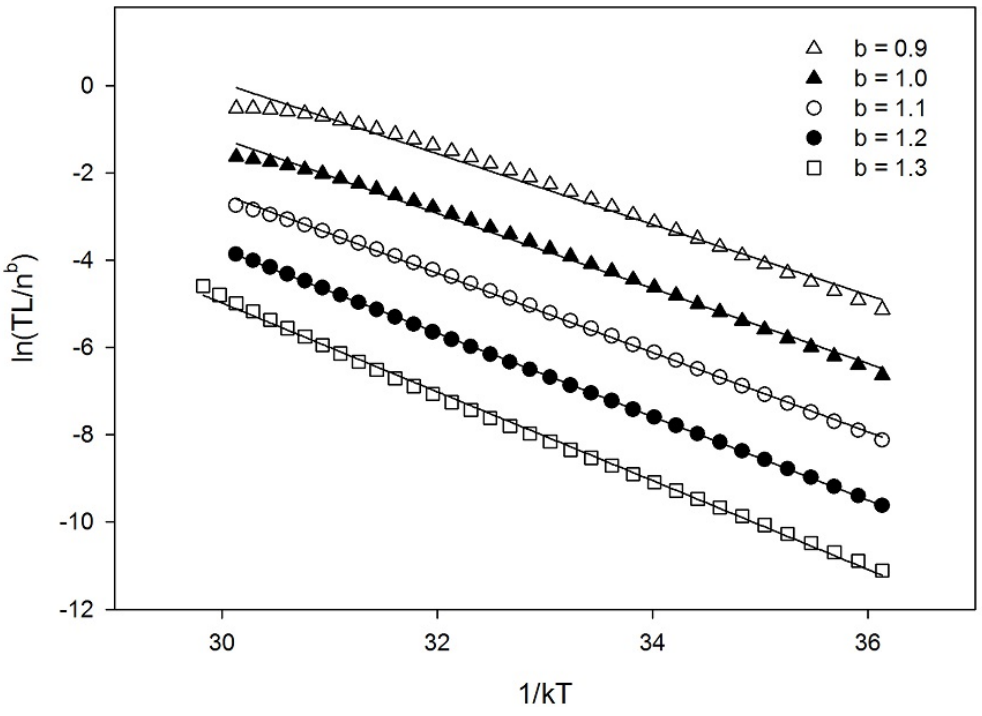

FIGURE 5.18: Plots used to determine the activation energy E and the order of kinetics b of the main TL peak of the unannealed sample. The glow curve onto which this method is applied was recorded from a sample irradiated to 10 Gy and heated at 5.0 °C/s as shown in Figure 5.4.

In Figure 5.18, the best straight line corresponds to $b = 1.2$ and the associated value of E is 0.96 ± 0.01 eV with $R^2 = 0.9996$. These values of E and b are consistent and in agreement with those derived from curve fitting and the PS method.

5.1.3.4 The IR analysis

The IR method was applied to the TL glow curves obtained from the study of the influence of repeated measurements as an independent way of evaluating the activation energy E of the main TL peak. The glow curves measured from the sample heated at the rate of 5.0 °C/s after irradiation to 10 Gy were used. Data in the initial rise part (5% to 15% of peak intensity) of the main TL peak were used to determine its activation energy E. A plot of $\ln(I)$ versus $1/kT$ is expected to yield a straight line with slope $-E$ in the initial rise part a the glow peak. Figure 5.19 is an example of such a plot made for evaluating E from the first of the sequence of the ten repeated TL measurements described in 5.1.1.2.

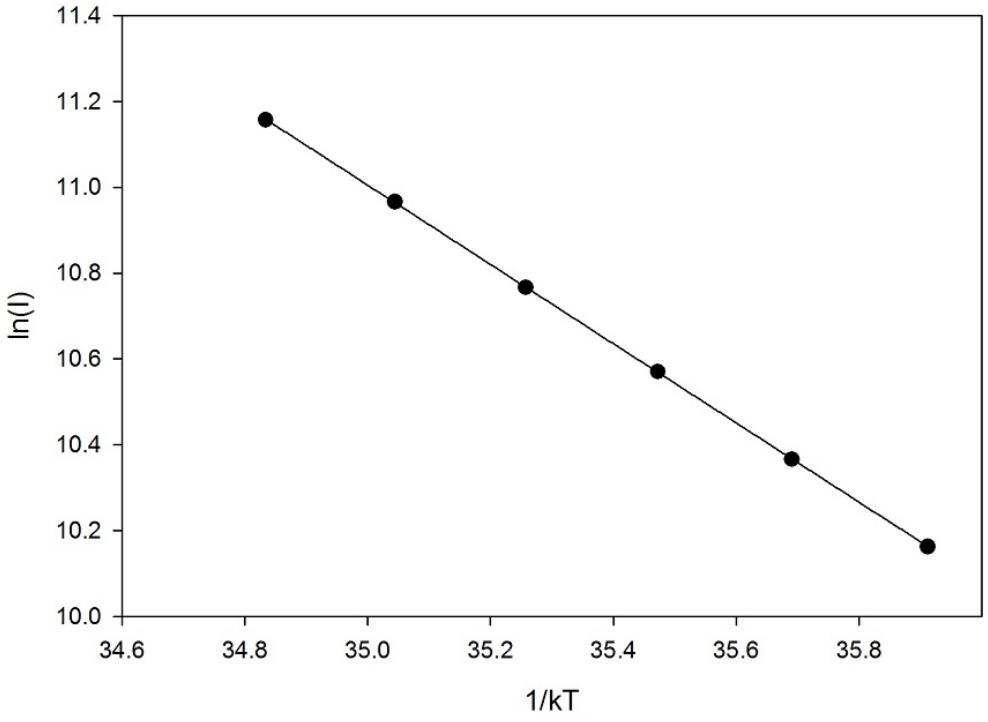

FIGURE 5.19: Example of a plot used to determine the activation energy E for the main TL peak. The original glow curve was measured at a heating rate of 5.0 °C/s after irradiation to 10 Gy.

Having fitted a straight line to the data shown in Figure 5.19, the activation energy was found as $E = 0.92 \pm 0.02$ eV with a regression square value, $R^2 = 0.9999$. Similarly, the activation energy was obtained for the remaining TL glow curves. The influence of repetitive measurement on the activation energy of the main TL peak is shown in Figure 5.20.

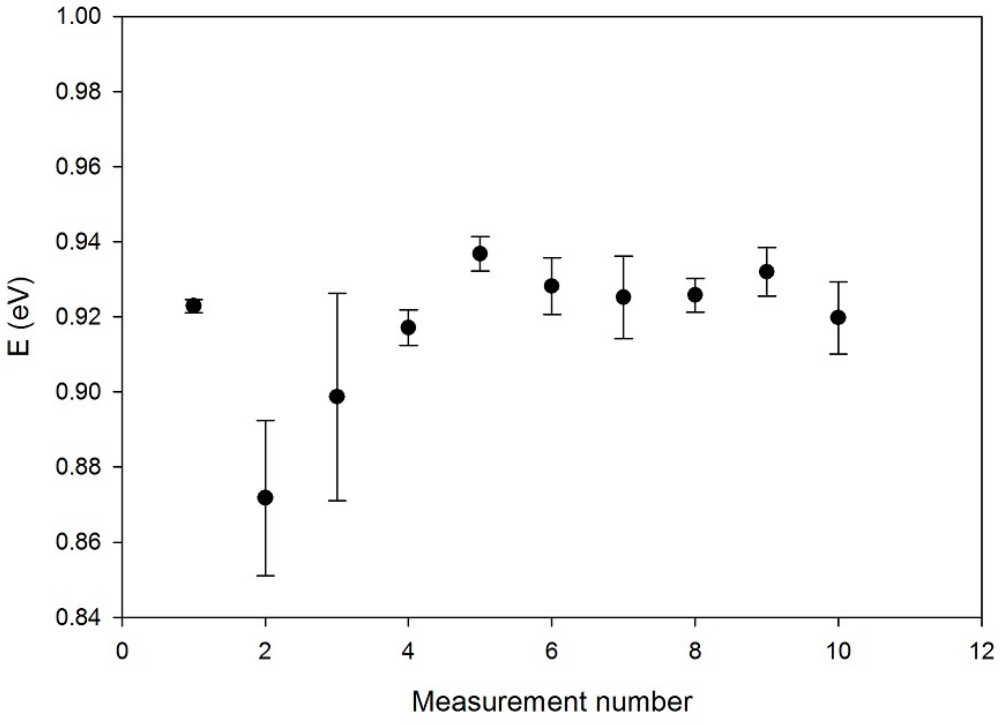

FIGURE 5.20: Influence of repetitive measurement on the activation energy E of the main TL peak for a sequence of ten TL measurements made on a sample irradiated to 10 Gy and heated at 5.0 °C/s.

By averaging all the values of E, we found $E_{avg} = 0.92 \pm 0.01$ eV. As seen in Figure 5.20, the error bars associated with the various E overlap. Hence, the influence of repetitive measurement on the activation energy E of the main peak is minimal. In addition, E_{avg} which is computed from a completely different set of data, obtained under different conditions (i.e., irradiation dose and heating rate), is in good agreement with the values of E found from curve fitting and PS method presented so far.

5.1.3.5 Various heating rate analysis

Various heating rate (VHR) methods exploit the shift in peak position with the change in heating rate to evaluate the trapping parameters E, s and b. For the VHR experiment, heating rates ranging from 0.2 to 5.0 °C/s were used. Starting with a fresh sample, the natural TL signal was measured before any further TL measurements. Each TL measurement was then taken at a different heating rate following irradiation to 123 Gy. Figure 5.21 shows the effect of variable heating rate on the position of the main TL peak.

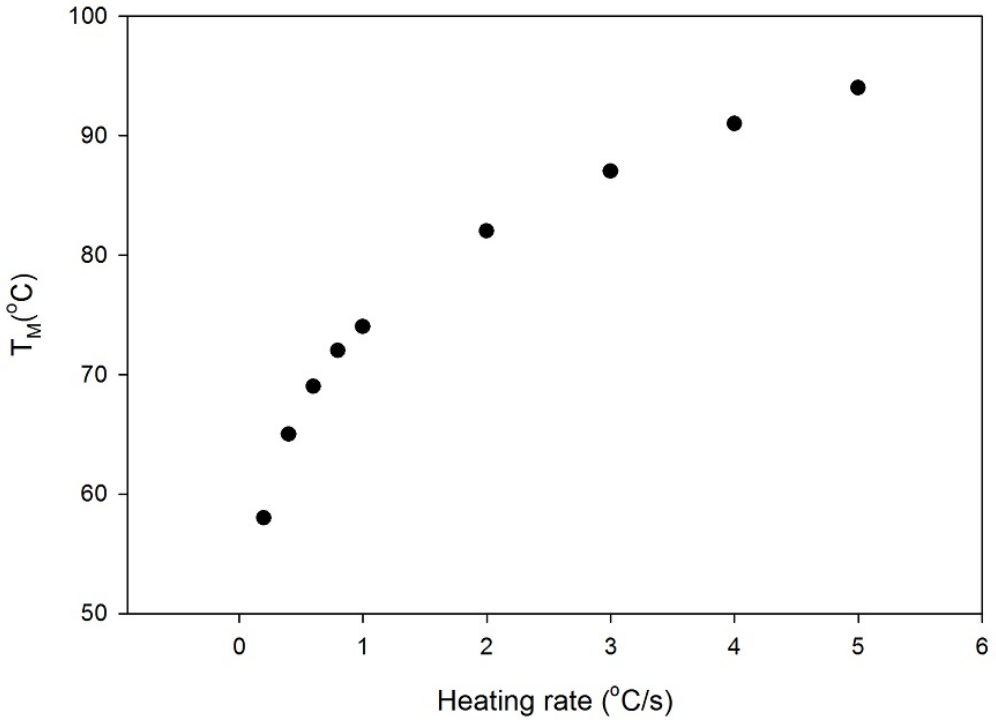

FIGURE 5.21: Shift in peak temperature with the increase in heating rate for the main TL peak.

From Figure 5.21, it is evident that the peak temperature T_M shifts to higher value with the increase in heating rate. For any two consecutive heating rates, the shift in peak temperature depends on the difference between the two rates in question. At lower heating rates, that is heating rates ranging from 0.4 to 1.0 °C/s, the shift in peak temperature is small compared with the shift at higher heating rates. This shift in peak temperature is consistent with the various formulae [4] stating the condition for maximum TL emission. This shift in peak temperature is accompanied by a decrease in peak intensity which is due to thermal quenching [45, 46]. A thermal quenching analysis [10] was therefore needed to determine the quenching parameters for the main TL peak.

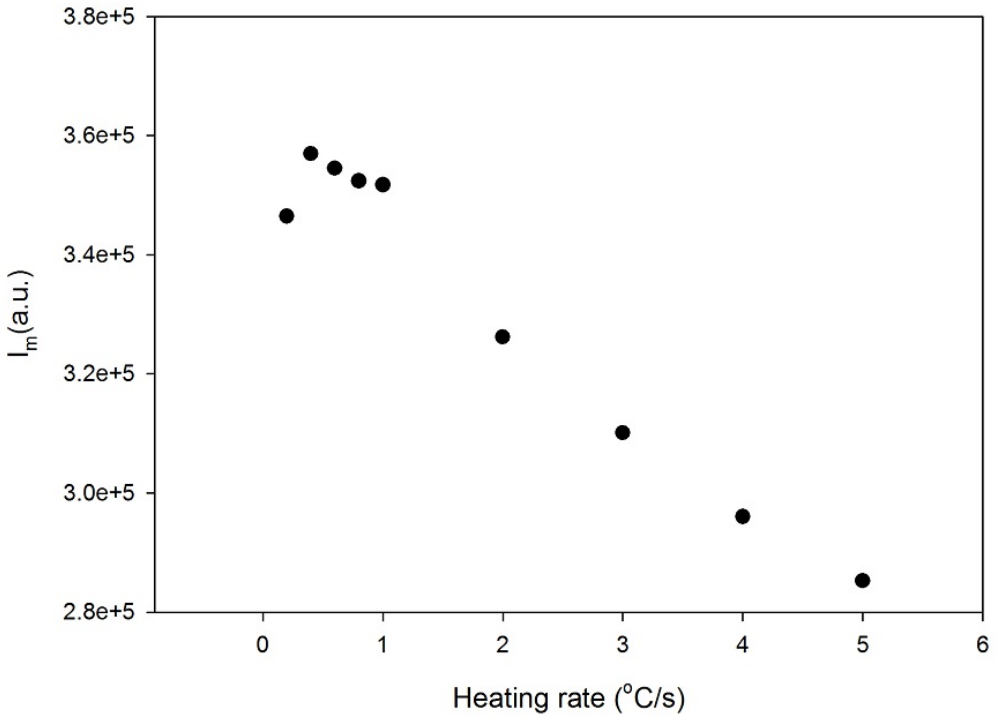

FIGURE 5.22: Influence of the heating rate on the intensity of the main TL peak for a dose of 123 Gy. The peak intensity is given in arbitrary units.

Table 5.3 shows the values of the activation energy E computed from equation (3.9). From Table 5.3, it is clear that the value of E depends on the choice of the pairs

TABLE 5.3: Estimates of E given by the Booth [28] method (equation (3.9))

$T_{M_1}(K)$	$T_{M_2}(K)$	E (eV)
331.15	338.15	0.92
364.15	367.15	0.79
331.15	367.15	0.88

(T_{M_1}, I_{M_1}) and (T_{M_2}, I_{M_2}). Therefore, values of E obtained from equations (3.9) can only be used as first estimates since there is no general rule concerning the choice of (T_{M_1}, I_{M_1}) and (T_{M_2}, I_{M_2}). The method suggested by Hoogenstraaten [29] and later extended to general-order kinetics by Chen and Winer [30] was also used to evaluate the activation energy E of the main TL peak. Figure 5.23 shows the plot of $\ln(T_M^2/\beta)$ as a function of $1/kT_M$.

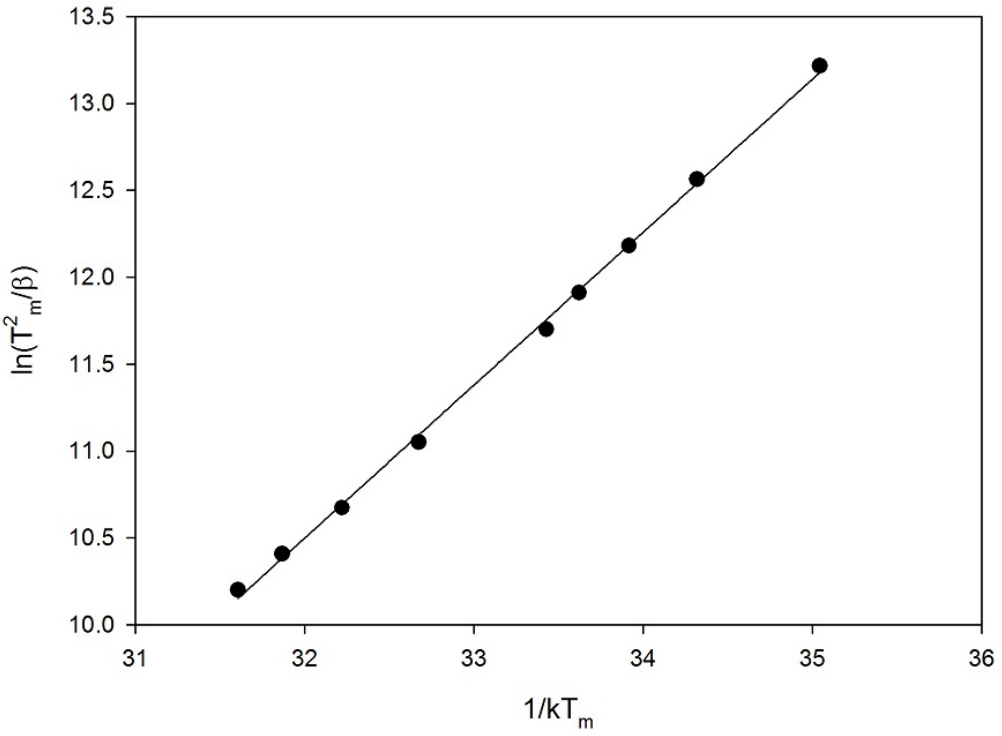

FIGURE 5.23: Plot of $\ln(T_M^2/\beta)$ as a function of $1/kT_M$ used to determine E and s.

From this plot, the activation energy E was found to be 0.88 ± 0.01 eV with $R^2 = 0.9987$. The value of E thus found was then substituted into $\ln(sk/E)$ to get the frequency factor $s = 4.8 \times 10^{12}$ s^{-1}. The value of E derived from the Hoogenstraaten [29] method is comparable to the value of 0.92 ± 0.01 eV obtained from the IR method and the values obtained from curve fitting and the PS method (see Table 5.1 and Table 5.2). However, it should be pointed out that the value of E reported here is smaller than the values of E derived from the other three methods. In their study of anomalous heating rate effects on TL intensity, using a simplified version of the semi-localised transition model of Mandowski [47], Pagonis et al. [48], showed that the VHR method can underestimate the activation energy E of a TL peak. In the present work, the value of E derived from the VHR method is lower than those obtained from the other methods. The value of the frequency factor s is of the same order of magnitude as the values of s derived from curve fitting (see Table 5.1).

The decrease in the intensity of the main peak with heating rate, as shown in Figure 5.22, is an indication of thermal quenching. The peak integral or area, I_{Que}, under

the quenched peak is defined by

$$I_{Que} = \eta(T)\, I_{Un} \tag{5.1}$$

where I_{Un} is the unquenched peak integral and $\eta(T)$ is the luminescence efficiency [10]. In practice, $\eta(T)$ is approximated to $\eta(T_M)$, the value at peak maximum. The quenching efficiency $\eta(T_M)$ is expressed as

$$\eta(T_M) = \frac{1}{1 + C\, \exp(-W/kT_M)}, \tag{5.2}$$

where C is a dimensionless constant, W is the activation energy of thermal quenching and k is Boltzmann's constant. Therefore, the quenching parameters C and W can be obtained from a plot of $\ln((\frac{I_{Un}}{I_{Que}}) - 1)$ against $1/kT_M$. Figure 5.24 shows the plot used to determine the quenching parameters C and W for the main TL peak of the unannealed sample.

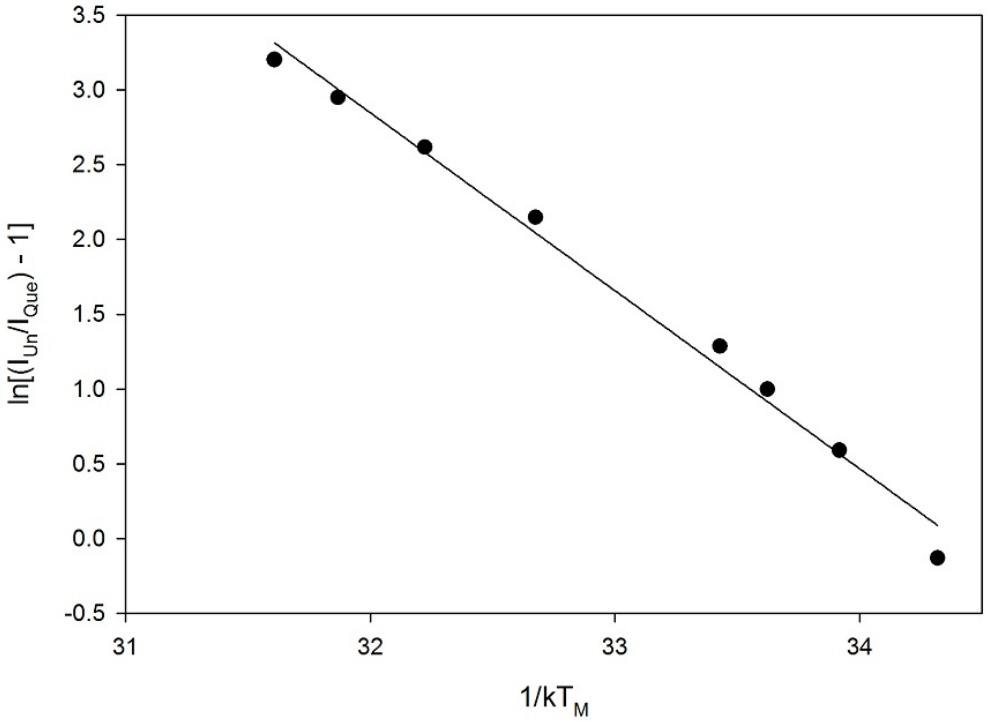

FIGURE 5.24: A plot of $\ln((\frac{I_{Un}}{I_{Que}}) - 1)$ against $1/kT_M$ for the main peak used to determine the quenching parameters W and C.

The activation energy of thermal quenching derived from the fit shown in Figure 5.24 was 1.20 ± 0.05 eV and the constant C was 5.9×10^{17}. Wintle [46] reported the quenching parameters $W = 0.64$ eV, and $C = 2.8 \times 10^7$ for radioluminescence emission spectra

centred at 465 nm. Nanjundaswamy et al. [45] cited values similar to those of Wintle (e.g., $W = 0.636$ eV, $C = 7.9 \times 10^6$). Similar values, obtained from the studied of luminescence lifetimes using time-resolved OSL are reported in Table 1 of Chithambo and Galloway [42]. The parameters W and C obtained in the present work are however larger than those cited here. The difference could be attributed to multiple reasons. One such reason is that the experimental conditions (e.g., transmission filter, irradiation source) and the method of investigations (e.g., TL, OSL, RL) are different. Hence, the value of W reported here could be associated to a recombination centre different from the one involved in the other studies. In addition as pointed out by Chithambo [49], the value of W depends on the emission wavelength of the luminescence. However it is more likely that the discrepancy between the value of W obtained in this work and those reported elsewhere is due to the use of $\eta(T_M)$ rather that $\eta(T)$.

5.1.3.6 Isothermal analysis

In addition to the methods discussed so far, isothermal analysis was used as yet another way of independently computing the trapping parameters of the main TL peak. The isothermal decay experiment consisted of four steps. In the first step, the natural TL signal was measured at a heating rate of 5.0 °C/s. Having measured the natural TL, the sample was irradiated to 123 Gy. Following the irradiation step, the TL was read out from room temperature up to 500 °C at the same heating rate of 5.0 °C/s and the position of the main TL peak was noted. This step was necessary to select the range of temperatures at which the isotherms could be measured. At this point, the sample was freshly irradiated to 123 Gy, preheated and held at a temperature T_i for some time t during which the TL signal was taken. The TL signal obtained at this stage decays with time so it is referred to as an isothermal decay curve. The final step consisted of recording a further TL glow curve up to 500 °C to ensure that there is no residual signal left before the next measurement. For subsequent measurements, only the three last steps were repeated namely; a fresh irradiation to 123 Gy, heating to a new temperature T_{i+1} at which a new isotherm was recorded and the subsequent TL taken up to 500 °C. All isothermal decay curves were measured for 150 seconds. The first TL, taken directly after the natural TL, had the main TL peak at 102 °C and for that reason, the isothermal decay curves were measured at 60, 66, 72, 78 and 84 °C respectively. The isotherm obtained at a temperature of 60 °C is shown in Figure 5.25 with the single exponential decay function described in equation (3.22) fitted to it.

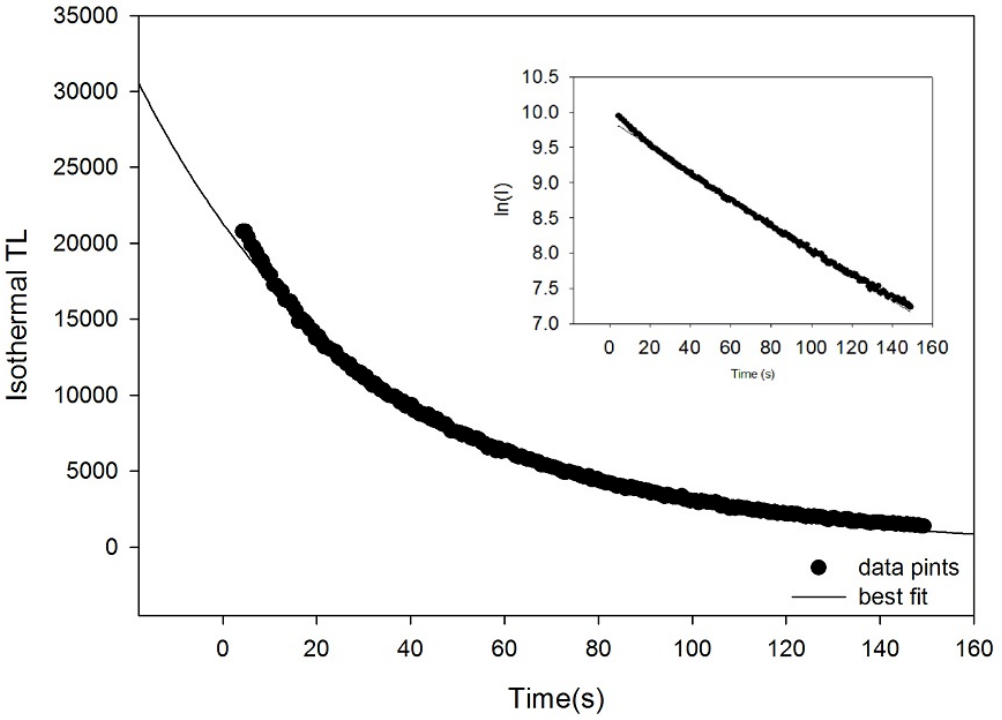

FIGURE 5.25: Isothermal decay curve obtained at 60 °C shown with a single exponential function fitted to it. The inset shows a plot of $\ln(I)$ against time. Such a plot is used to test if the decay curve can indeed be described by an exponential function.

To estimate the order of kinetics b, a series of plots of $(\frac{I}{I_0})^{\frac{1-b}{b}}$ versus time t were made for values of b ranging from 0.9 to 2.3 and the value of b which gave the best straight line was retained as the order of kinetics. I and I_0 are the isothermal intensity at time t and t_0 respectively. Figure 5.26 shows the lines obtained for the isothermal decay curve measured at 60 °C with b taking the values 1.1, 1.2 and 1.3 respectively. The best straight line found corresponds to $b = 1.2$ with $R^2 = 0.9996$.

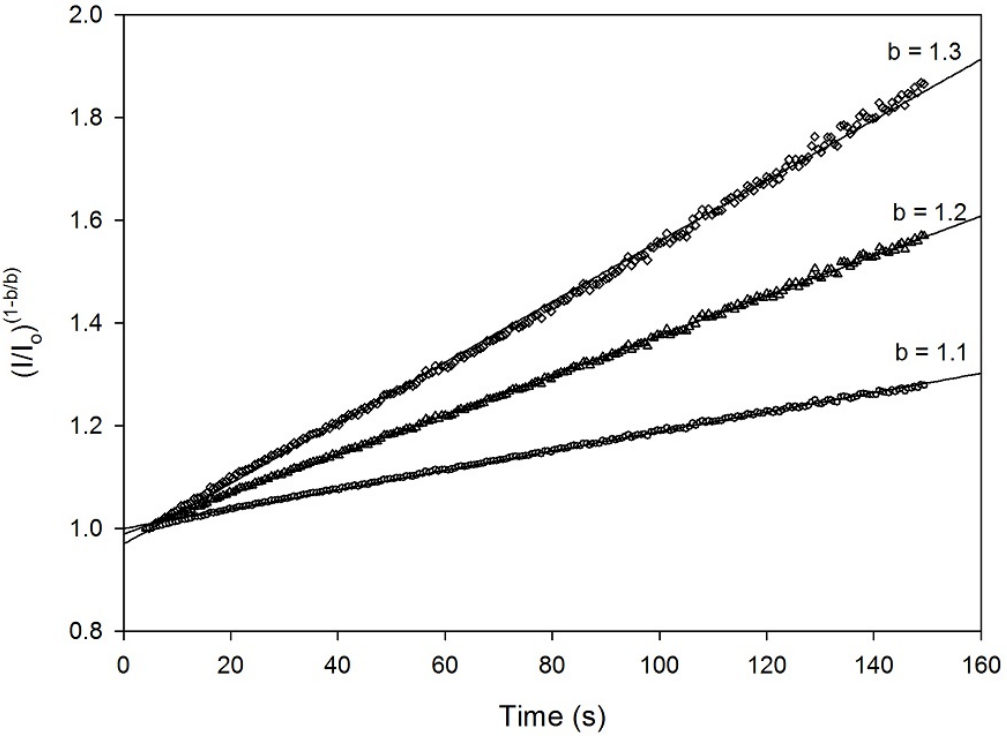

FIGURE 5.26: plots of $(\frac{I}{I_0})^{\frac{1-b}{b}}$ versus t for the isothermal at 60 °C and b taking values 1.1, 1.2 and 1.3. The best straight line corresponds to $b = 1.2$.

5.1.3.7 TL-like phosphorescence analysis

Randall and Wilkins [9] suggested that kinetic features of a glow peak could also be studied from the isothermal decay curves by first transforming them into TL-like curves. As suggested by Randall and Wilkins [9], we plotted It against $\ln(t)$ where I is the isothermal TL intensity at time t. The resulting curves had a structure similar to that of TL glow curves. Figure 5.27 shows the TL-like curves obtained for the isotherms recorded at 60 and 66 °C respectively.

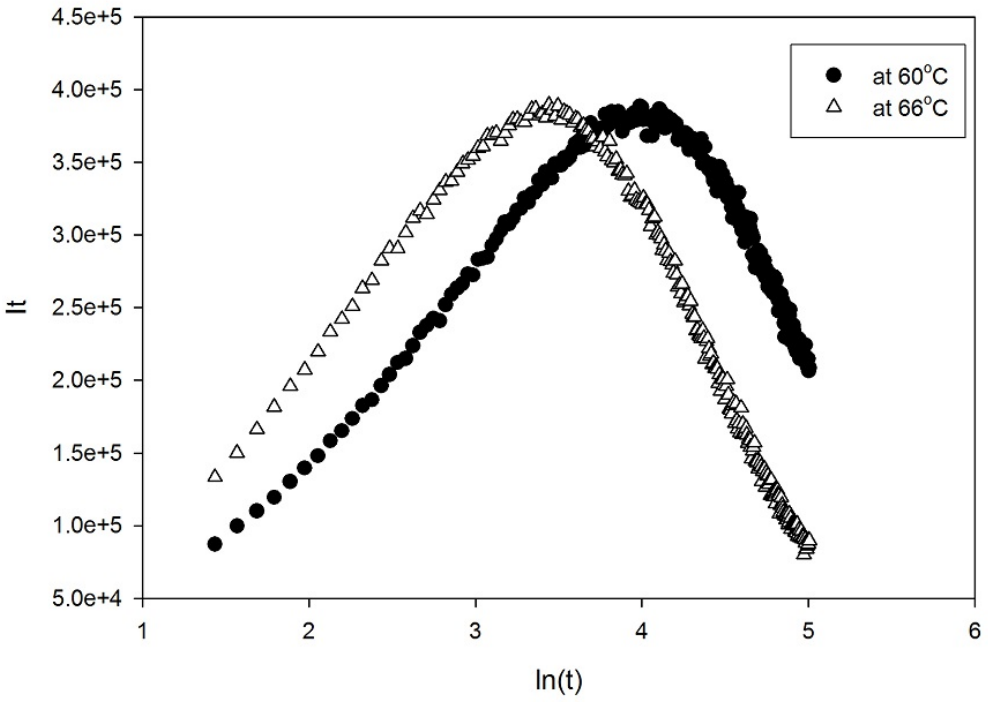

FIGURE 5.27: TL-like curves for isotherms measured at 60 and 66°C respectively.

Figure 5.27 shows that the peak of the TL-like phosphorescence curve shifts with temperature. For isotherms measured at higher temperatures, we noticed the same shift in the corresponding TL-like curves. As discussed by Chen and McKeever [4], this shift in peak position can be used to determine the activation energy E of the TL peak. In the case of first-order kinetics, It yields

$$It = sn_0 t \exp(-E_t/kT) \exp[-st \exp(-E_t/kT)], \tag{5.3}$$

where all the terms have their usual meaning. Defining $x = ln(t)$, and $y = It$, equation (5.3) becomes

$$y = (n_0/\gamma) \exp(x) \exp[-\exp(x)/\gamma], \tag{5.4}$$

with $\gamma = s^{-1} \exp(E_t/kT)$. Taking the derivative of y with respect to x and equating the result to zero, we obtain

$$\exp(x_{max}) = \gamma. \tag{5.5}$$

Hence by the definition of x, $t_{max} = \gamma$. For two TL-like curves obtained from isotherms measured at temperatures T_1 and T_2 with respective maximum at $\ln \gamma_1$ and $\ln \gamma_2$, the

shift in maxima is defined as

$$\Delta = \ln \gamma_2 - \ln \gamma_1 = (E_t/k)(1/T_2 - 1/T_1). \tag{5.6}$$

From the two curves shown in Figure 5.27, the value of E_t obtained from equation (5.6) was 0.89 eV. In this particular case, the temperature difference between T_1 and T_2 is 6 °C. The calculations were repeated using temperatures T_1 and T_2 which yield larger temperature differences to check, if there was any correlation between the shift in temperatures and the activation energy E_t. The results are summarised in Table 5.4.

TABLE 5.4: Values of E_t obtained from TL-like curves corresponding to isotherms at different temperatures.

T_1(°C)	T_2(°C)	ΔT(°C)	E_t (eV)
60	66	6	0.89
66	72	6	0.87
72	78	6	1.04
78	84	6	0.78
60	72	12	0.88
66	78	12	0.97
72	84	12	0.92
60	78	18	0.93
66	84	18	0.90

TABLE 5.5: Average value of E_t for a given shift in temperature.

ΔT (°C)	E_{avg} (eV)
6	0.89
12	0.92
18	0.91

For each shift in temperature, the average value of E_t, given in Table 5.5, are in good agreement with the values of E found from the previous methods (see Table 5.1 and Table 5.2).

5.1.4 Dosimetric features

5.1.4.1 Dose dependence of the main peak

To study the influence of irradiation dose on the main TL peak, glow curves were measured on a fresh sample for doses between 2 and 151 Gy. The natural TL signal was initially read out from the sample at a rate of 5.0 °C/s before exposure to the irradiation source. If the natural TL is not measured first, the dose response will be affected by

the natural dose. For each subsequent TL measurement, the sample was then irradiated for some time t and the glow curve was recorded by heating at the same rate of 5.0 °C/s. The background signal was taken after each TL measurement and subtracted accordingly during analysis. Knowing the exposure time t for each measurement, the corresponding dose was calculated as the product $t \times d_r$ where d_r is the dose rate (0.1028 Gy/s). Figure 5.28 shows the influence of irradiation dose on the temperature T_M of the main peak. It is evident that the temperature of the main peak is not affected by the dose, which is a characteristic of first-order glow peaks [2, 4]. This result therefore implies that the main TL peak is a first-order peak which is consistent with the results presented earlier in this section.

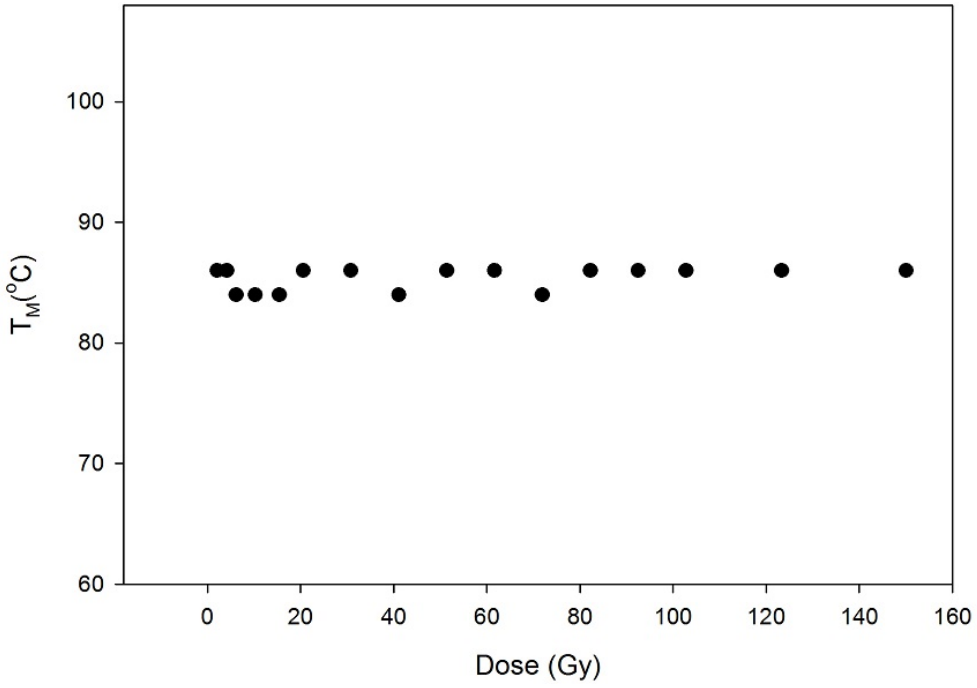

FIGURE 5.28: Influence of irradiation dose on the temperature T_M of the main TL peak for doses between 2 and 151 Gy and a heating rate of 5.0 °C/s.

Figure 5.29 shows the influence of irradiation dose on the intensity of the main TL peak. For low doses, typically between 2 and 10 Gy, the dose response of the peak is linear. In the intermediate dose range from 10 to 60 Gy, the growth of the main peak is sub-linear and for doses greater than 60 Gy, the peak has a linear dose response. This dependence of the main TL peak on the irradiation dose could be described by the function

$$S(D) = A\,(1 - \exp(-d\,D)) + c\,D, \tag{5.7}$$

where $S(D)$ is the peak intensity for some dose D ranging from 2 to 151 Gy; A, d and c are all positive numbers. For the fit shown in Figure 5.29, we found $A = 18919.16$, $d = 0.0666$ and $c = 35.90$. Since $S(D)$ is in arbitrary units, d and c must be in arbitrary units/Gy.

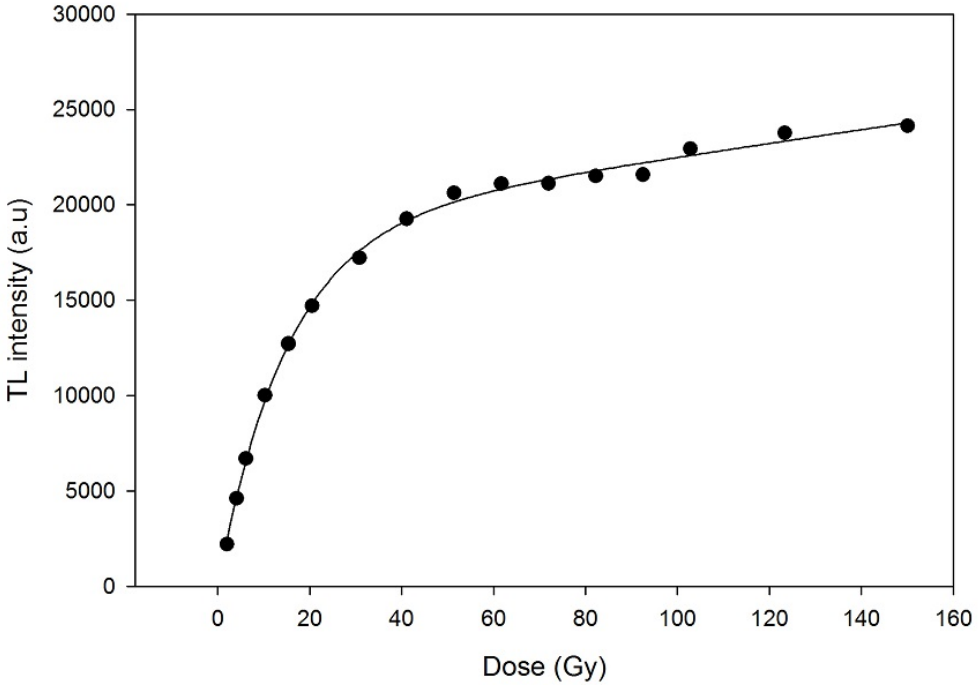

FIGURE 5.29: Influence of the irradiation dose on the main TL peak for a series of measurements made at 5.0 °C/s on a sample irradiated to doses between 2 and 151 Gy. The solid line is the fit obtained from equation (5.7).

For a quantitative description of the dose response of the main peak, we computed the super-linearity function $g(D)$ as

$$g(D) = \frac{D\,S"(D)}{S'(D)} + 1 \tag{5.8}$$

where S' and $S"$ are the first and second derivatives of the dose response function $S(D)$. By definition, the dose response of a TL peak is linear if the super-linearity index $g(D) = 1$, sub-linear if $g(D) < 1$ and super-linear if $g(D) > 1$ [4]. Figure 5.30 shows the behaviour of the super-linearity index g for the main peak as a function of the dose.

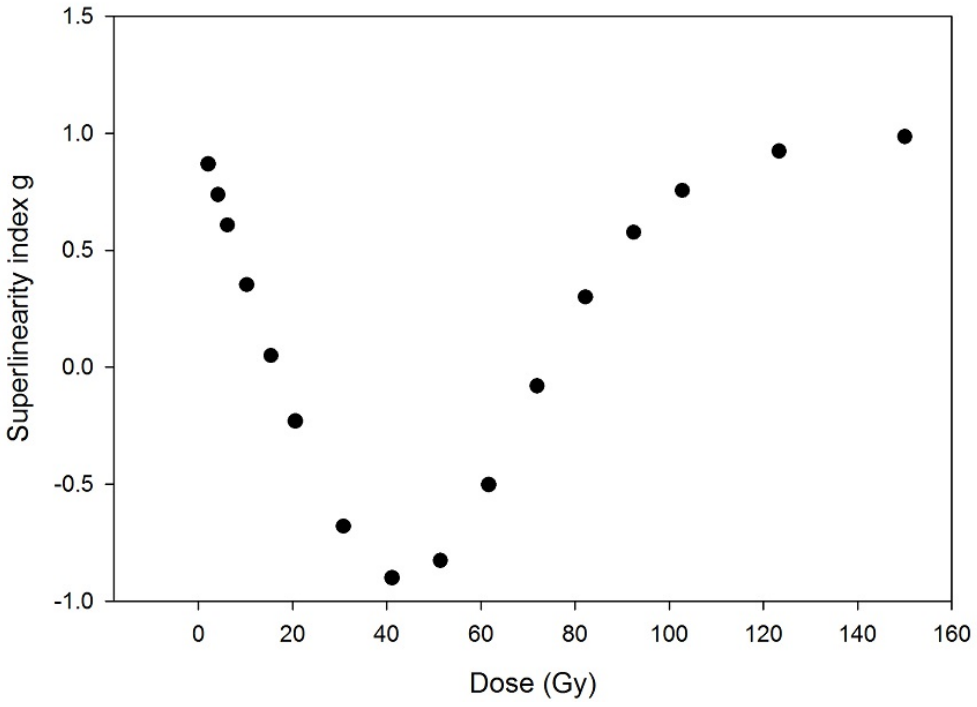

FIGURE 5.30: Super-linearity index g describing the dose dependence of the main peak. The sample was heated at 5.0 °C/s for each measurement.

As shown in Figure 5.30, $g(D) < 1$ for all doses D in the range from 2 to 151 Gy. Hence by the definition of g, the dose response of the main peak is sub-linear. The analysis with the super-linearity index does not render the qualitative description invalid because the deviation from linearity is with respect to the initial region from 2 to 10 Gy.

The IR method was used to evaluate the activation energy E of the main peak for each of the TL glow curves measured at various doses. Figure 5.31 is a plot of the activation energy E of the main TL peak against the irradiation dose.

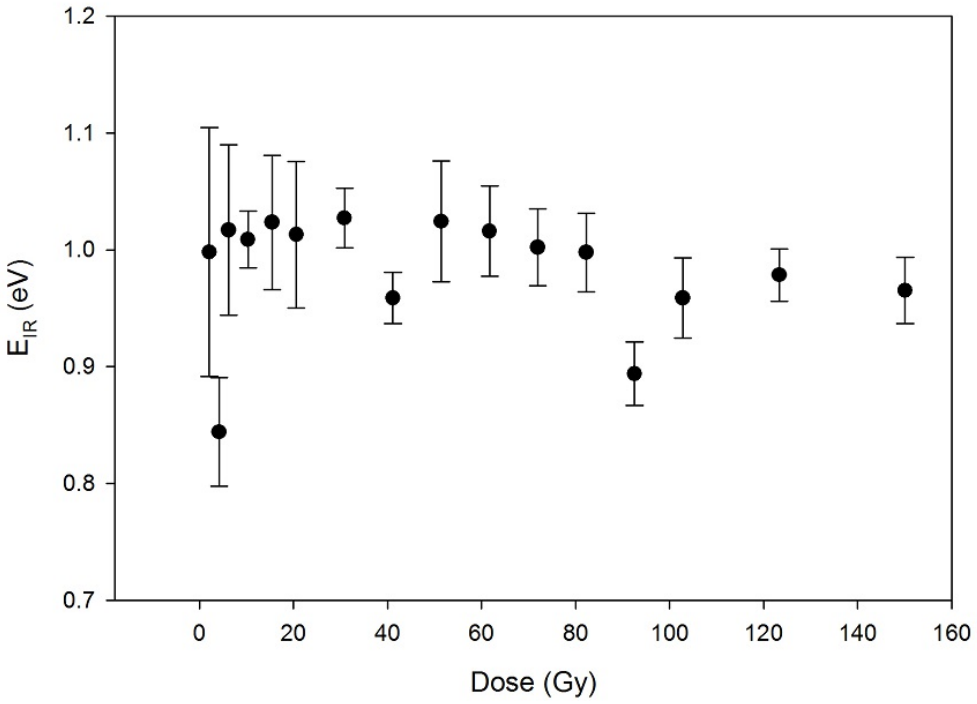

FIGURE 5.31: Influence of the irradiation dose on the activation energy E of the main peak

As depicted in Figure 5.31, the influence of irradiation on the activation energy is minimal over the dose range from 2 to 151 Gy. The average value of the activation energy for this dose range is $E_d = 0.99 \pm 0.04$ eV. As the size of the error bars suggests, the values of E corresponding to higher irradiation dose are more precise than those associated with the values of E calculated for lower doses. The intensity of a TL glow peak increases with the irradiation dose as such, the values of calculated from the IR method are more precise.

5.1.4.2 Influence of delayed stimulation on the main peak

The influence of delay between irradiation and TL measurement on the main peak was investigated on a sample irradiated to 93 Gy and heated at 5.0 °C/s. After each irradiation, the heating was delayed for 1, 2, 4 or 6 h respectively. Figure 5.32 shows the glow curve measured after a 6 h delay.

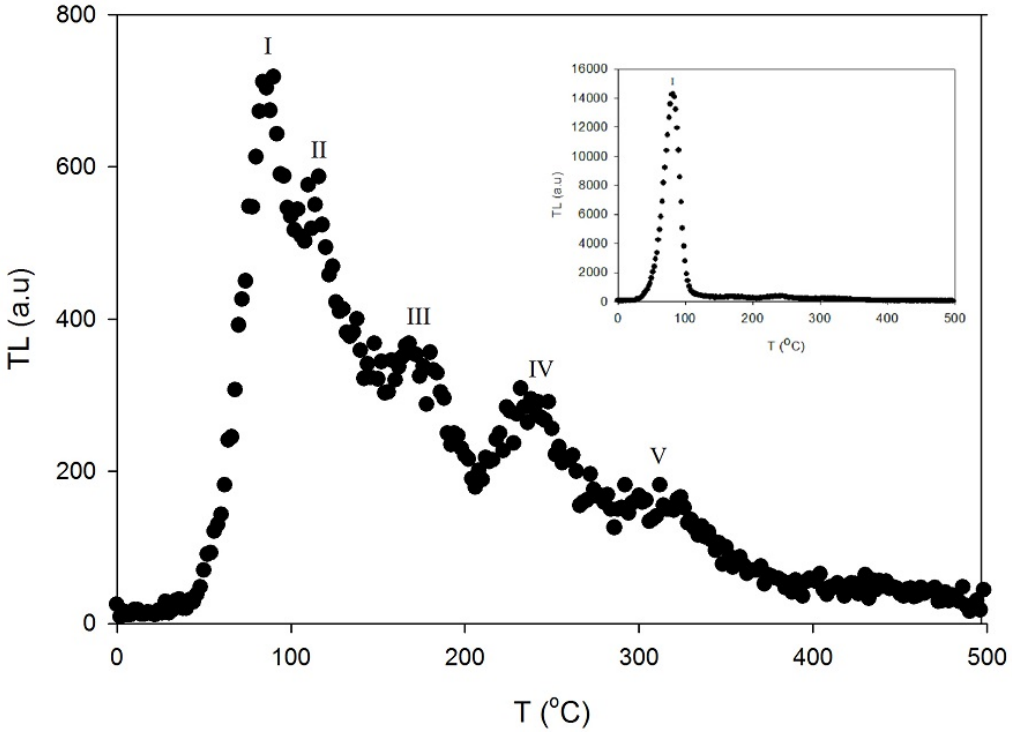

FIGURE 5.32: TL glow curve taken at a heating rate of 5.0 °C/s after a 6 h delay from a sample irradiated to 93 Gy. The TL glow curve measured directly after irradiation is shown in the inset.

The inset in Figure 5.32 shows the glow curve measured directly after irradiation (i.e., without delay). It is evident from this figure that as the main TL peak fades, the other peaks become more apparent. The fading of the main TL peak could be described by a exponential function of the form

$$I(t) = I_0 \exp(-f\,t), \tag{5.9}$$

where I_0 is the initial intensity (i.e., no delay), f is the decay constant and t is the delay time. Figure 5.33 shows the effect of delayed stimulation on the intensity of the main TL peak.

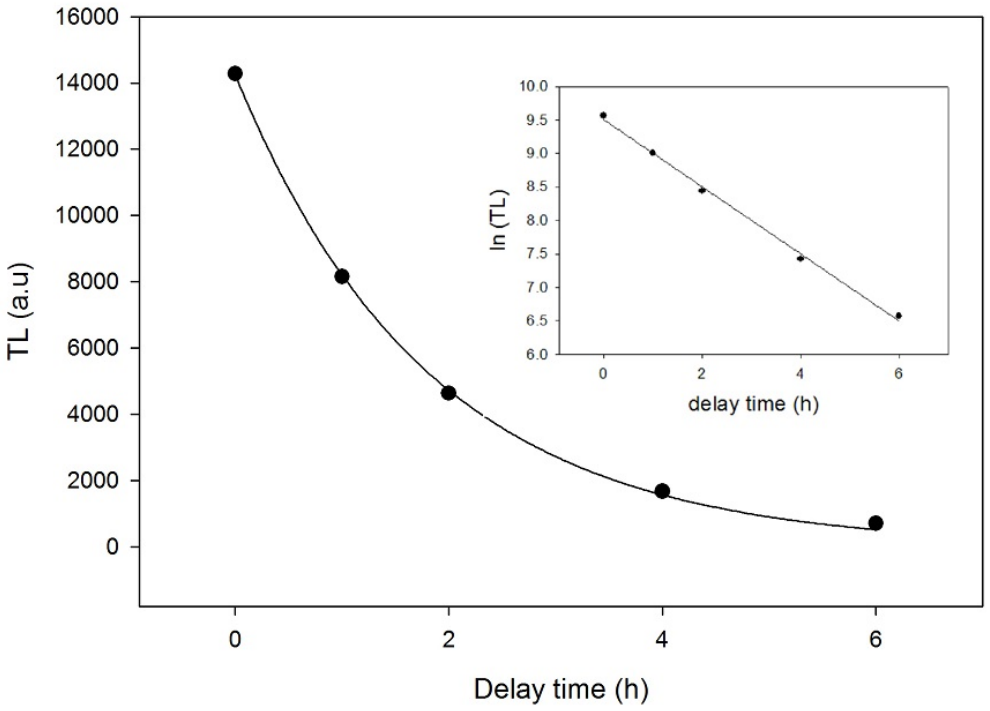

FIGURE 5.33: Influence of delay on the intensity of the main TL peak. For each measurement, the sample was irradiated to 93 Gy and heated at 5.0 °C/s after delay. The solid line is the best fit obtained from equation (5.9). The inset, which shows the plot of $\ln(TL)$ versus delay time confirms the exponential nature of the decay.

The decay constant f obtained from the fit shown in Figure 5.33 is 0.55 h^{-1}. The initial intensity of the main TL peak decreases by approximately 42 % after 1 h and for a 6 h delay, only 5 % of the initial TL intensity is left. The half-life of the peak is given by $\ln(2)/f$. Therefore the half-life of the main TL peak is approximately 1.26 h, which is consistent with the reported values of half-life for the main TL peak of quartz. Aitken [50] reported values of half-life between 1 and 2 h. Hence, the short half-life of peak I implies that this peak results from the recombination with holes of electrons trapped at shallow traps. In addition, re-trapping at the traps responsible for peak I is negligible, which is valid for a first-order peak. The fading is therefore due to the fact that the shallow traps are unstable at room temperature.

5.1.5 Summary of the kinetics of the main TL peak: unannealed sample

Table 5.6 compares the values of trap depth E and the order of kinetics b of the main TL peak to those published elsewhere. The reader is referred to Table 4 of Preusser et al. [13]

for a listing of typical values of E for the other peaks as well. The methods of analysis are abbreviated as follows: IR (initial rise), VHR (Hoogenstraaten [29] variable heating rate method), CF (curve fitting), IT (isothermal analysis), TLP (TL-like phosphorescence analysis), WCM (whole curve method) and GCD (glow curve deconvolution). The heating rate is abbreviated as HR. As shown in Table 5.6, the values of E and b obtained

TABLE 5.6: Values of the trap depth E and the order of kinetics b for the main TL peak of the unannealed sample

main peak T_M (°C)	HR (°C/s)	E (eV)	b	Method	Reference
72	1.0				Figure 5.3
92	5.0	0.92 ± 0.02		IR	Figure 5.19
58 -> 94	0.2 -> 5.0	0.88 ± 0.01		VHR	Figure 5.23
74	1.0	0.91 ± 0.01	1.01±0.01	CF	Figure 5.15
94	5.0	0.93 ± 0.02	1.08±0.01	CF	Table 5.1
92	5.0	0.96 ± 0.01	1.2	WCM	Figure 5.18
	5.0		1.2	IT	Figure 5.26
		0.92		TLP	Table 5.5
100	5.0	1.02 ± 0.03		PS	Mebhah et al. [51]
		0.92 ± 0.09	1.32 ± 0.09	WCM	Mebhah et al. [51]
		0.97 ± 0.02	1.11 ± 0.08	GCD	Mebhah et al. [51]
		1.00			Kitis et al. [52]

in the present work are consistent and compare favourably to those published elsewhere.

5.2 Kinetic and dosimetric features of the annealed sample

In this section, we report on the results obtained from TL studies on natural quartz annealed at 500 °C for 10 minutes. The aim was to study the effect of annealing on the kinetic and dosimetric features of the main peak in natural quartz.

5.2.1 General features

A preliminary measurement was carried out to observe the effect of annealing on the natural TL signal. In contrast to the unannealed sample, a TL glow curve measured from the annealed sample at a heating rate of 5.0 °C/s prior to irradiation yielded a signal comparable to the background signal. Figure 5.34 shows the signal obtained in this case. Such a result was expected from the annealed sample since annealing empties traps populated from previous irradiation.

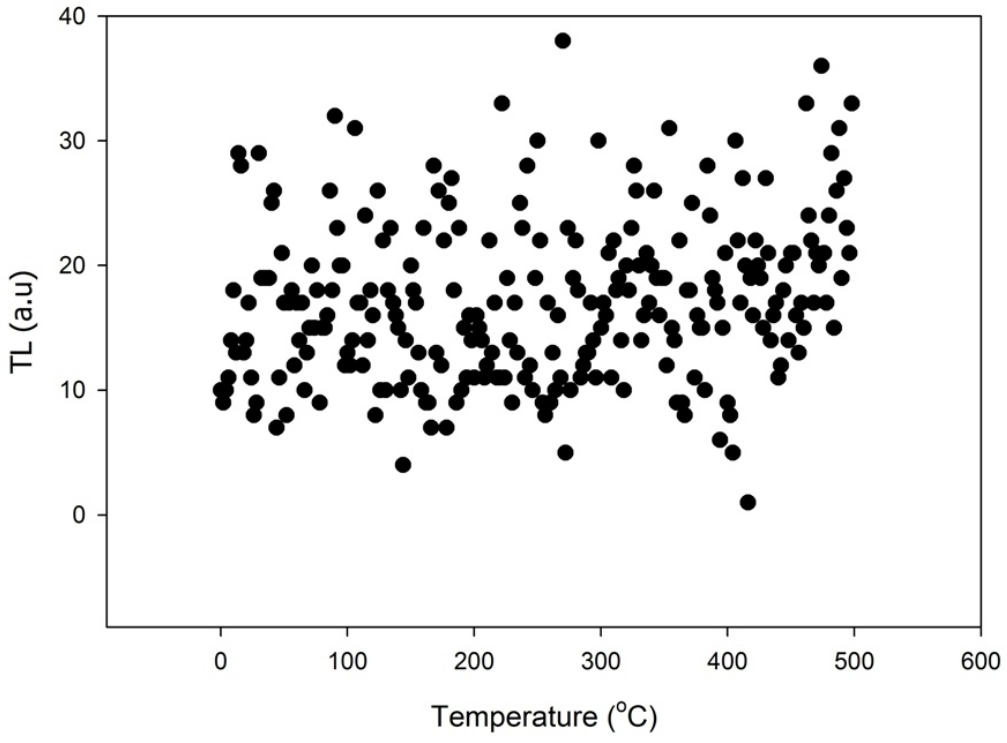

FIGURE 5.34: TL signal measured at heating rate of 5.0 °C/s from the annealed sample prior to irradiation.

Subsequently, the sample was then irradiated to 93 Gy and the TL was read out at the same rate of 5.0 °C/s up to 500 °C. The resulting glow curve is shown in Figure 5.35.

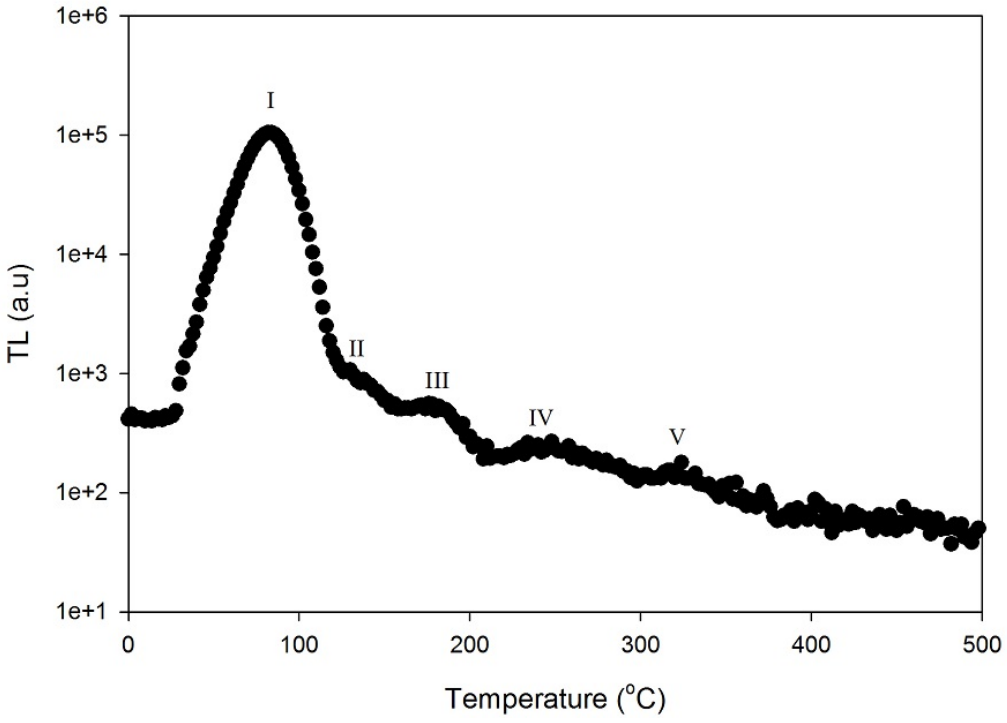

FIGURE 5.35: TL glow curve from annealed natural quartz irradiated to 93 Gy and heated at a rate of 5.0 °C/s.

The glow curve shown in Figure 5.35 has the main peak at 82 °C (peak I) and secondary peaks around 110 °C (peak II), 180 °C (peak III) and 230 °C (peak IV). The high temperature region starting from 200 °C is somewhat complex and further analyses are needed to determine the total number of peaks present in the glow curve. The peak positions reported here are however similar to those found for the unannealed sample.

5.2.1.1 Influence of repeated TL measurements

The influence of repeated measurement on the main TL peak of the annealed sample was investigated to check the peak reproducibility and the effect of sample re-use on the peak intensity. A sequence of ten consecutive TL measurements were performed on the same aliquot. For each measurement, the aliquot was irradiated to 10 Gy and heated at 5.0 °C/s. The background reading was taken and subtracted from each TL measurement during analysis. Figure 5.36 shows that the intensity of the main TL peak increases linearly with repeated measurement. This increase in TL intensity with repeated measurement is probably due to sensitisation [4, 25].

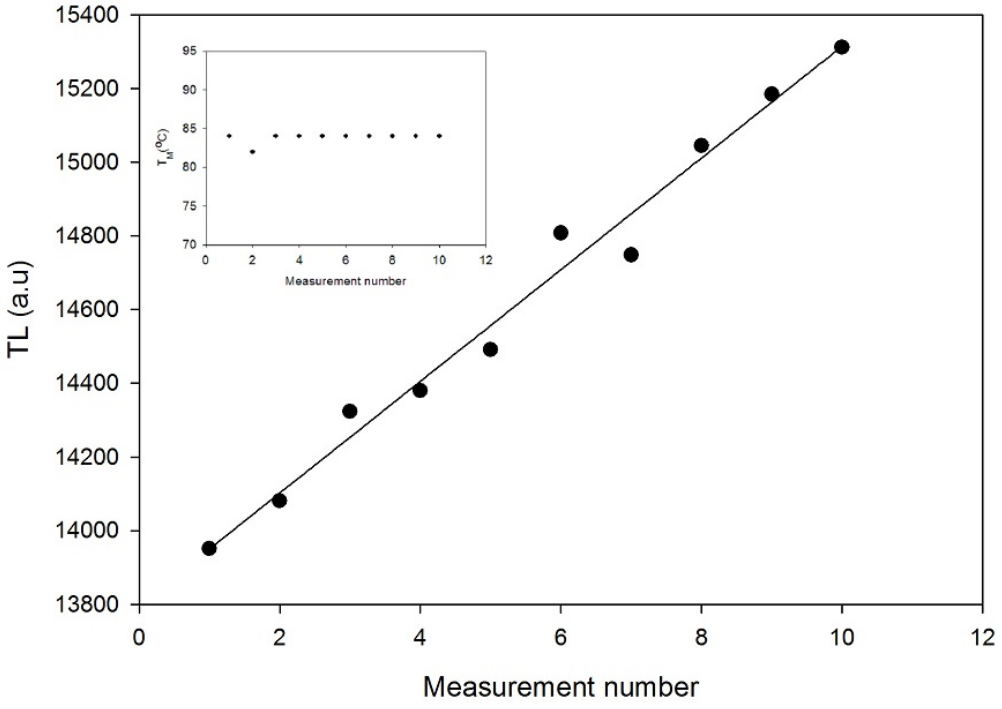

FIGURE 5.36: Influence of repeated measurement on the intensity of the main TL peak for a dose of 10 Gy and a heating rate of 5.0 °C/s.

The inset in Figure 5.36 shows the influence of repetitive measurement on the temperature of the main peak of the annealed sample. The peak position, as shown in the inset, is not affected by sample re-use. Hence, as in the case of the unannealed sample, the position of the main peak is reproducible.

5.2.1.2 T_M - T_{stop} method

The T_M - T_{stop} [2] method, whose aim is to determine the number of peaks in a given glow peak, was applied to the rising edge of the main peak. The experiment was performed on a fresh aliquot of the annealed sample. As in the case of the unannealed sample, an irradiation dose of 93 Gy and a heating rate of 5.0 °C/s were used. The T_{stop} temperature was increased from 40 to 70 °C in steps of 3 °C. Figure 5.37 and Figure 5.38 show the influence of partial heating on the main peak temperature and intensity respectively. The temperature of the main TL peak is essentially independent of the T_{stop} temperature and its intensity decreases with increase in the T_{stop} temperature. These results imply that there is no subsidiary peak on the low temperature side of the main peak and that it is a first-order peak. As mentioned earlier, the decrease in the peak intensity with the

increase in T_{stop} is due to the partial depletion of electrons from the traps associated with the main peak.

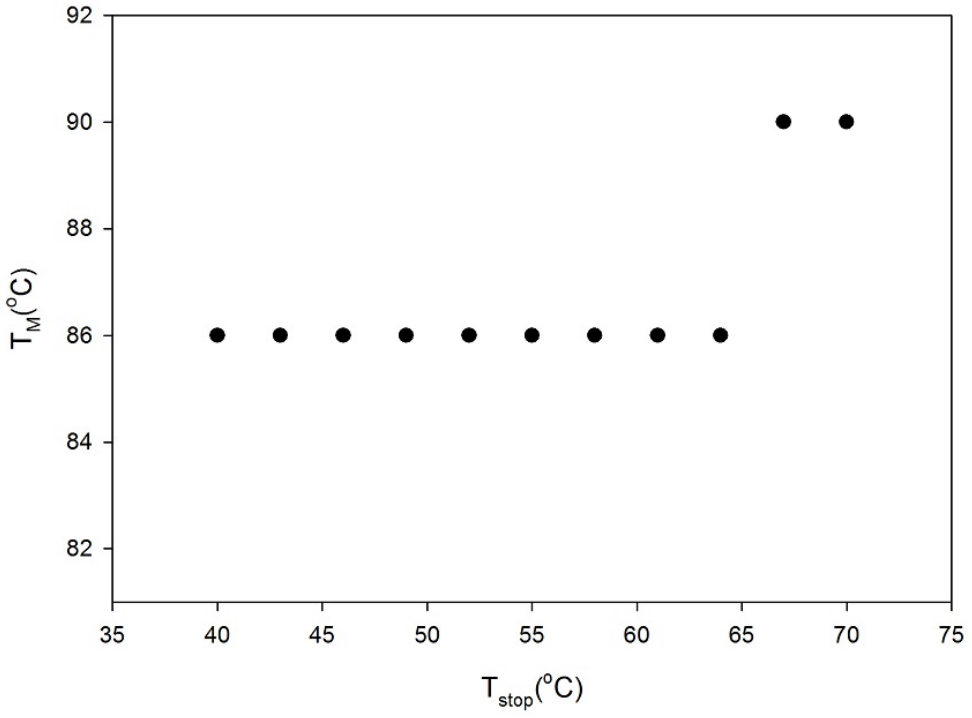

FIGURE 5.37: Dependence of the peak temperature T_M on the T_{stop} temperature for an irradiation dose of 93 Gy and a heating rate of 5.0 °C/s.

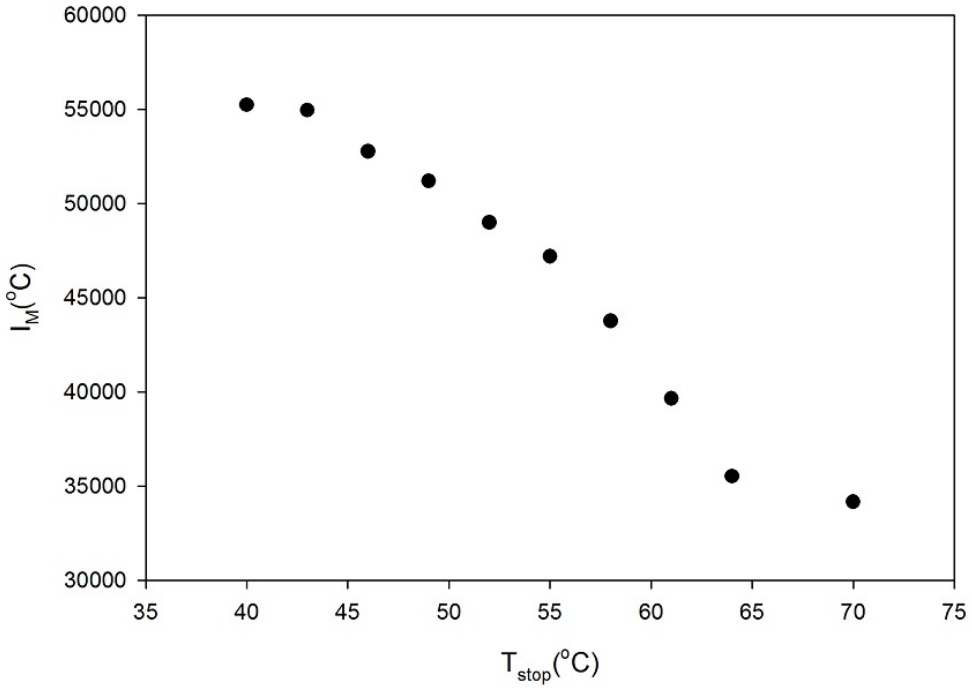

FIGURE 5.38: Dependence of the peak intensity I_M on the T_{stop} temperature for an irradiation dose of 93 Gy and a heating rate of 5.0 °C/s.

5.2.2 Evaluation of the kinetic parameters

5.2.2.1 Curve fitting

An equation consisting of a sum of five general-order terms of the form given by equation (3.33) was fitted to glow curves measured from the annealed sample. A sum of five terms was used because as shown in Figure 5.35, a glow curve measured from the annealed sample shows at least five visible peaks. The fitting was performed with the commercial software Sigmaplot (Systat Software, San Jose, CA). Figure 5.39 shows the experimental glow curve and the generated fit for a sample irradiated to 93 Gy and heated at 5.0 °C/s. The fit is shown as the solid line through the data points. The kinetic parameters obtained for the main peak from the fit in Figure 5.39 were $E = 1.00 \pm 0.01$ eV and $b = 1.09 \pm 0.01$. Given these values of E and b, the frequency factor s was calculated from equation (3.6) to be $3.60 \times 10^{13}\ s^{-1}$. The figure of merit (FOM) and the coefficient of regression R^2 were 1.6% and 0.9998 respectively.

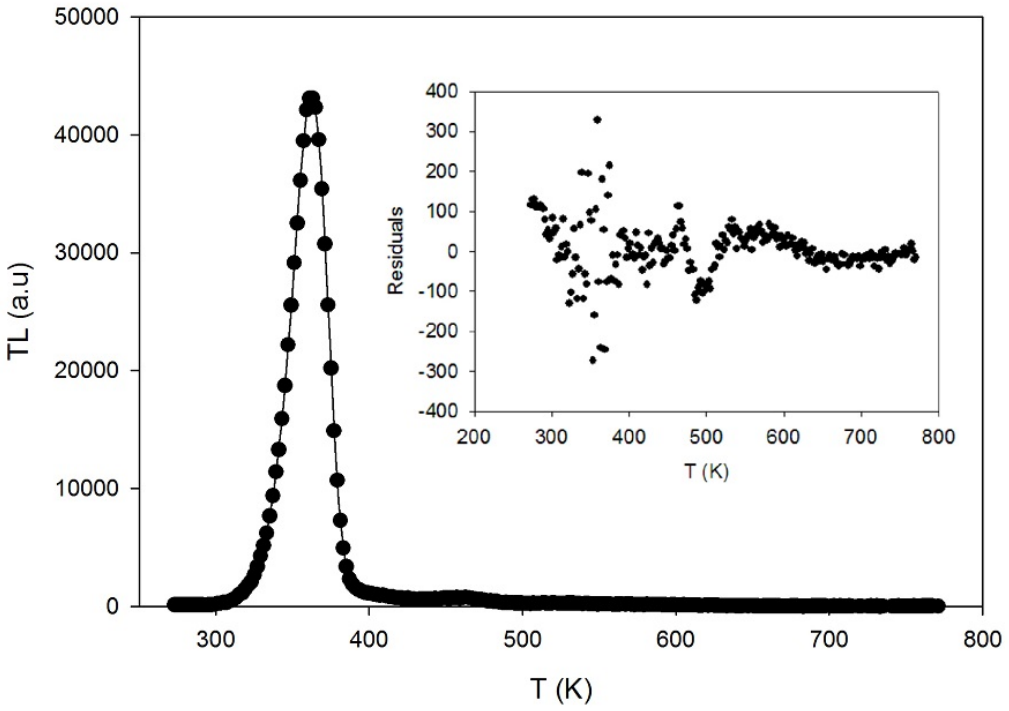

FIGURE 5.39: Experimental TL glow curve and best fit generated from a sum of five general-order terms. Each term is given by the general-order equation of Kitis et al. [37](i.e., equation (3.33)). The glow curve was measured at 5.0 °C/s after irradiation to 93 Gy.

As reflected by the plot of the residuals in the inset in Figure 5.39, the cumulative fit is fairly satisfactory. Table 5.7 presents the kinetics parameters obtained from curve fitting. As evident in Table 5.7, the goodness of the fit is affected by the heating rate at

TABLE 5.7: Kinetic parameters of the main TL peak. These parameters were obtained from curve fitting. Each of the glow curve fitted was measured from the sample irradiated to 93 Gy.

HR (°C/s)	T_M (K)	$T_{M_{fit}}$ (K)	E (eV)	b	s $(\times 10^{13} s^{-1})$	FOM	R^2
0.1	321.15	321.86 ± 0.14	0.99 ± 0.02	1.00 ± 0.04	3.52	11%	0.9916
0.2	327.15	327.84 ± 0.04	0.99 ± 0.08	1.00 ± 0.04	3.54	6.1%	0.9970
0.4	333.15	333.93 ± 0.54	0.99 ± 0.07	1.01 ± 0.03	3.60	4.1%	0.9988
0.6	338.15	337.70 ± 0.06	0.98 ± 0.08	1.01 ± 0.01	2.53	4.4%	0.9996
0.8	341.15	340.73 ± 0.16	0.99 ± 0.02	1.03 ± 0.01	3.48	2.1%	0.9997
1.0	343.15	342.79 ± 0.27	0.99 ± 0.03	1.02 ± 0.02	3.51	4.0%	0.9998
2.0	349.15	349.38 ± 0.30	1.02 ± 0.03	1.20 ± 0.12	9.92	5.5%	0.9986
3.0	355.15	355.16 ± 1.11	0.98 ± 0.07	1.06 ± 0.08	2.17	2.5%	0.9994
4.0	359.15	359.08 ± 0.54	1.01 ± 0.05	1.07 ± 0.03	5.43	2.4%	0.9997
5.0	363.15	362.23 ± 0.03	1.00 ± 0.01	1.09 ± 0.01	3.60	1.6%	0.9998

which the glow curve was measured. This is probably due to the fact at some heating

rates, the higher temperature peaks (i.e peak II, peak III, peak IV and peak V) are not always distinguishable. However, since a sum consisting of five terms was used for fitting, some of the terms may be irrelevant because the glow curve appears to contain less peaks. The activation energy E and the order of kinetics b are not affected by the heating rate. The order of kinetics b of the main peak is close to 1.0. In addition, the values of b reported in Table 5.7 correspond to values of μ_g between 0.42 and 0.45 on Chen's [34] graph. Therefore, for the heating rates used, the order of kinetics b of the main peak is close to 1.0.

5.2.2.2 The whole curve method

The WCM was applied to determine the activation energy E and the order of kinetics b of the main peak. As described in section 3.5, several lines of $\ln(TL/n^b)$ versus $1/kT$ were plotted for a range of b values and the correct values of E and b were retained from the best straight line. Figure 5.40 shows the lines obtained for the main peak for b taking values 0.9, 1.0, 1.1, 1.2 and 1.3 respectively.

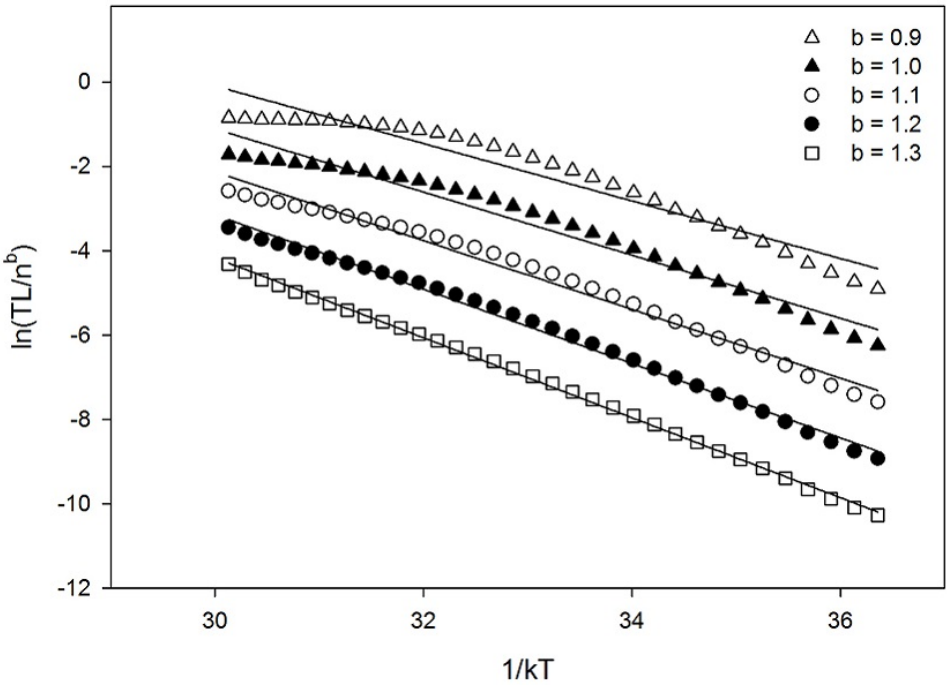

FIGURE 5.40: Plots used to determine the activation energy E and the order of kinetics b of the main TL peak of the annealed sample. The glow curve onto which this method is applied was recorded from a sample irradiated to 10 Gy and heated at 5.0 °C/s.

The best straight line in Figure 5.40 was obtained for $b = 1.3$ and $E = 0.95 \pm 0.01$ eV. The coefficient of regression, R^2, was 0.9986. These values of E and b compare favourably to those derived from curve fitting and subsequent methods.

5.2.2.3 The IR analysis

The IR method was used to evaluate the activation energy E of the main TL peak of the annealed sample. Figure 5.41 shows a plot of $\ln(I)$ against $1/kT$ for data in the initial rise part of the main peak. From the plot in Figure 5.41, the value of E was found to be 0.96 ± 0.03 eV ($R^2 = 0.9969$). This value of the activation energy E is in good agreement with the value of 0.92 ± 0.02 eV found for the unannealed sample. The agreement between the two values of E suggests that the activation energy E of the main peak is not affected by annealing at 500 °C.

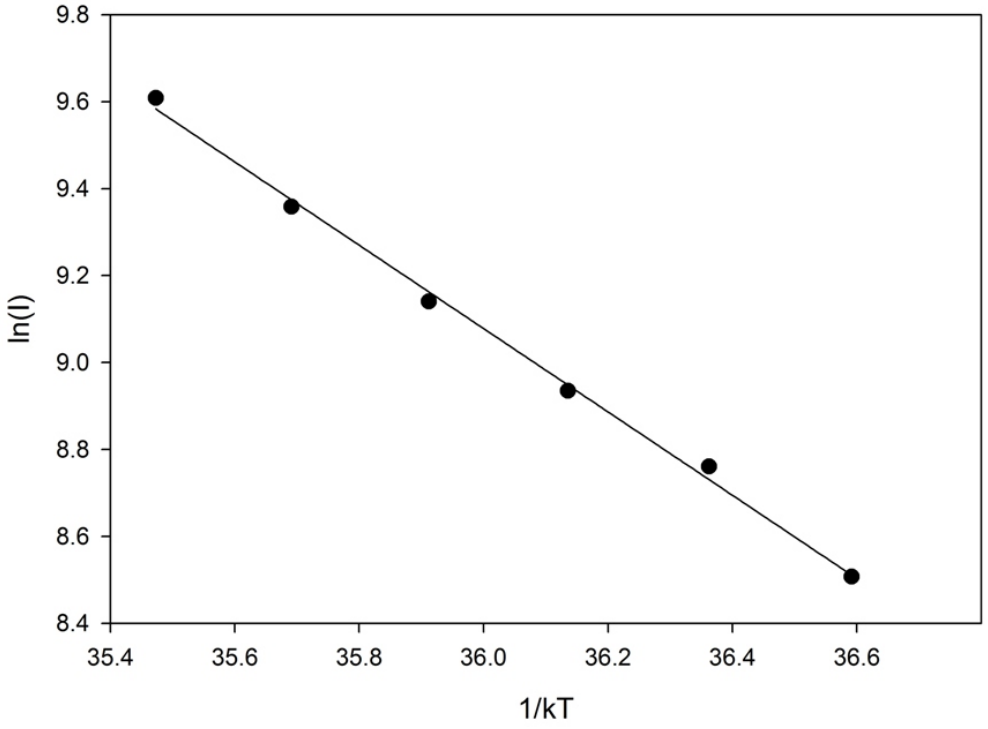

FIGURE 5.41: Plot of $\ln(I)$ versus $1/kT$ used to determine the activation energy E of the main TL peak for a sample heated at 5.0 °C/s after irradiation to 93 Gy (see Figure 5.35).

The IR method was also used to study the influence of repetitive measurement on the activation energy of the main TL peak. Figure 5.42 shows the effect of repeated measurement on the activation energy E of the main TL peak for the annealed sample.

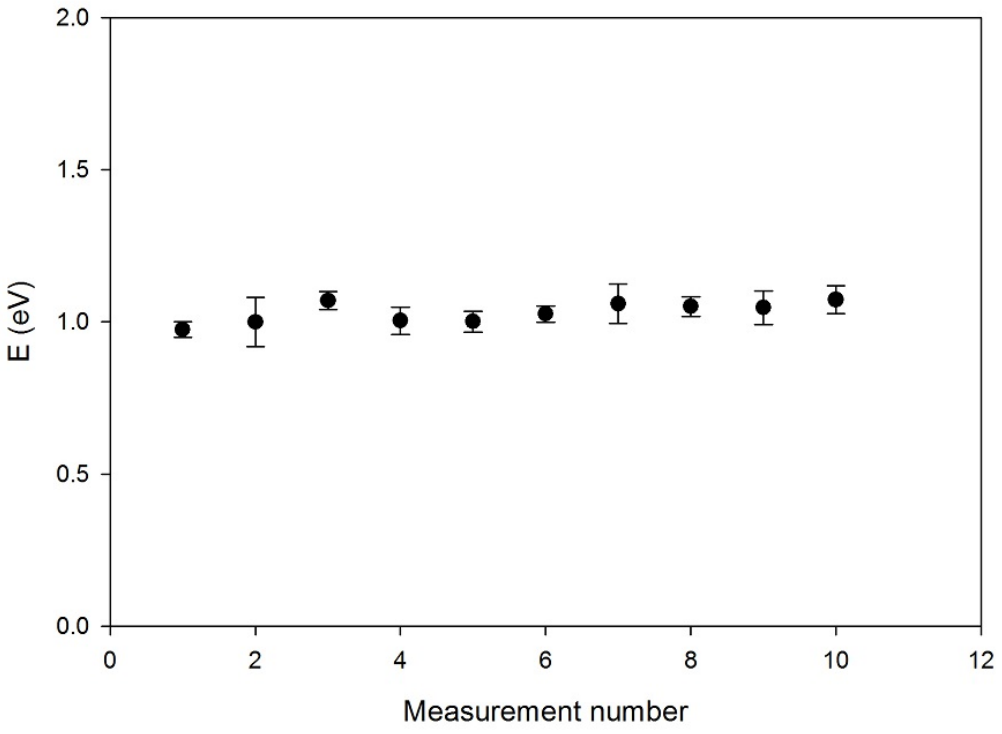

FIGURE 5.42: Influence of repeated measurement on the activation energy E of the main TL peak for a dose of 10 Gy and a heating rate of 5.0 °C/s.

The error bars associated with the values of E shown in Figure 5.42 overlap and as for the main TL peak of the unannealed sample, the influence of repetitive measurement on the activation energy E of the main TL peak of the annealed sample is minimal. The average value of E calculated from the repeated TL measurements was 1.03 ± 0.04 eV.

5.2.2.4 Various heating rate analysis

The effect of heating rate on the main TL peak of the annealed sample was studied for heating rates ranging from 0.1 to 5.0 °C/s. For each TL measurement, the sample was irradiated to 93 Gy. Figure 5.43 shows the shift in the temperature of the main TL peak with heating rate. As shown in Figure 5.43, the peak temperature shifts from 48 °C (at 0.1 °C/s) to 90 °C (at 5.0 °C/s).

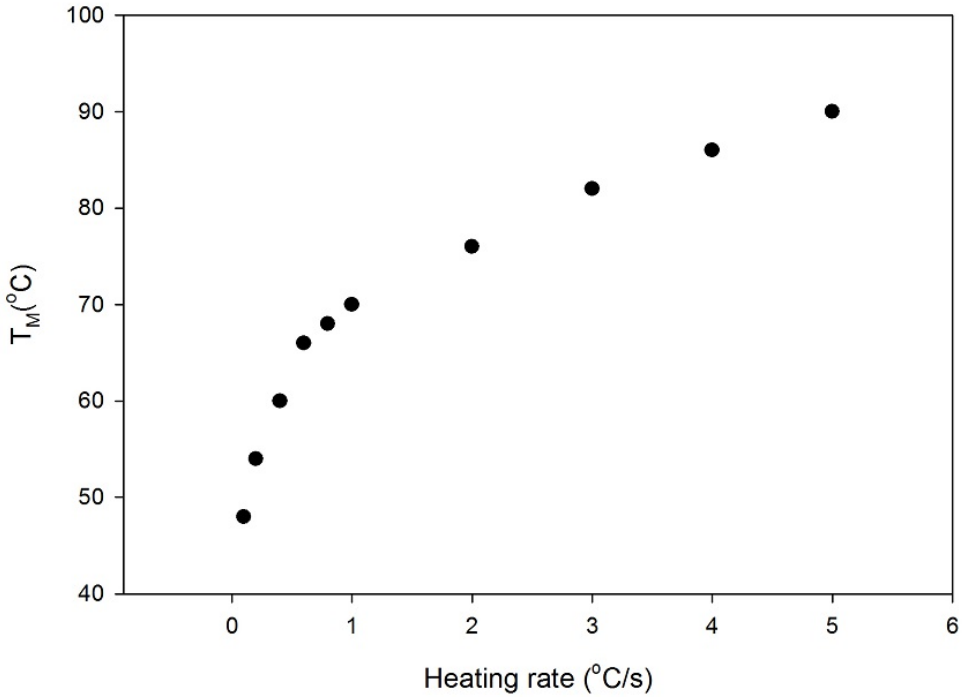

FIGURE 5.43: Shift in the temperature of the main TL peak for a sample of annealed quartz irradiated to 93 Gy.

The peak intensity also shifts as a result of the increase in heating rate. We noticed however that for all the variable heating experiments performed, the peak intensity, in arbitrary units, increases with the second measurement of the series before decreasing afterwards. This implies that the sensitivity of the sample possibly increases directly after the first measurement. Figure 5.44 shows the influence of heating rate on the intensity of the main TL peak.

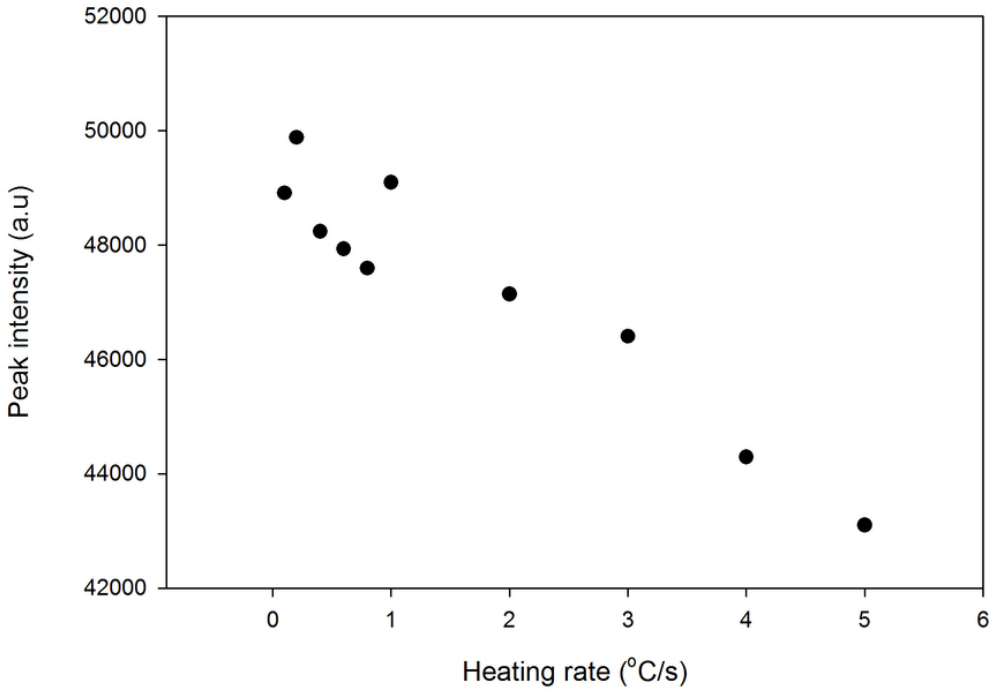

FIGURE 5.44: Influence of heating rate on the intensity of the main TL peak for a sample of annealed quartz irradiated to 93 Gy.

We then computed the activation energy E of the main TL peak of the sample using the Hoogenstraaten [29] VHR method of analysis and found 0.89 ± 0.02 eV (R^2 = 0.9946). This value of E is comparable to the value of 0.96 ± 0.03 eV obtained from the IR method for the same peak. For both samples, annealed and unannealed, the VHR method yielded a smaller value of E. As pointed earlier in 5.1.3.5, in a recent study of variable heating rate effects on TL, Pagonis et al. [48] showed that the VHR method can systematically underestimate the value of the activation energy E of a peak. The plot from which the value of E was derived is shown in Figure 5.45.

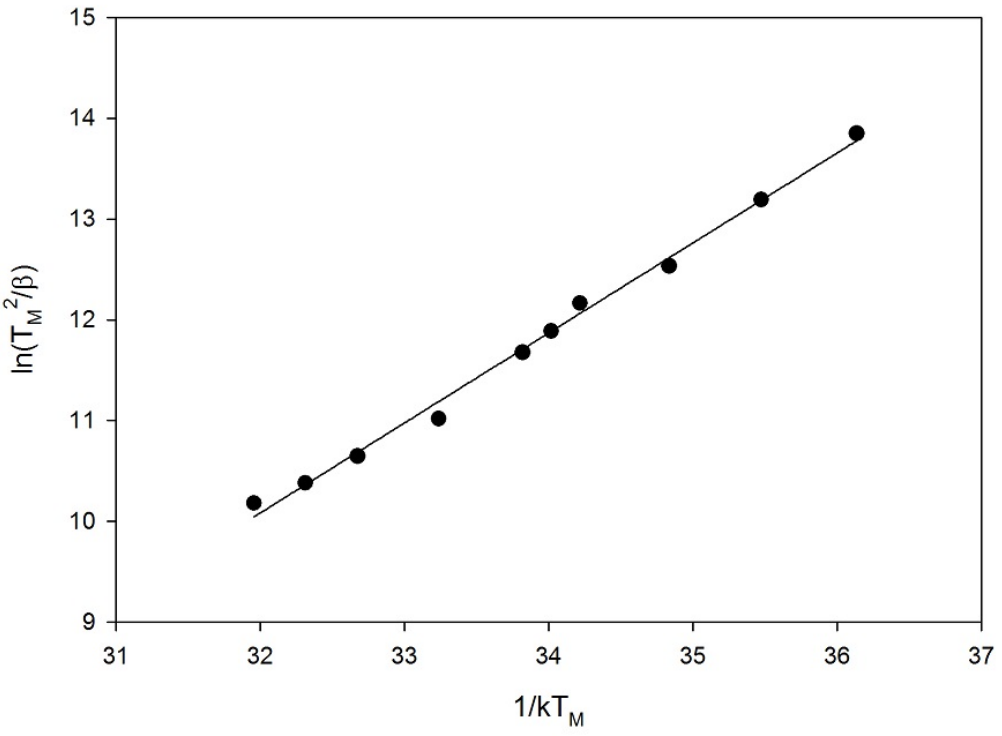

FIGURE 5.45: Plot of $\ln(T_M^2/\beta)$ against $1/kT_M$ used to determine E and s.

The frequency factor s resulting from this analysis was 1.10×10^{12} s^{-1}, which is two orders of magnitude less than the values of s found from curve fitting. This value of s is however of the same order of magnitude as the value ($s = 4.8 \times 10^{12}$ s^{-1}) derived for the unannealed sample.

The decrease in peak intensity with heating rate (Figure 5.44) is an indication of thermal quenching. To obtain the quenching parameters (C and W) associated with the main peak of the annealed sample, we plotted $\ln((\frac{I_{Un}}{I_{Que}}) - 1)$ against $1/kT_M$. The peak integral under the unquenched peak is given by I_{Un} whereas that under the quenched peak is I_{Que}. Figure 5.46 shows the plot of $\ln((\frac{I_{Un}}{I_{Que}})-1)$ against $1/kT_M$ used to determine the quenching parameters.

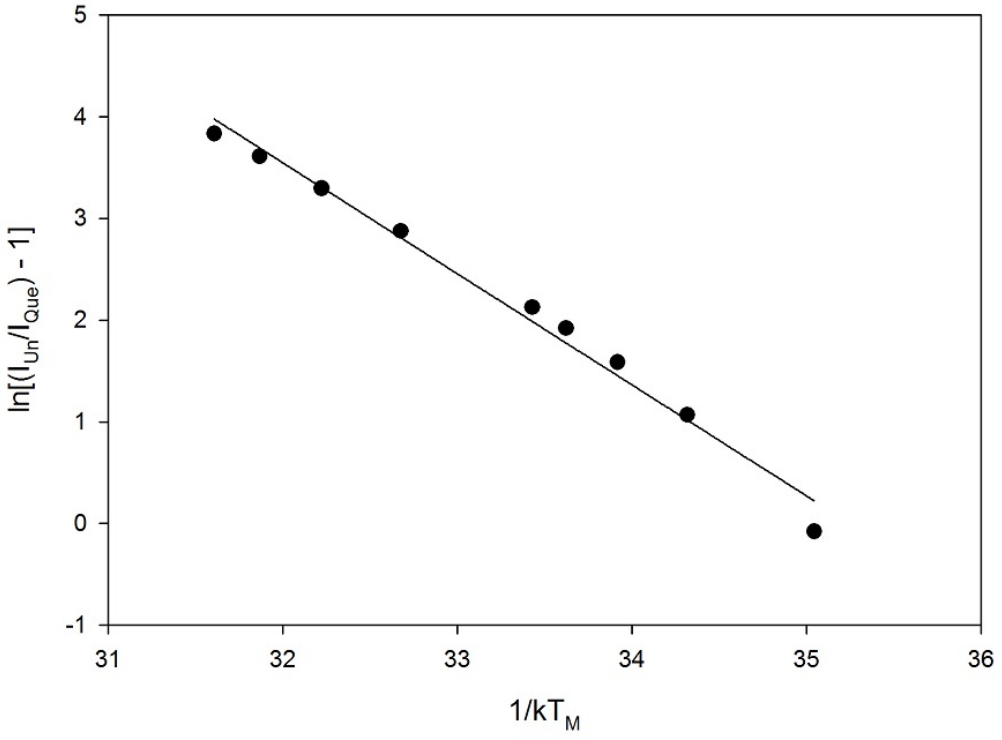

FIGURE 5.46: Determination of the quenching parameters W and C from the plot of $\ln((\frac{I_{Un}}{I_{Que}}) - 1)$ against $1/kT_M$ for the main peak of the annealed sample.

The quenching parameters C and W obtained from the fit shown in Figure 5.46 were respectively 5.2 $\times$ 10^{16} and 1.09 $\pm$ 0.05 eV. These values of C and W are comparable to those obtained for the unannealed sample (1.20 $\pm$ 0.05 eV and 5.2 $\times$ 10^{16}).

5.2.3 Dosimetric features

5.2.3.1 Dose dependence of the main peak

The study of the dosimetric features of a peak gives information about the order of kinetics and the applicability of the peak in dosimetry and dating [4, 43]. The dose response of the main TL peak of the annealed sample was investigated by carrying out a sequence of TL measurements on a single aliquot of the sample. To ease comparison, the experimental procedure was identical to that used for the unannealed sample. As such, the TL glow curves were taken at a heating rate of 5.0 °C/s and the irradiation doses were between 2 and 151 Gy. Figure 5.47 shows that the temperature of the main TL peak is independent of the irradiation dose.

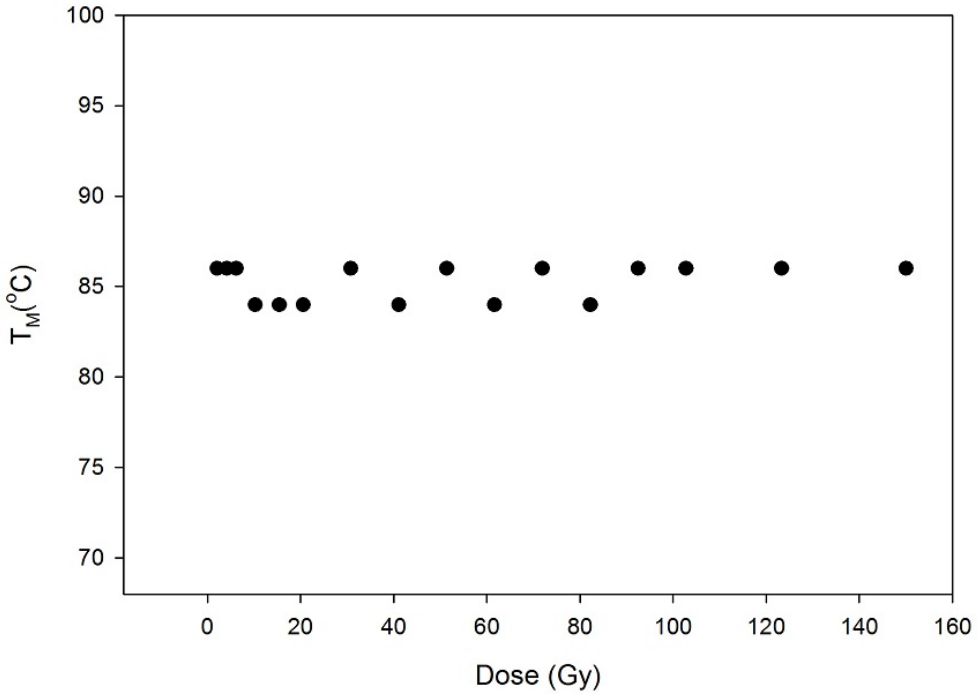

FIGURE 5.47: Dependence of the temperature of the main TL peak on the irradiation dose for a heating rate of 5.0 °C/s.

This behaviour of the main peak is an indication of first-order kinetics [2, 4].

Figure 5.48 shows the intensity of the main TL peak as a function of the irradiation dose.

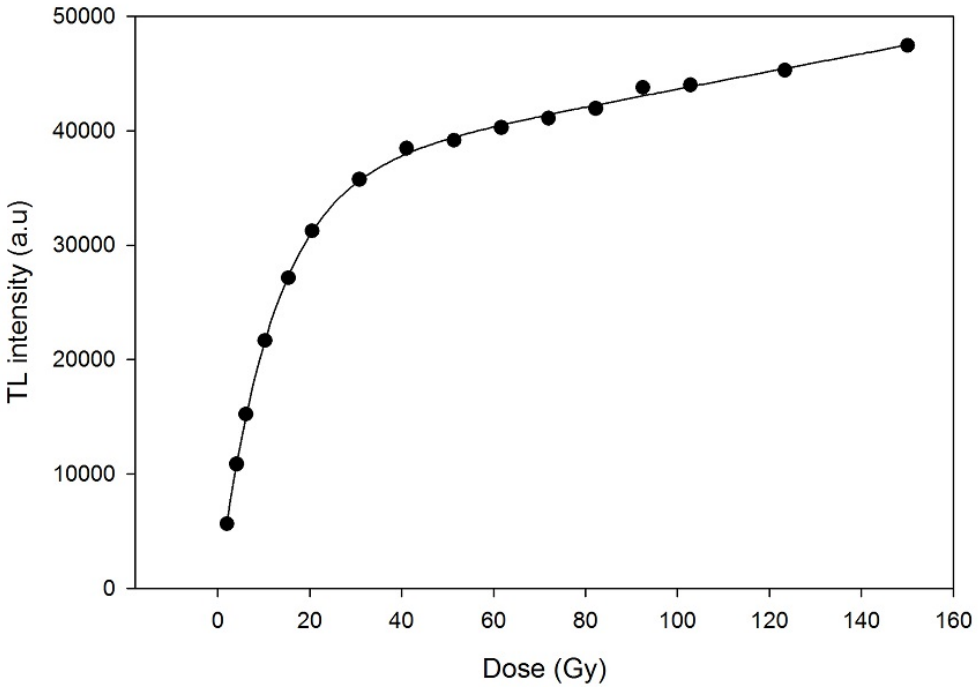

FIGURE 5.48: The peak intensity is shown as a function of irradiation dose for TL glow curves taken at a heating rate of 5.0 °C/s. The solid line through the data is given by a function of the form $S(D) = 35922.67(1 - \exp(-0.0844D)) + 77.04D$ where D is the variable representing the dose.

As in the case of the unannealed sample, we were able to describe the dose response S as the sum of a saturating exponential and a power law as in equation (5.7). The second derivative of the dose response function is negative and the super-linearity index g remains less than 1. Hence, as in the case of the unannealed sample, the growth of the main peak with irradiation dose is sub-linear with respect to the initial linear range from 2 to 10 Gy.

The activation energy E of the main peak at each irradiation dose was computed from the IR method. Figure 5.49 shows that the effect of irradiation on the activation energy is minimal. The activation energy E is nearly constant and its average value is 1.00 ± 0.03 eV. This average value of E is in very good agreement with the values obtained from curve fitting (see Table 5.7) and the VHR analysis.

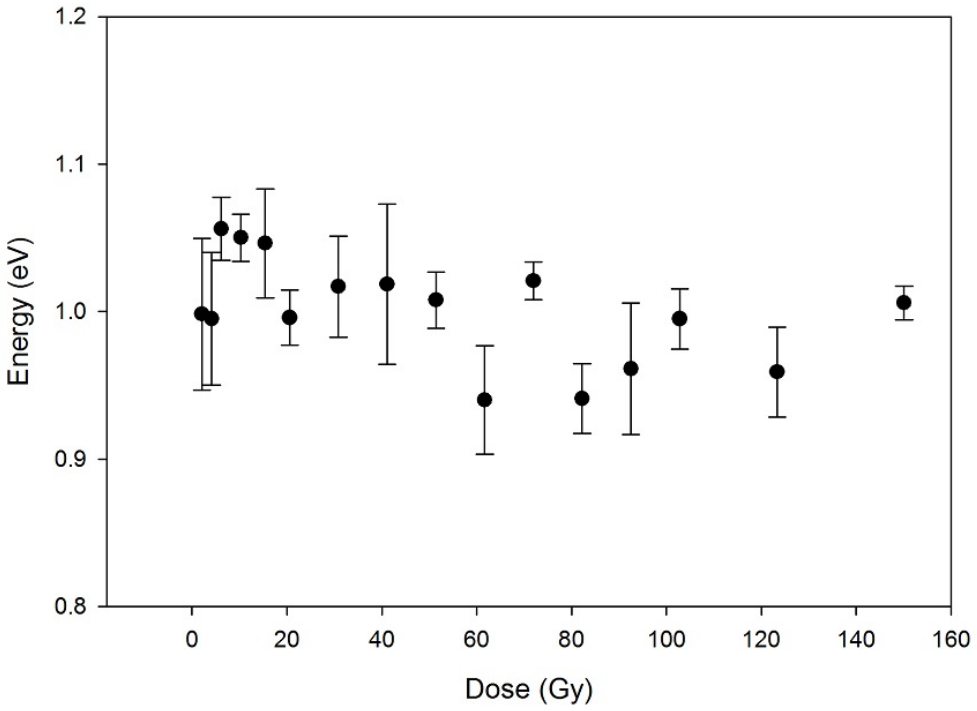

FIGURE 5.49: Influence of the irradiation dose on the activation energy E of the main TL peak for the annealed sample. TL glow curves were read out at a heating rate of 5.0 °C/s.

5.2.3.2 Influence of delayed stimulation on the main TL peak

The effect of delay between irradiation and TL read out was also investigated for the annealed sample. For each measurement, the sample was irradiated to 93 Gy and the heating at 5.0 °C/s was delayed. As in the case of the unannealed sample, the stimulation was delayed for 1, 2, 4, or 6 h respectively. Figure 5.50 shows the glow curve measured 6 h after irradiation. The inset shows the glow curve measured directly after irradiation.

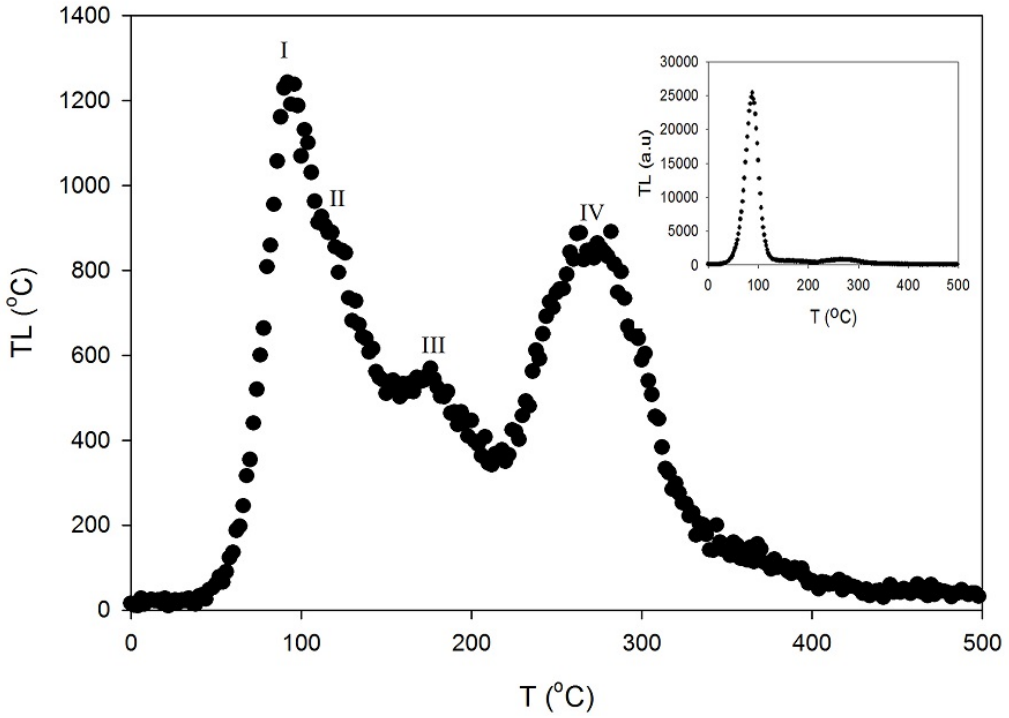

FIGURE 5.50: TL glow curve measured at a heating rate of 5.0 °C/s a 6h delay from a sample irradiated to 93 Gy. The inset shows the glow curve taken from the same sample directly after irradiation.

Figure 5.50 shows that as in the case of the unannealed sample, the peaks at higher temperature become more apparent as the main peak fades. However, as shown in the inset of Figure 5.50, for a 6 h delay, the intensity of the peak around 300 °C is greater than that of the intermediate peaks between 110 and 250 °C. This was not the case for the unannealed sample (Figure 5.32). Figure 5.51 shows the decrease in the intensity of the main TL peak as a function of the delay time. As in the case of the unannealed sample, the fading of the main TL peak of the annealed sample could also be described by equation (5.9).

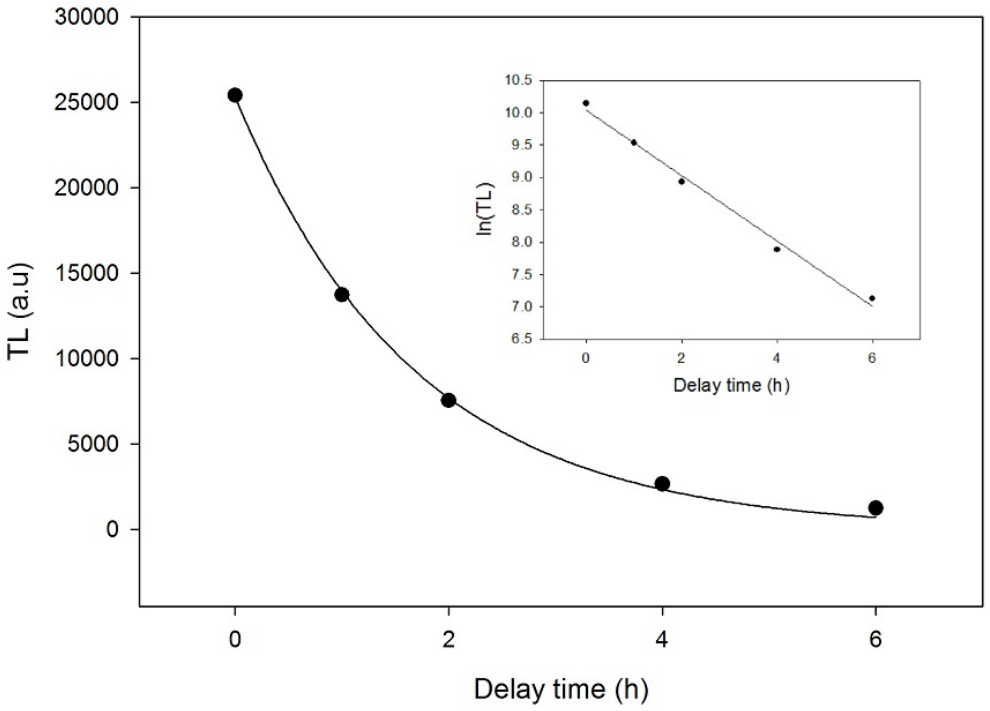

FIGURE 5.51: Effect of delayed stimulation on the main TL peak of the annealed sample for a heating rate of 5.0 °C/s and a dose of 93 Gy. The solid line is the best fit obtained from equation (5.9). The inset shows a plot of $\ln(TL)$ against delay time confirming the exponential nature of the fading.

The exponential nature of the fading suggests a negligible amount of re-trapping into the traps associated with the main peak. The decay constant obtained from the fit is $f = 0.59\ \mathrm{h}^{-1}$. This value of b is greater than that of the unannealed sample ($f = 0.55\ \mathrm{h}^{-1}$). Hence, the half-life of the main TL peak which is approximately 1.17 h is smaller than that of the main TL peak of the unannealed sample. The values of half-life obtained here are consistent with previous knowledge of the stability of the "110" °C TL peak in quartz (e.g., Koul [43] and references therein). As in the case of the unannealed sample, the fading is due to the loss of electrons from the shallow traps associated with the main peak at room temperature.

5.2.4 Summary of kinetics parameters of the main TL peak

Table 5.8 summarises and compares the kinetic parameters E and b of the main TL peak of the annealed sample to those found for the unannealed sample and to those reported in literature. The results published by Mebhah et al. [51] and shown in Table 5.8, which were obtained for quartz samples fired over 400 °C compare well with the values reported

TABLE 5.8: Values of the trap depth E and the order of kinetics b for the main TL peak of quartz. The abbreviations are as follows: IR (initial rise), VHR (Hoogenstraaten [29] variable heating rate method), CF (curve fitting), IT (isothermal analysis), TLP (TL-like phosphorescence analysis), WCM (whole curve method),GCD (glow curve deconvolution) and HR (heating rate).

main peak T_M(°C)	HR (°C/s)	E (eV)	b	Method	Reference
annealed sample					
82	5.0	0.96 ± 0.03		IR	Figure 5.41
48 -> 90	0.1 -> 5.0	0.89 ± 0.02		VHR	Figure 5.45
48	0.1	0.99 ± 0.02	1.00 ± 0.04	CF	Figure 5.39
90	5.0	1.00 ± 0.01	1.09 ± 0.01	CF	Table 5.7
86	5.0	0.95 ± 0.01	1.3	WCM	Figure 5.40
unannealed sample					
72	1.0				Figure 5.3
92	5.0	0.92 ± 0.02		IR	Figure 5.19
58 -> 94	0.2 -> 5.0	0.88 ± 0.01		VHR	Figure 5.23
74	1.0	0.91 ± 0.01	1.01±0.01	CF	Table 5.1
94	5.0	0.93 ± 0.02	1.08±0.01	CF	Figure 5.15
92	5.0	0.96 ± 0.01	1.2	WCM	Figure 5.18
	5.0		1.2	IT	Figure 5.26
		0.92		TLP	Table 5.5
100	5.0	1.02 ± 0.03		PS	Mebhah et al. [51]
		0.92 ± 0.09	1.32 ± 0.09	WCM	Mebhah et al. [51]
		0.97 ± 0.02	1.11 ± 0.08	GCD	Mebhah et al. [51]
		1.00			Kitis et al. [52]

here for the unannealed and annealed samples. The values of the order of kinetics b found in this work also compare well with those published elsewhere.

5.3 Phototransferred TL in natural quartz

Phototransferred TL (PTTL) was studied in unannealed samples and samples annealed at 500 °C for 10 minutes. Each of the sample used for PTTL (annealed or unannealed) was irradiated to 93 Gy at room temperature. Following irradiation, the sample was preheated to a temperature T_i at a heating rate of 5.0 °C/s. After preheating, the sample was then exposed to 470 nm blue light for some time t at room temperature. The final step consisted in heating the sample to 500 °C at the same rate of 5.0 °C/s to measure the induced PTTL. The heating was done in a nitrogen atmosphere. The choice of the preheat temperatures was guided by the knowledge of peak positions in the TL glow curves recorded. Unless otherwise stated, the dose and heating rate were varied only for the study of dose dependence and heating rate effects. For convenience,

a glow curve recorded after preheating and subsequent illumination, will be referred to as a PTTL glow curve. However, the term "PTTL glow curve" does not imply that all the peaks in such a glow curve are due to phototransfer.

5.3.1 PTTL glow curves of the unannealed sample

For the unannealed sample, most of the TL glow curves measured at 5.0 °C/s after irradiation to 93 Gy have prominent peaks at 84 (peak I), 178 (peak III), 240 (peak IV) and 325 °C (peak V). There is also a peak around 450 °C (peak VI) which is not always evident and only becomes apparent after peak I has been thermally removed. As such, for the first PTTL experiment, the sample was preheated to 120 °C after irradiation in order to remove peak I and then illuminated for 5 s. Figure 5.52 shows the PTTL glow curve obtained upon subsequent heating to 500 °C.

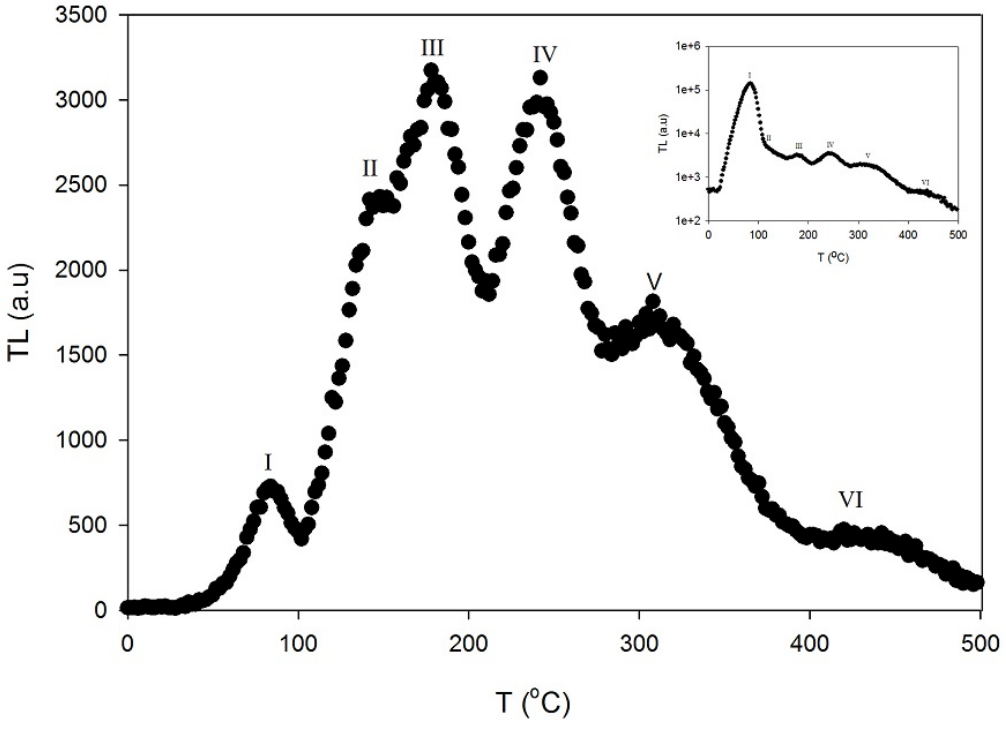

FIGURE 5.52: A PTTL glow curve obtained from the unannealed sample irradiated to 93 Gy, preheated to 120 °C, illuminated for 5 s and heated at a rate of 5.0 °C/s. Peak I, at 84 °C, is due to phototransfer. The original TL glow curve measured at the same rate of 5.0 °C/s after irradiation to 93 Gy is shown in the inset.

The PTTL glow curve in Figure 5.52 consists of six distinctive peaks. Peak I, which occurs at 84 °C, is due to phototransfer since the original TL peak at 84 °C is removed by a 120 °C preheat. This PTTL peak is low in intensity compared with peak I of

the original TL glow curve. The weak intensity of the PTTL peak is probably due to the fact that only a fraction of the electrons released from the donor traps during illumination ended up at traps responsible for peak I. Some of the electrons released from the donor traps recombine with holes to give off light during illumination while others are probably re-trapped. In addition, the population of electrons released from the donor traps depends on the duration of the illumination. It is worth noting that the PTTL peak in Figure 5.52 appears at the same temperature as the original TL peak. Subsequent PTTL glow curves taken for longer illumination times have a structure similar to that shown in Figure 5.52. Varying the illumination time allowed us to study the effect of illumination on the phototransferred peak. Figure 5.53 shows the dependence of the PTTL intensity on the illumination time. The PTTL intensity refers to the intensity of the PTTL peak.

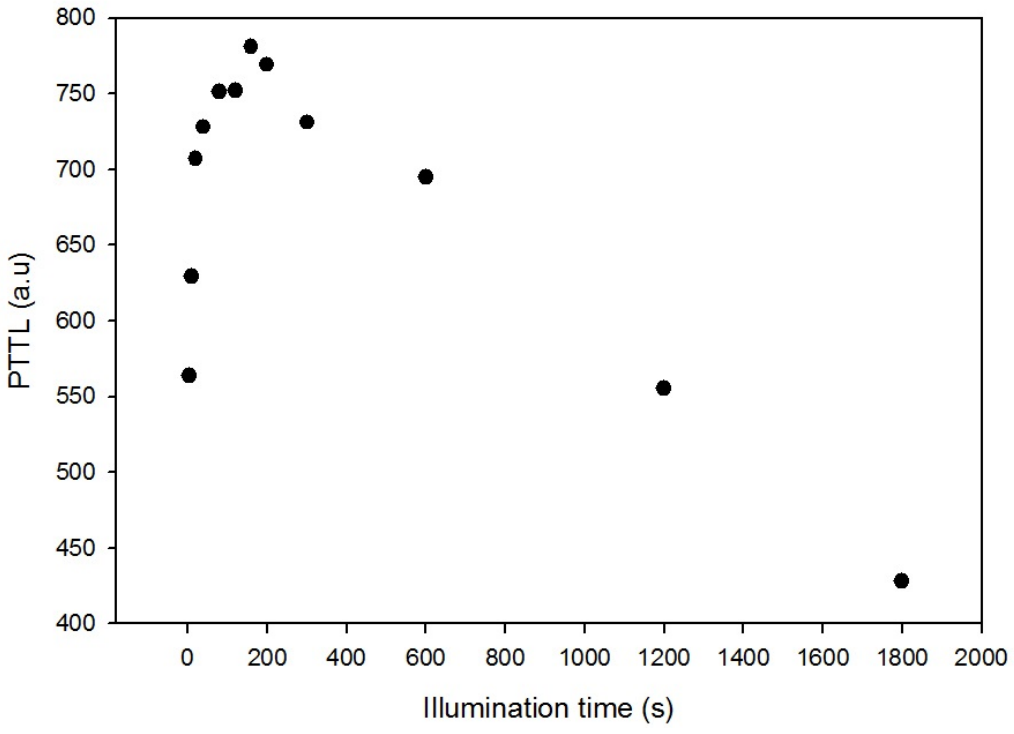

FIGURE 5.53: Dependence of the PTTL peak intensity on illumination time for the unannealed sample irradiated to 93 Gy, preheated to 120 °C and heated at 5.0 °C/s.

As shown in Figure 5.53, the PTTL intensity increases with illumination time from 5 up to 160 s and then decreases for greater illumination times. In order to improve our understanding of the dynamics of charge movement during illumination and subsequent heating, it was important to study the influence of illumination on the intensity of the

other peaks. Peaks III, IV and V, shown in Figure 5.52, are not removed by a preheat to 120 °C. In addition to these peaks, the peak at 140 °C (peak II) is clearly visible in the PTTL glow curve. Peak II is present in the original TL glow curve but because of its proximity to peak I (also known as the main peak or the "110" °C peak), it is barely seen. Figure 5.54 shows the relative intensity (I_2/I_1) of peak II as a function of illumination time. The relative intensity of a peak is defined as the ratio between its peak maximum and that of peak I, where peak I is due to phototransfer.

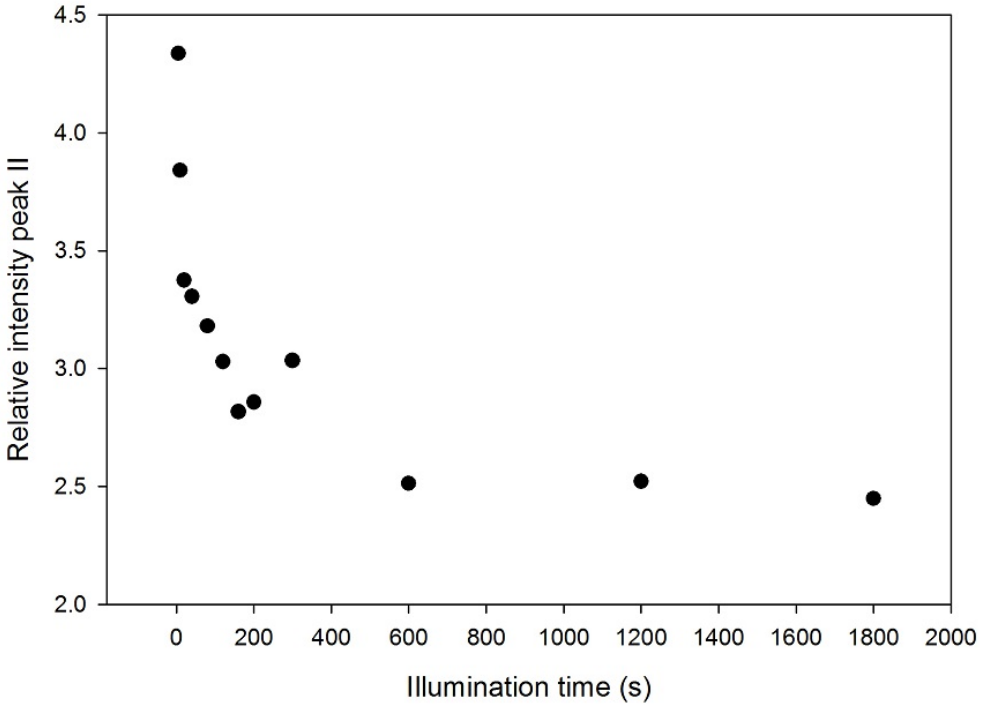

FIGURE 5.54: Influence of illumination on peak II for an irradiation dose of 93 Gy, a 120 °C preheat and a heating rate of 5.0 °C/s. The relative intensity of peak II is given by the ratio between its peak maximum and that of the PTTL peak (I_2/I_1).

The relative intensity of peak II decreases with illumination times from 5 to 600 s and remains constant with illumination time up to 1800 s the maximum time used. The region from 5 to 160 s where the intensity of the PTTL increases as shown in Figure 5.53 corresponds to a region of decreasing intensity for peak II. This implies that traps responsible for peak II are losing electrons due to illumination. However, for illumination times between 600 and 1800 s, the relative intensity of peak II is constant implying that the loss of electrons from the corresponding traps for longer illumination is negligible. As evident in Figure 5.55, illumination has a similar effect on peak III.

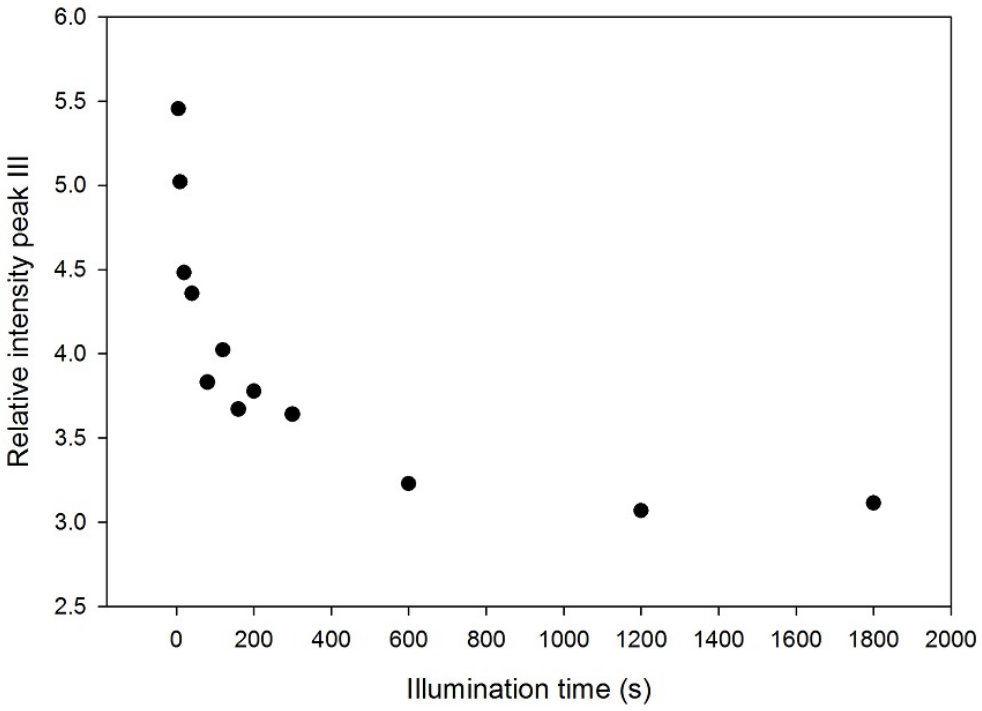

FIGURE 5.55: Influence of illumination on peak III for an irradiation dose of 93 Gy, a 120 °C preheat and a heating rate of 5.0 °C/s.

For peaks IV and V, the relative intensities were found to decrease with illumination times from 5 to 600 s. However for illumination times greater than 600 s, as shown in Figure 5.56 and Figure 5.57, an increase in these relative intensities was noticed. This increase at higher illumination time suggests the re-trapping of electrons into the traps associated with peaks IV and V.

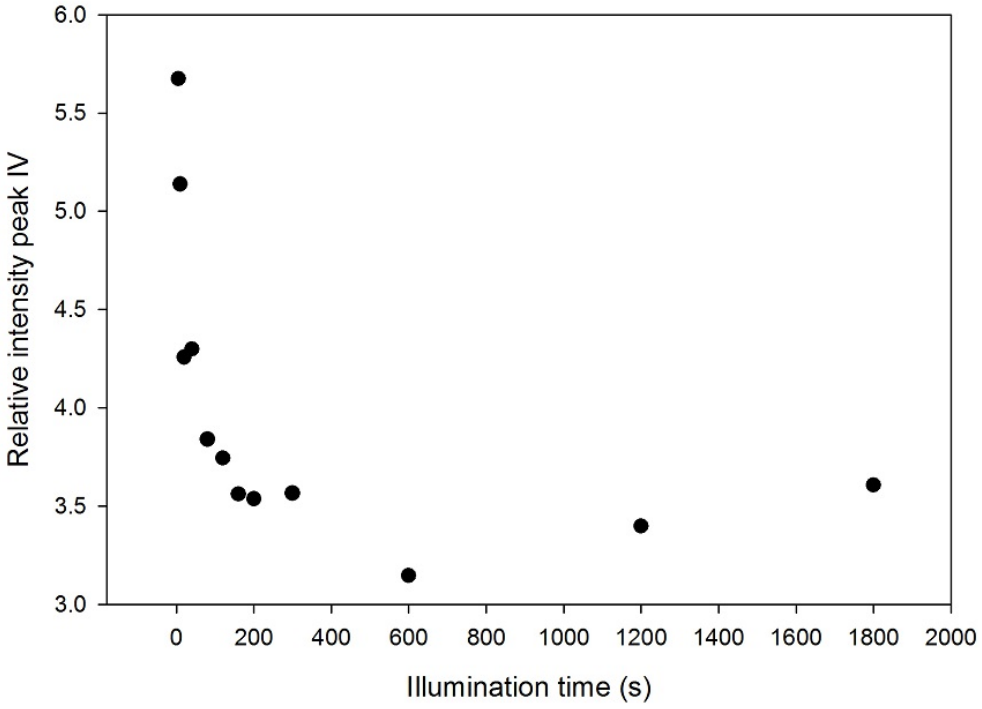

FIGURE 5.56: Relative intensity of peak IV against illumination time for an irradiation dose of 93 Gy, a 120 °C preheat and a heating rate of 5.0 °C/s.

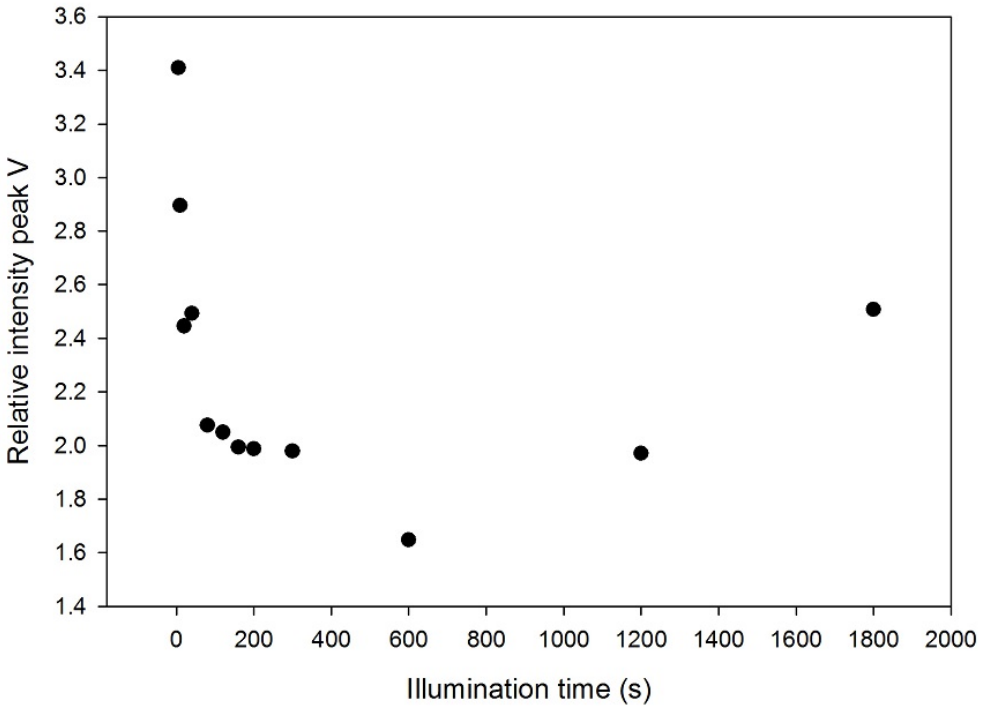

FIGURE 5.57: Relative intensity of peak V against illumination time for an irradiation dose of 93 Gy, a 120 °C preheat and a heating rate of 5.0 °C/s.

In the next PTTL experiment, the sample was preheated to 200 °C to remove peaks I, II and III. Upon illumination and heating, peak I was regenerated at 84 °C but peaks II and III were not. The PTTL glow curve obtained after a 200 °C preheat and 5 s of illumination is shown in Figure 5.58.

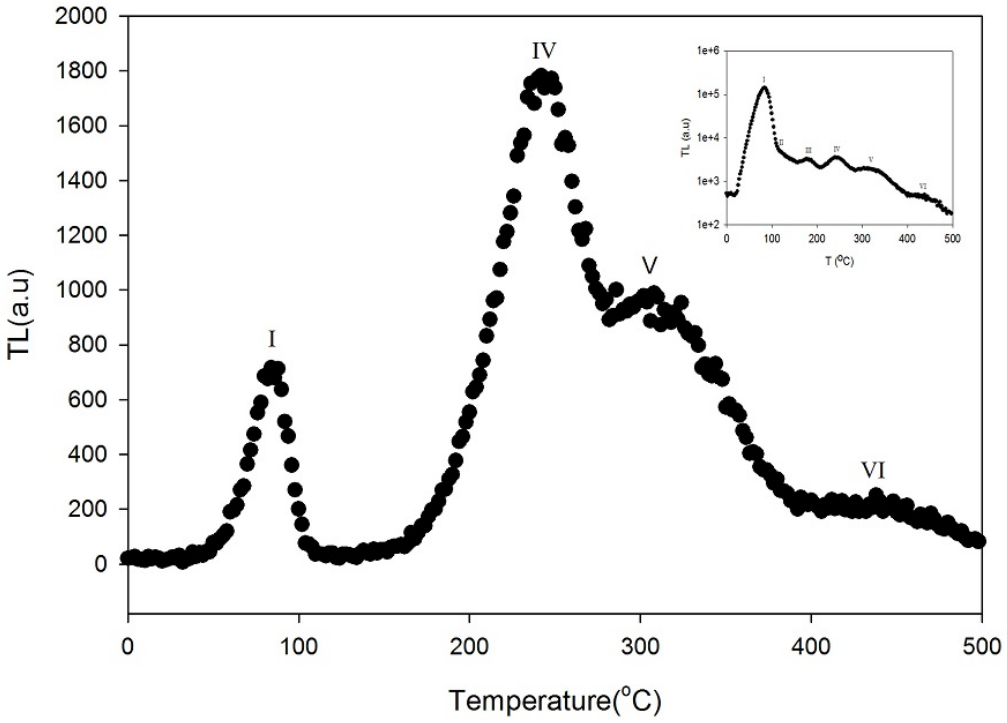

FIGURE 5.58: PTTL glow curve recorded at a heating rate of 5.0 °C/s from the sample irradiated to 93 Gy, preheated to 200 °C and illuminated for 5 s. Peak I is the regenerated PTTL peak. The original TL glow curve measured at a heating rate of 5.0 °C/s after irradiation to 93 Gy is shown in the inset.

The PTTL glow curve in Figure 5.58 shows four peaks centred at 84 (peak I), 240 (peak IV), 320 (peak V) and 450 °C (peak VI) respectively. Peak I is the only peak due to phototransfer. PTTL glow curves measured for longer illumination times had the same number of peaks and the same structure as in Figure 5.58. The dependence of the PTTL peak intensity on the illumination time is presented in Figure 5.59. The increasing part observed with a preheat to 120 °C is not present in Figure 5.59. The second point to note is that the PTTL intensity decreases with illumination time from 5 to 300 s in a non linear way. The dynamics of charge movement was further investigated by monitoring the effect of illumination on peak IV and V.

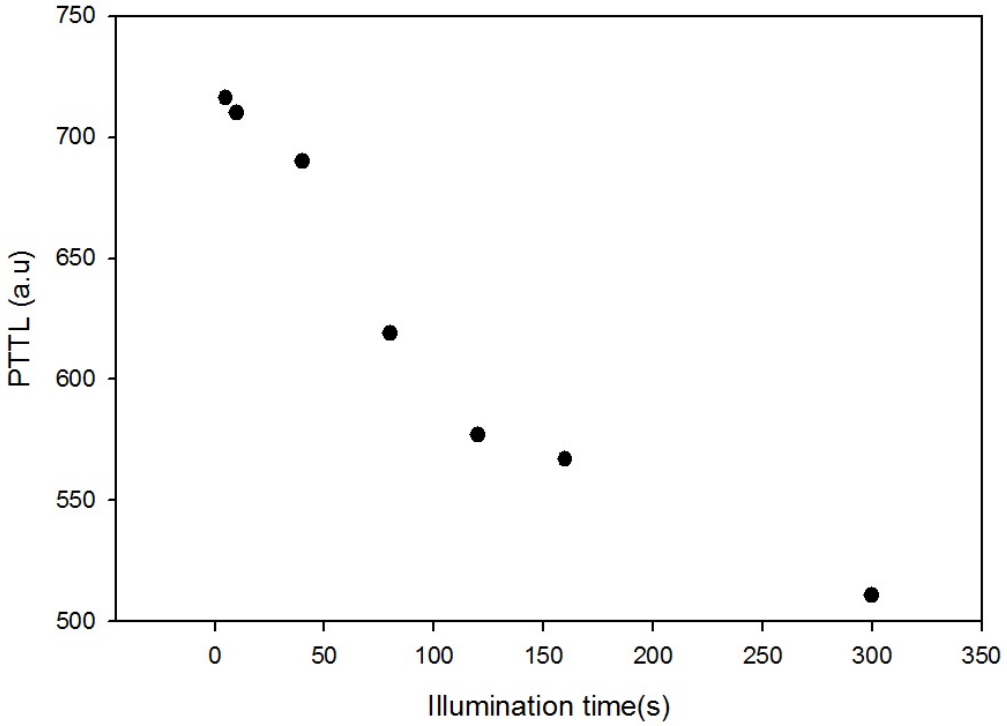

FIGURE 5.59: Effect of illumination on the PTTL peak intensity of peak I for an irradiation dose of 93 Gy, a 200 °C preheat and a heating rate of 5.0 °C/s.

Figure 5.60 and 5.61 show the influence of illumination on the intensity of peak IV and V respectively. In contrast to Figures 5.56 and 5.57, the y-axis in Figure 5.60 and 5.61 is not the relative intensity of each peak.

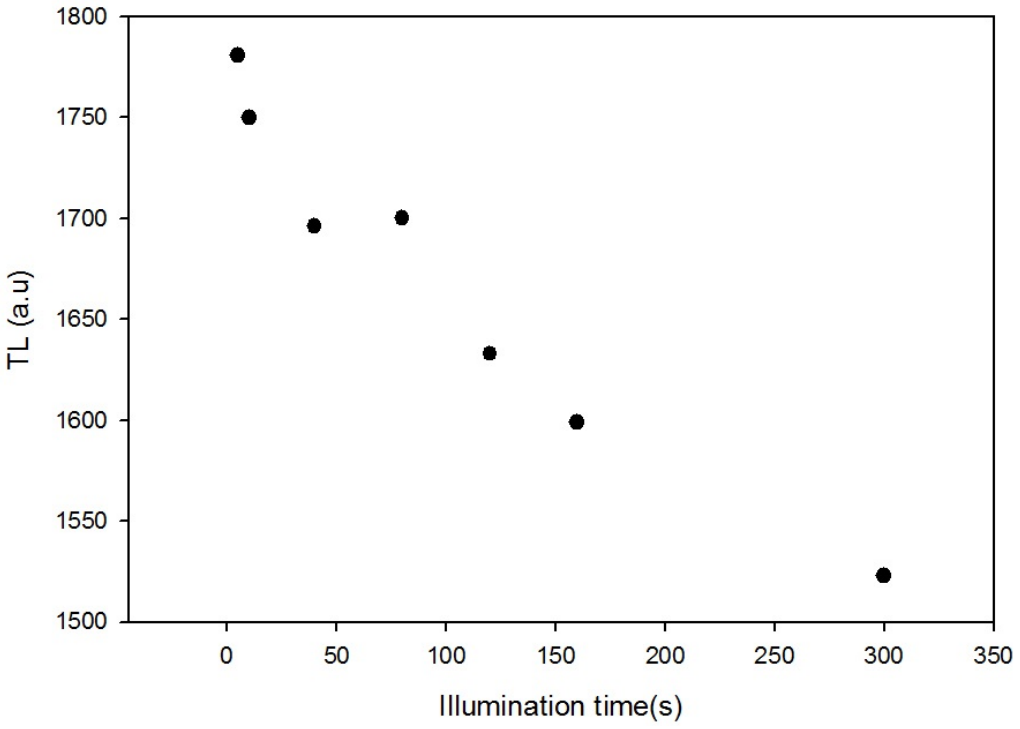

FIGURE 5.60: Variation in the intensity of peak IV with illumination for an irradiation dose of 93 Gy, a 200 °C preheat and a heating rate of 5.0 °C/s.

As depicted in Figure 5.60, the intensity of peak IV decreases continuously with increasing illumination time. This decrease in TL intensity is due to a loss of electrons from traps responsible for peak IV during illumination.

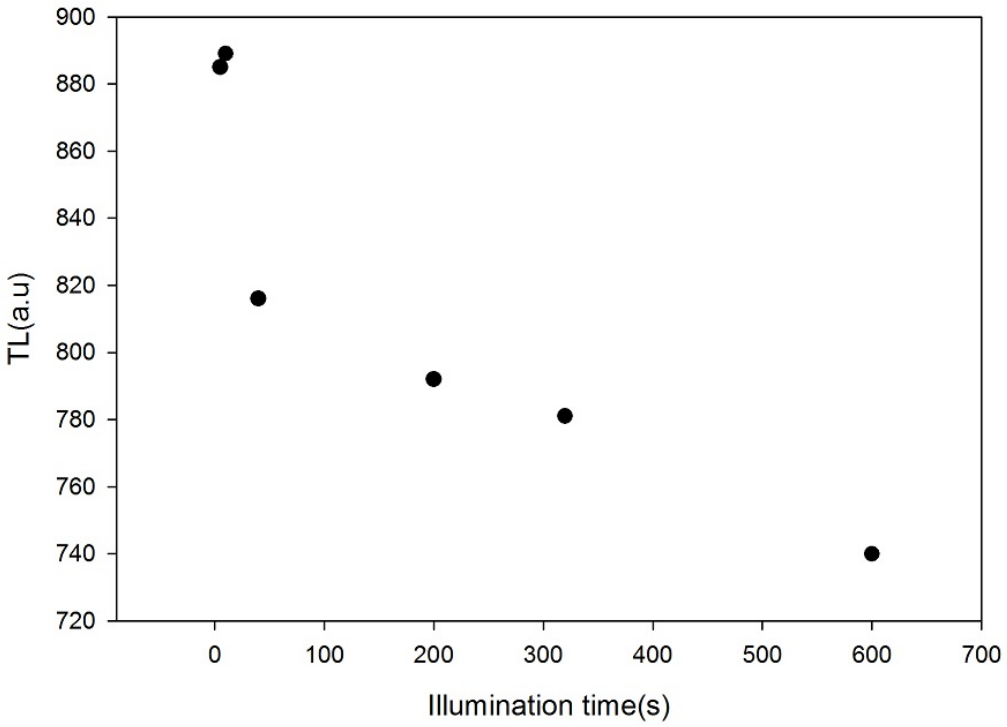

FIGURE 5.61: Influence of the illumination time on peak V for an irradiation dose of 93 Gy, a 200 °C preheat and a heating rate of 5.0 °C/s.

For peak V, it was difficult to accurately determine the peak position so we evaluated the area under the glow curve from 290 to 390 °C. As shown in Figure 5.61, the area under peak V decreases continuously with illumination time, suggesting the loss of electrons from the associated traps.

In a subsequent PTTL experiment on the same sample, the preheat temperature was increased to 280 °C. A preheat temperature of 280 °C is expected to remove all peaks occurring at temperatures less than 280 °C. Peak IV, at 240 °C, is included in the list of peaks removed by this preheat temperature. So upon illumination and heating, any peak which occurs at a temperature less than 280 °C will be due to phototransfer. However as also noticed previously, only peak I (at 84 °C) was regenerated. PTTL glow curves obtained in this case show only two clear peaks i.e., peak I, the induced PTTL peak and peak V which is not removed by a 280 °C preheat. Figure 5.62 shows an example of such a glow curve recorded after 5 s of illumination.

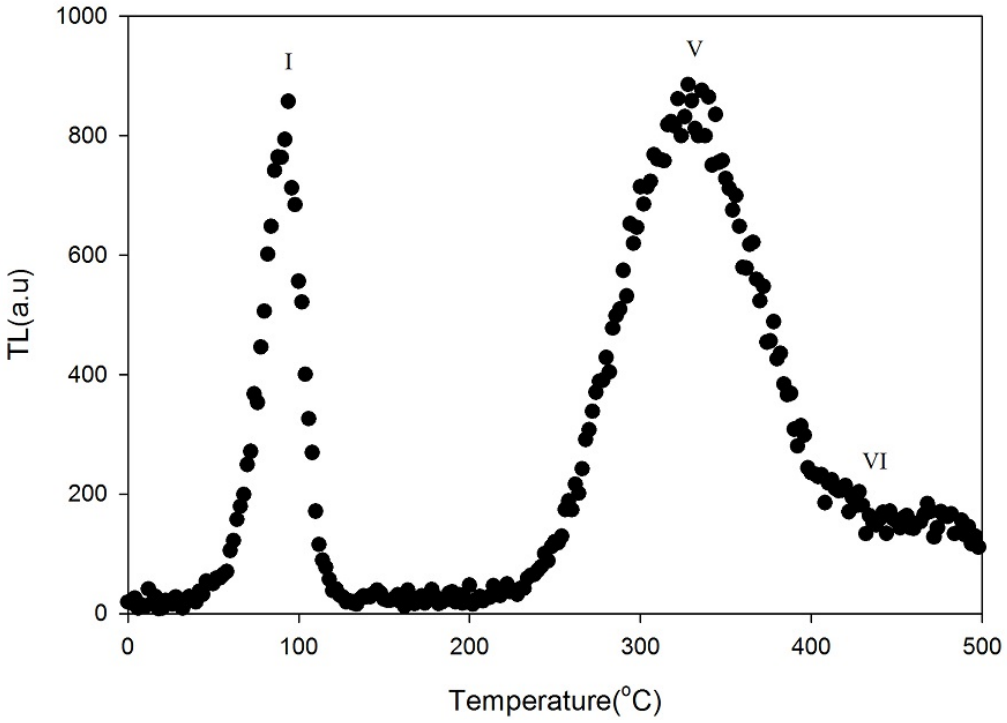

FIGURE 5.62: Example of PTTL glow curve taken at a heating rate of 5.0 °C/s after irradiation to 93 Gy, a 280 °C preheat and 5 s illumination.

At longer illumination times, Peaks II, III and IV which occur between 110 and 325 °C were still not regenerated. As shown in Figure 5.63, the intensity of the PTTL peak (peak I) decreases with illumination time. Again, the increasing part observed for a preheat to 120 °C was not seen. The fact that no increasing part was seen in Figure 5.63 may have been due to the choice of initial illumination time, so for subsequent experiments, we started at shorter illumination times (e.g., 3 s) for higher preheat temperatures (e.g., $T > 120$ °C).

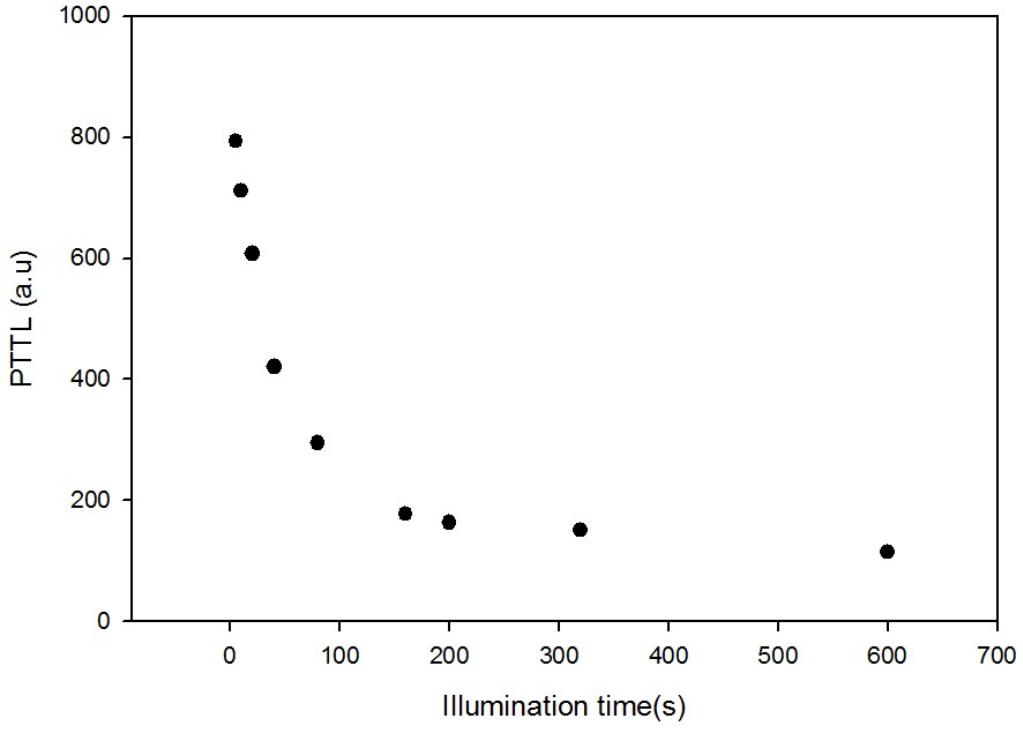

FIGURE 5.63: Influence of illumination on the intensity of the PTTL peak (peak I in Figure 5.62) for a 93 Gy irradiation dose, a 280 °C preheat and a 5.0 °C/s heating rate.

Figure 5.63 shows that for illumination times greater than 300 s, the PTTL intensity is nearly constant. A decrease in the intensity of peak V with the increase in illumination time was also observed. This decrease in the intensity of peak V (see Figure 5.64) suggests a loss of electrons from the associated traps during illumination. The regeneration of peak I may be due to some of these electrons. This therefore implies that the traps responsible for peak V may be donor traps associated with the PTTL peak.

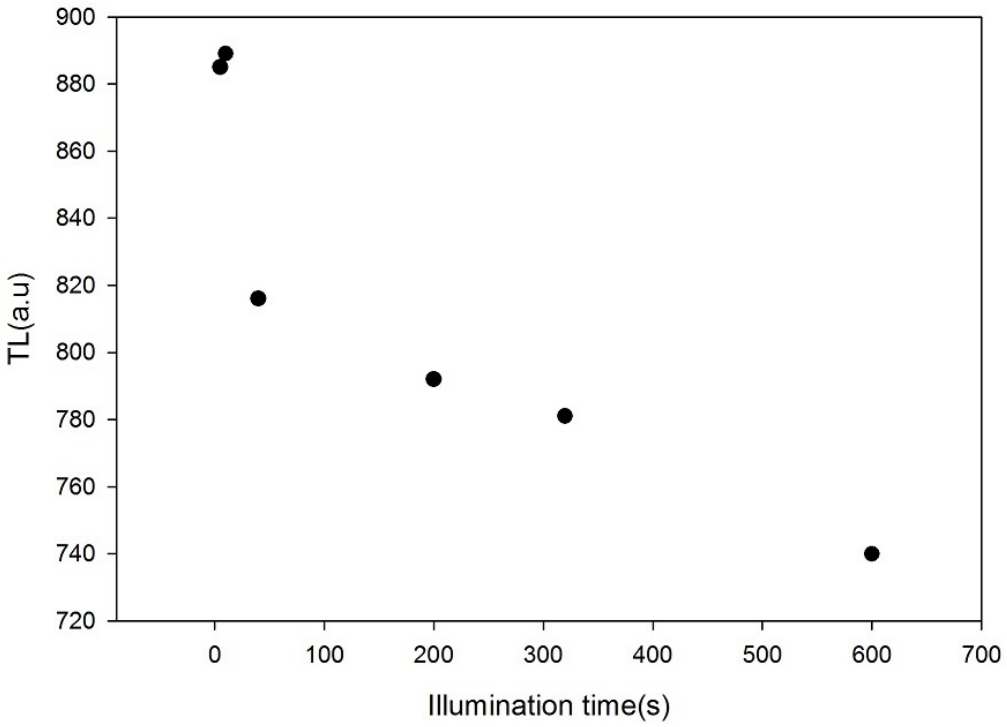

FIGURE 5.64: Effect of illumination on the intensity of peak V

We finally measured PTTL glow curves for a preheat temperature of 375 °C. Preheating to 375 °C removes all peaks including the 325 °C peak whose traps are believed to be the donor traps in this case [53, 54]. Upon heating after illumination, none of the peaks could be regenerated. Glow curves recorded in this case only showed a high temperature peak around 430 °C (peak VI) which is not due to phototransfer. An example of such a glow curve is shown in Figure 5.65.

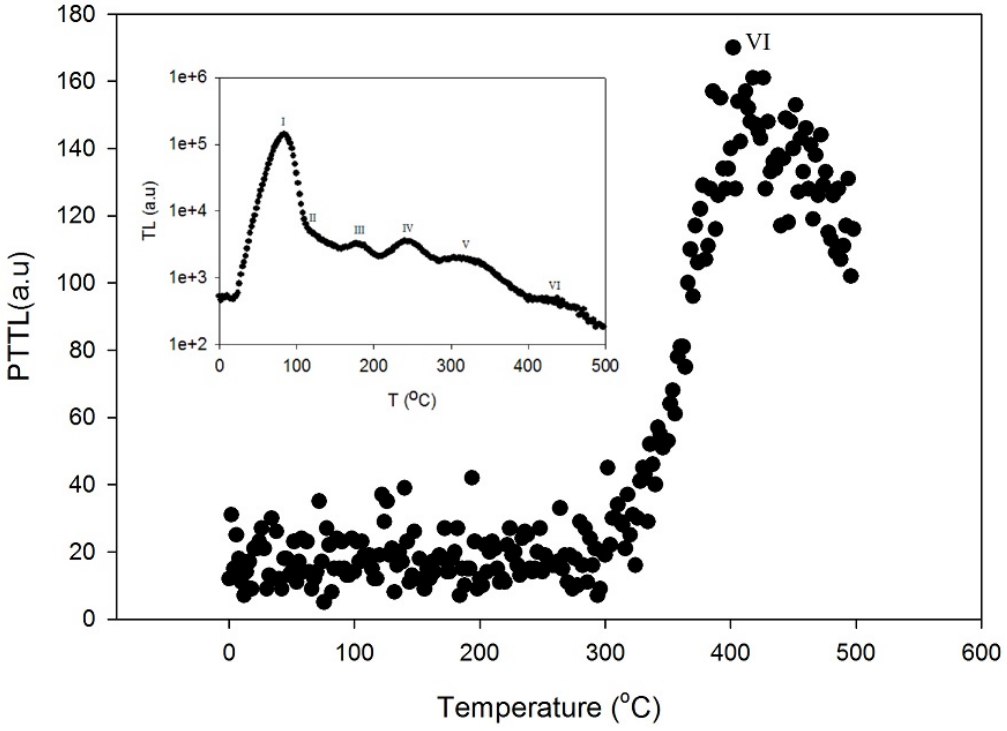

FIGURE 5.65: Glow curve measured at a rate of 5.0 °C/s from a sample irradiated to 93 Gy, preheated to 375 °C and illuminated for 5 s.

From the PTTL experiments conducted on the unannealed sample with various preheat temperatures, we found that only the main TL peak (i.e., peak I at 84 °C for a heating rate of 5.0 °C/s) was regenerated upon illumination and heating. In addition, the results suggest that the traps associated with the 325 °C peak are the main donors. However, a contribution to the PTTL from the intermediate peaks is not excluded since their respective intensities were found to decrease with illumination time.

5.3.2 Pulse annealing: unannealed sample

The influence of the preheat temperature on the peak due to phototransfer (PTTL peak) was investigated on the unannealed sample. The sequence of PTTL measurements was carried out with preheat temperatures varying from 110 °C to 600 °C in steps of 20 °C each. For each measurement, the sample was irradiated to 93 Gy, preheated, exposed to 470 nm blue light for 80 s at room temperature and heated. The heating was done at a rate of 5.0 °C/s. The sequence of measurements was carried on 3 aliquots with similar mass. Figure 5.66 shows the dependence of the PTTL signal on preheating where the PTTL signal is the average of the intensity of the PTTL peak. The uncertainty

associated with each of the measurement from the 3 aliquots is evaluated as the standard deviation from the average intensity.

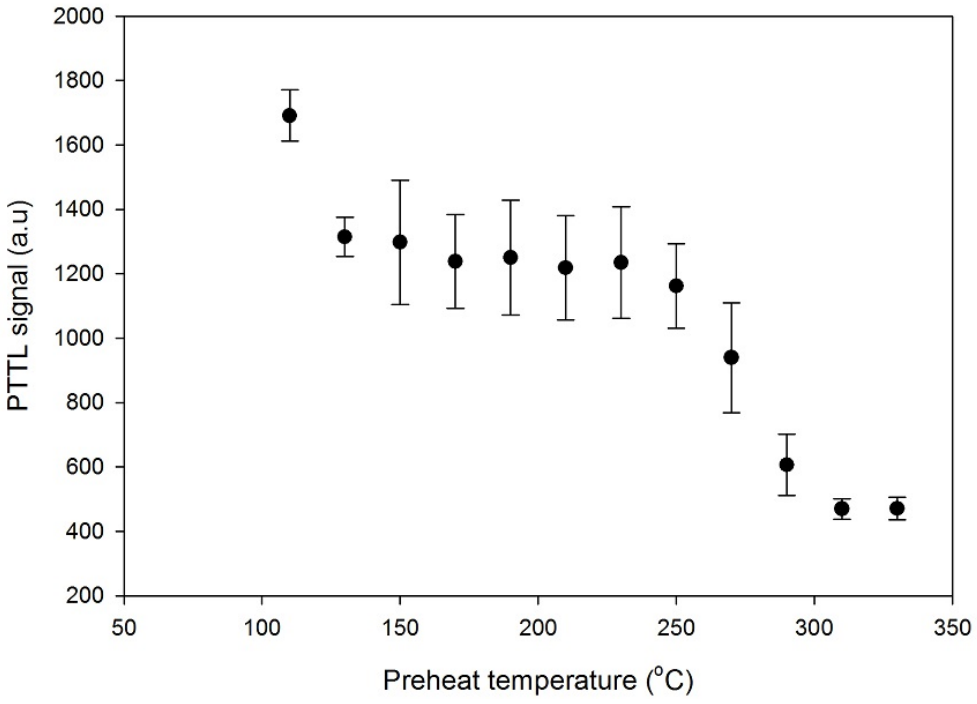

FIGURE 5.66: Effect of preheating on the PTTL peak intensity. The sample was irradiated to 93 Gy for each PTTL measurement and illuminated for 80 s.

The PTTL peak appeared at 84 °C as such, preheating to 110 °C may not have emptied the associated trap completely. This is the reason while the first data point in Figure 5.66 is relatively higher than the rest of the data points. For preheat temperatures ranging from 130 to 230 °C, the PTTL signal is constant whereas for preheat temperatures ranging from 250 to 330 °C, there is a drop in the PTTL intensity. At preheat temperatures greater than 330 °C, no PTTL was found. The result of Figure 5.66 implies that the traps associated with the intermediate peaks between 130 and 230 °C contribute little to the PTTL whereas those associated with the 325 °C peak are the main source of the PTTL. As suggested in subsection 5.3.1, for our samples, deeper traps (350 °C and above) do not contribute to the PTTL. In analytical grade quartz, Bertucci et al. [18] observed that traps at temperatures greater than 500 °C contributed to the PTTL. This is clearly not the case with our result. The difference in behaviour could be attributed to many factors such as, the sample origin and the various treatments (irradiation, heating, experimental procedure).

5.3.3 PTTL glow curves of the annealed sample

In comparison to the unannealed sample, thermal cleaning in the annealed sample revealed peaks at 83 (peak I), 154 (peak II), 178 (peak III), 240 (peak IV), 322 (peak V) and 420 °C (peak VI) for a sample irradiated to 93 Gy and heated at the rate of 5.0 °C/s. The PTTL glow curve obtained after a 120 °C preheat and 5 s of illumination is shown in Figure 5.67.

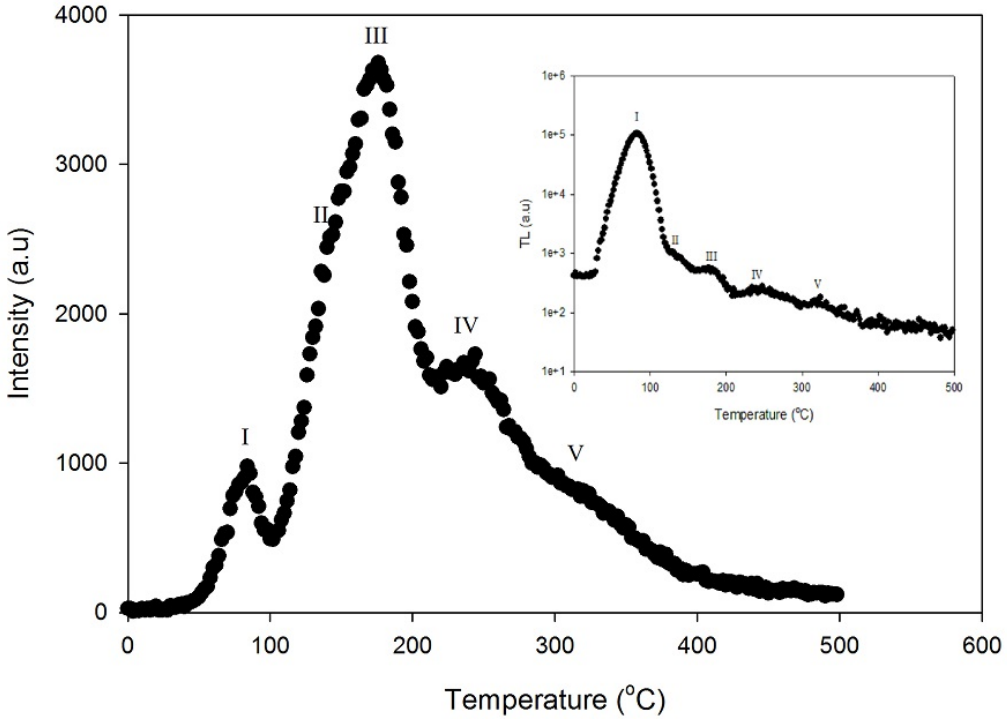

FIGURE 5.67: PTTL glow curve from natural quartz annealed at 500 °C for 10 minutes, irradiated to 93 Gy, preheated to 120 °C, illuminated for 5 s and heated at 5.0 °C/s. The peak found at 83 °C is due to phototransfer.

The PTTL glow curve shown in Figure 5.67 has prominent peaks at 83 (PTTL peak), 178 (peak III) and 240 °C (peak IV). Peak III has a weak intensity peak around 150 °C (peak II). The region of the PTTL glow curve from 250 to 500 °C is not well resolved but seems to contain at least one peak around 320 °C (peak V). As in the case of the unannealed sample, the influence of illumination time on the PTTL signal was investigated. Figure 5.68 shows the dependence of the intensity of the PTTL peak on illumination.

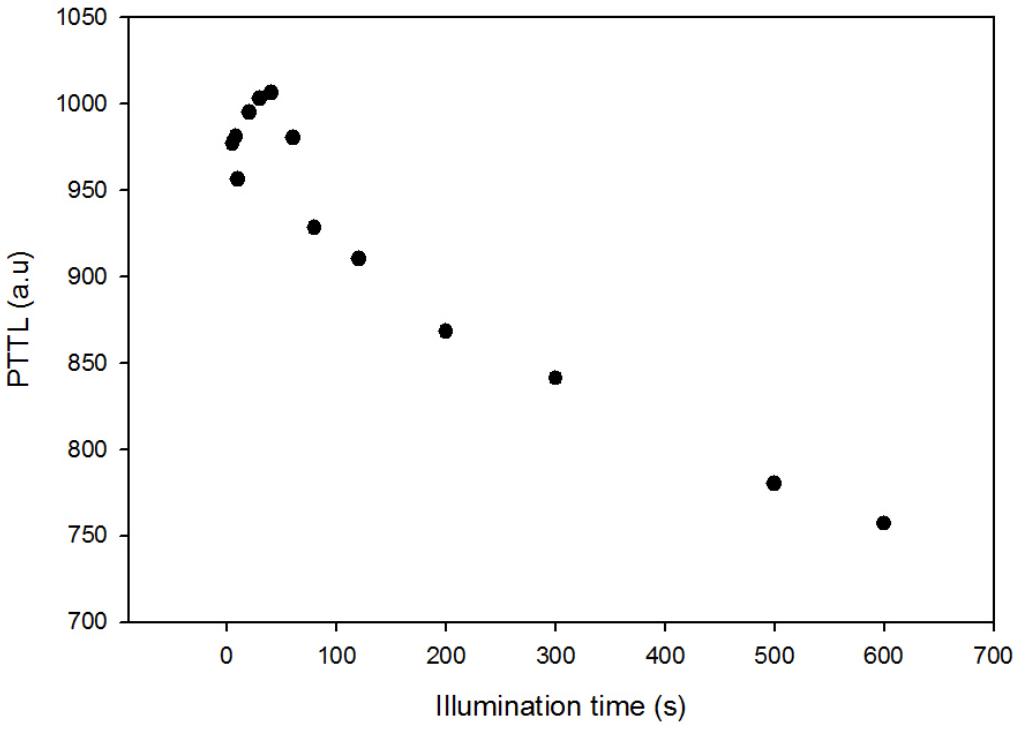

FIGURE 5.68: Dependence of the intensity of the PTTL peak on illumination time. The sample was irradiated to 93 Gy, preheated to 120 °C and measured at heating rate of 5.0 °C/s.

The PTTL peak (i.e., peak I) intensity of the annealed sample increases with illumination time up to 40 s and then decreases with further illumination up to 600 s, the maximum illumination time used. For the unannealed sample, the maximum PTTL intensity was reached at 160 s of illumination. However, for the annealed sample, the maximum intensity is reached at 40 s of illumination. The structure of the decreasing part of the dependence of PTTL peak intensity on illumination is similar for both the unannealed and annealed sample. Analysis of the peaks which are not removed by a preheat of 120 °C showed that in general, their respective intensity decreases with illumination time. Such a decrease in TL intensity with illumination time for these higher temperature peaks implies that their associated traps lose electrons as a result of illumination. Hence, they probably contribute to the PTTL resulting in peak I. Figure 5.69 shows how the TL intensity of peak III decreases with illumination time.

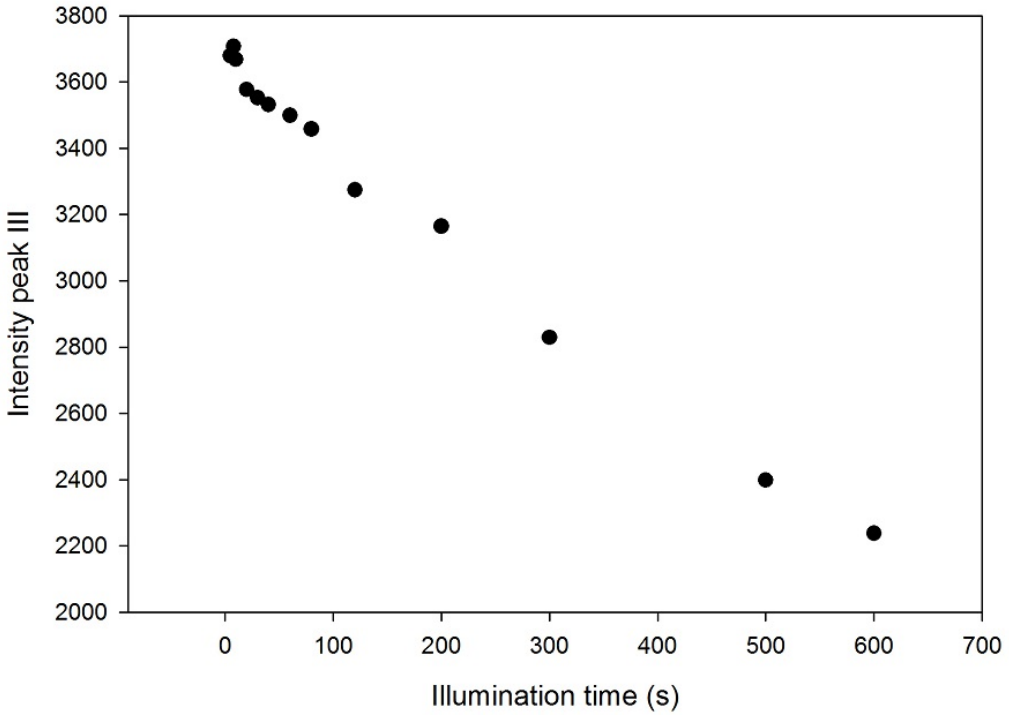

FIGURE 5.69: Effect of illumination on the TL intensity of the 178 °C peak for an irradiation dose of 93 Gy, a 120 °C preheat and a heating rate of 5.0 °C/s.

In a later experiment on the same sample, a 160 °C preheat was used to remove peak I and II. Upon illumination and heating, peak I was regenerated but peak II was not. As in the case of the unannealed sample, a plot of PTTL intensity as a function of illumination time did not show an increasing part as found when a 120 °C preheat was used. The corresponding PTTL intensity curve is shown in Figure 5.70

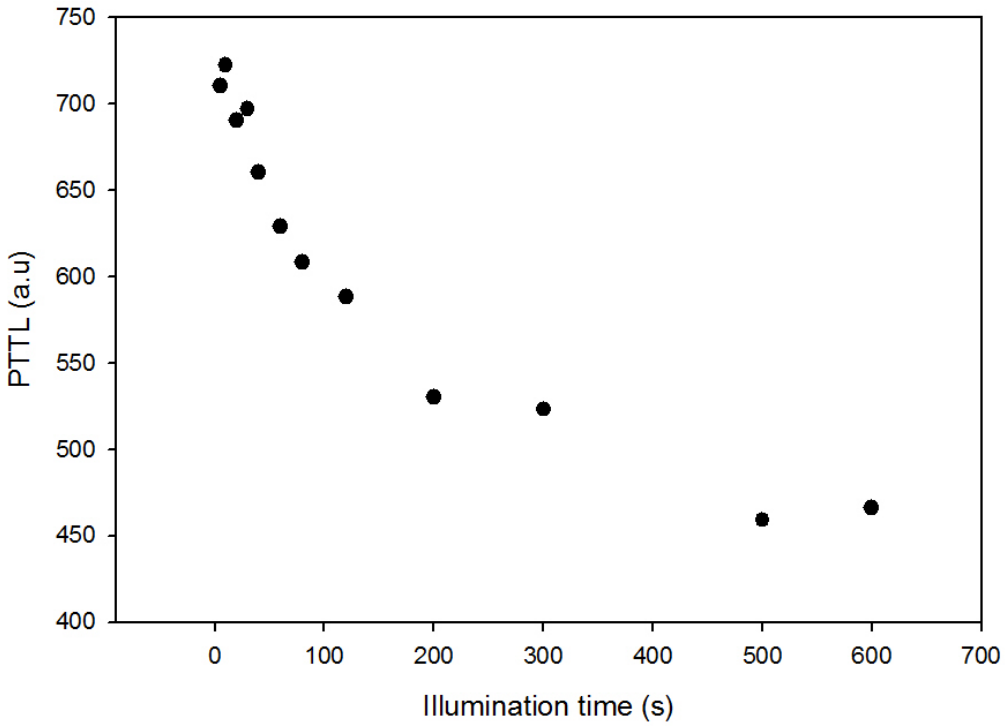

FIGURE 5.70: Effect of illumination on the PTTL peak intensity for an irradiation dose of 93 Gy, a 160 °C preheat and a heating rate of 5.0 °C/s.

To check if the intensity of the PTTL decreases continuously to a negligible value, PTTL glow curves were taken for illumination time greater than 1000 s. Figure 5.71 show the PTTL glow curve obtained with a 200 °C preheat. Again, only the main TL peak was regenerated with illumination whereas peaks II and III were not.

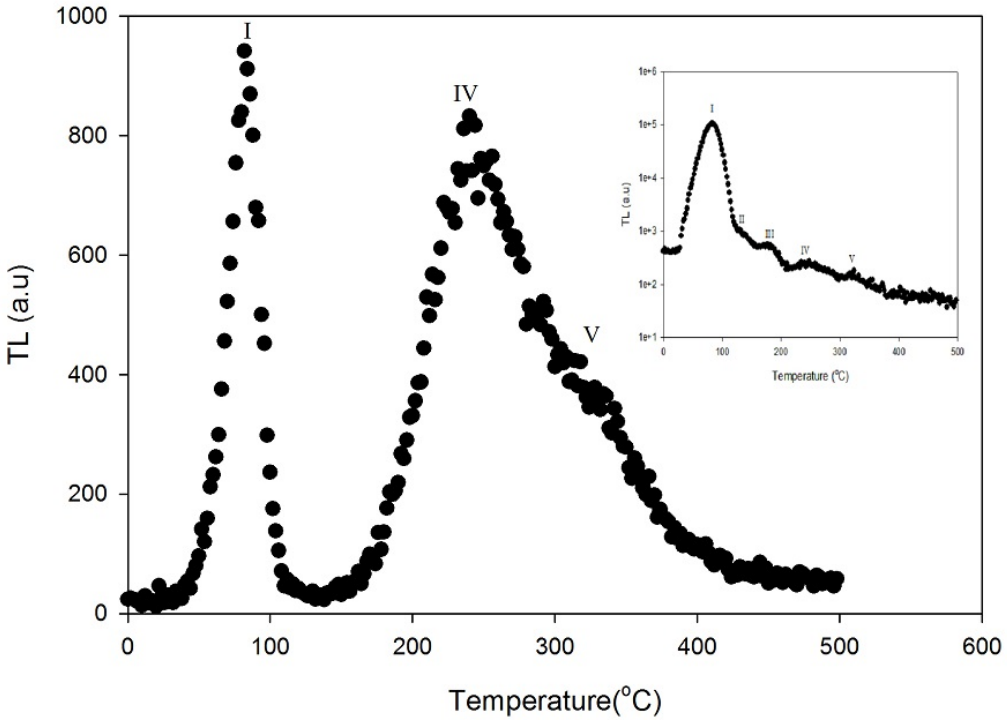

FIGURE 5.71: PTTL glow curve obtained after 5 s of illumination and 200 °C preheat for an irradiation dose of 93 Gy and a heating rate of 5.0 °C/s.

The PTTL glow curve in Figure 5.71 has 3 visible peaks namely the PTTL peak at 83 °C, peak IV at 240 °C and peak V around 330 °C. The intensity of the PTTL peak, as shown in Figure 5.72, decreases continuously with illumination time up to 2400 s the maximum time used. The intensity drops rapidly with illumination time up to 300 s but for longer illumination times, it decreases at a slower rate towards at steady value. In a subsequent PTTL experiment, a final illumination time of 3600 s was used to check if the intensity of the PTTL peak would eventually drop to zero.

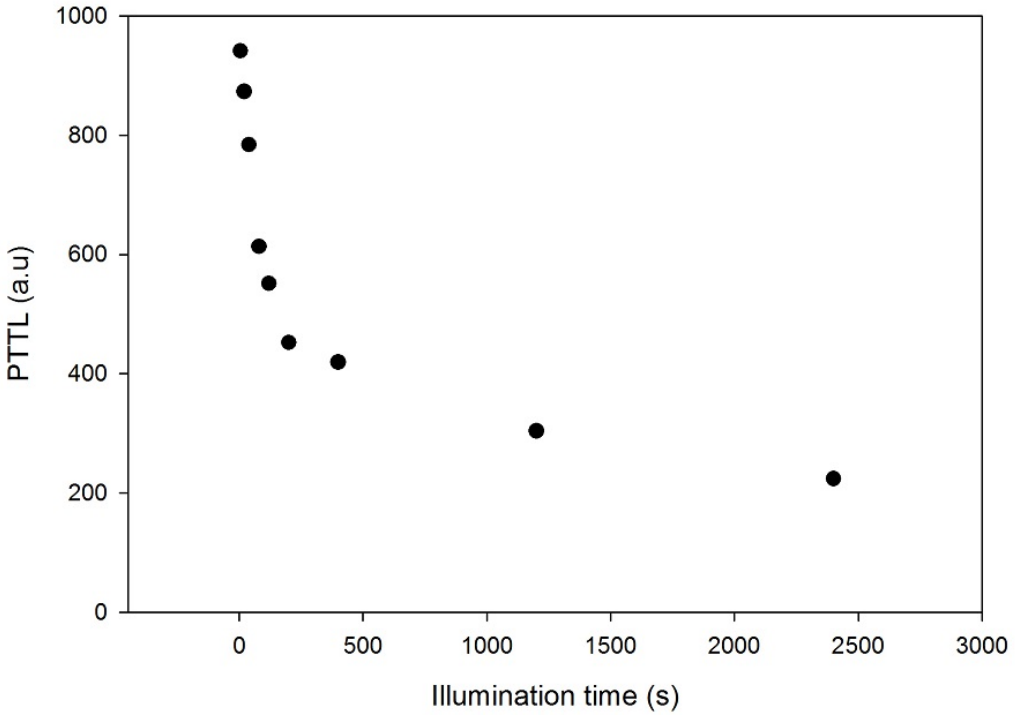

FIGURE 5.72: Influence of illumination on the PTTL peak for an irradiation dose of 93 Gy, a 200 °C preheat and a heating rate of 5.0 °C/s.

The intensity of peak IV (at 240 °C), which is not removed by preheating at 200 °C, was found to decrease with illumination time (see Figure 5.73). For short illumination times, the plot in Figure 5.73 shows some data points which we believe to be statistical scatter. It would be erroneous to think that the intensity of peak IV increases in this case before decreasing at longer illumination times because, these scattered data points do not correspond exactly to intensities measured at the smallest illumination times.

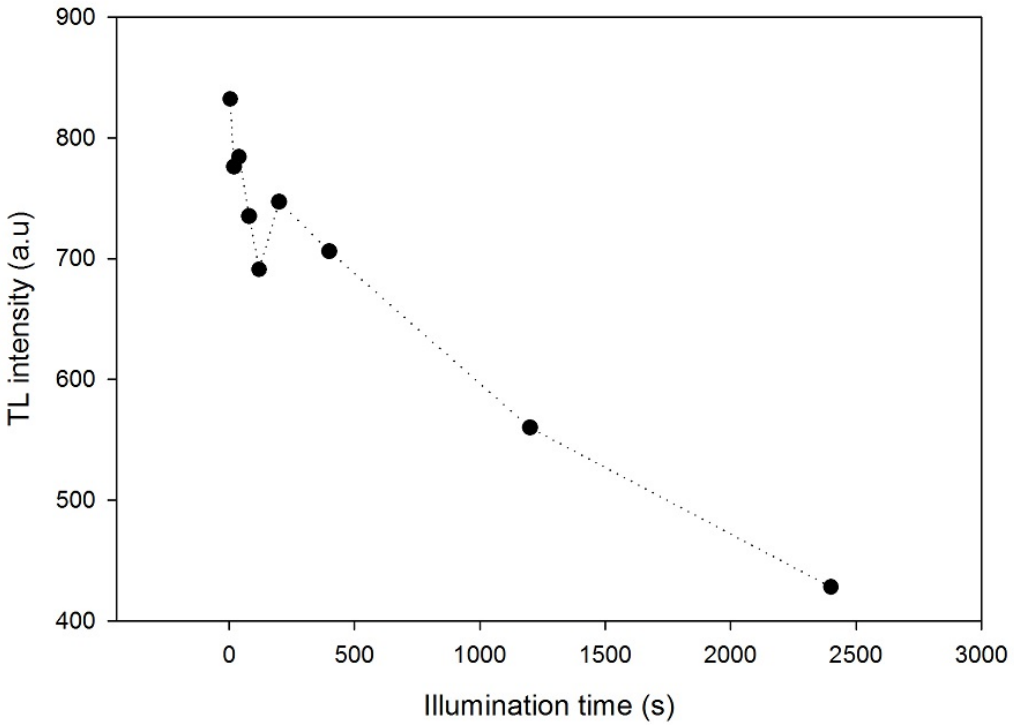

FIGURE 5.73: Dependence of peak IV (at 240 °C) on the illumination time. The dotted show the trend in the TL signal of peak IV.

Peak V (at 325 °C) is complex and difficult to analyse. However, by comparing the PTTL glow curves measured at different illumination times, it is apparent that the intensity of peak V decreases with increase in illumination time. To illustrate this observation, we present in Figures 5.74 and 5.75 the two glow curves measured after 5 s and 2400 s of illumination time respectively.

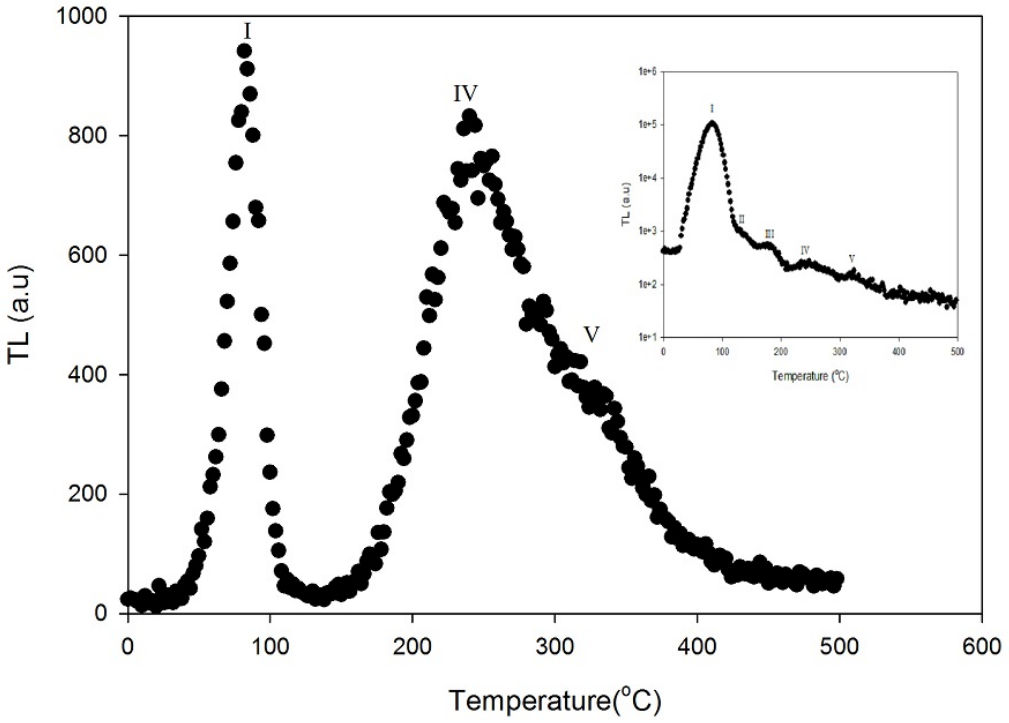

FIGURE 5.74: Glow curve measured from the sample irradiated to 93 Gy and heated at 5.0 °C/s after a 200 °C preheat and 5 s of illumination.

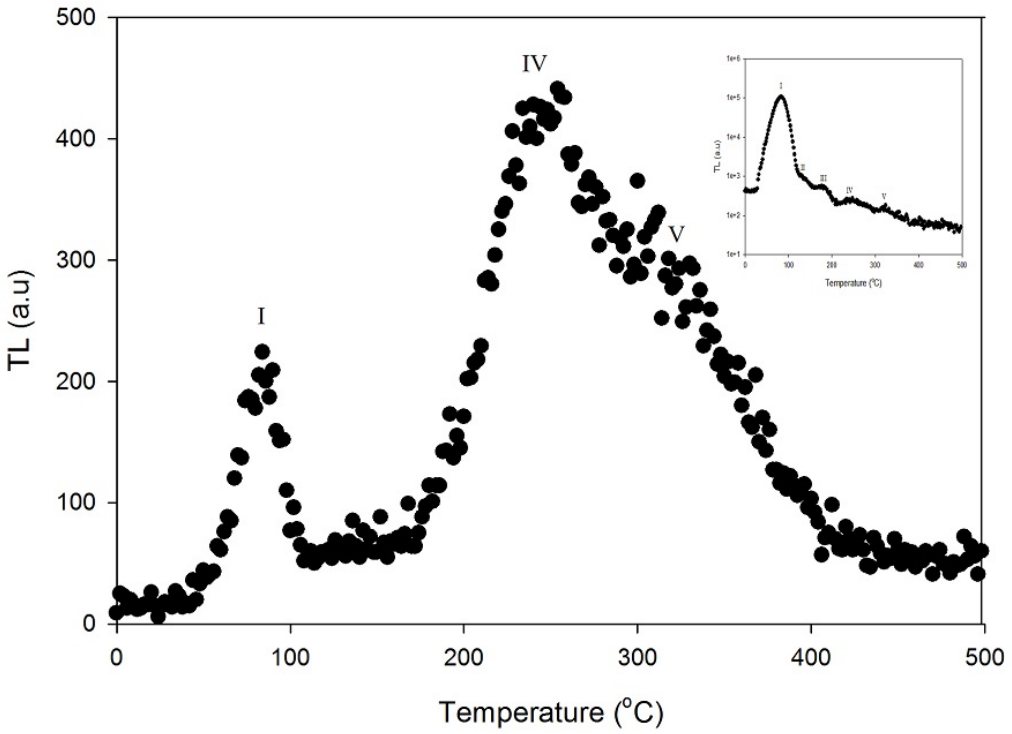

FIGURE 5.75: Glow curve measured from the sample irradiated to 93 Gy and heated at 5.0 °C/s after a 200 °C preheat and 2400 s of illumination.

From Figures 5.74 and 5.75, it can be seen that the intensity of peak V has decreased with illumination time and it becomes more difficult to distinguish peak V from the tail of peak IV.

In the following phototransfer experiment on the influence of illumination time on the intensity of the PTTL peak, we preheated the sample to 280 °C thereby removing all peaks which occur at temperatures less than 280 °C. After illumination and subsequent heating, the resulting PTTL glow curve showed only two peaks namely the PTTL peak (or peak I) at 84 °C and peak V. Figure 5.76 shows the glow curve obtained for a preheat temperature of 280 °C and 3 s of illumination.

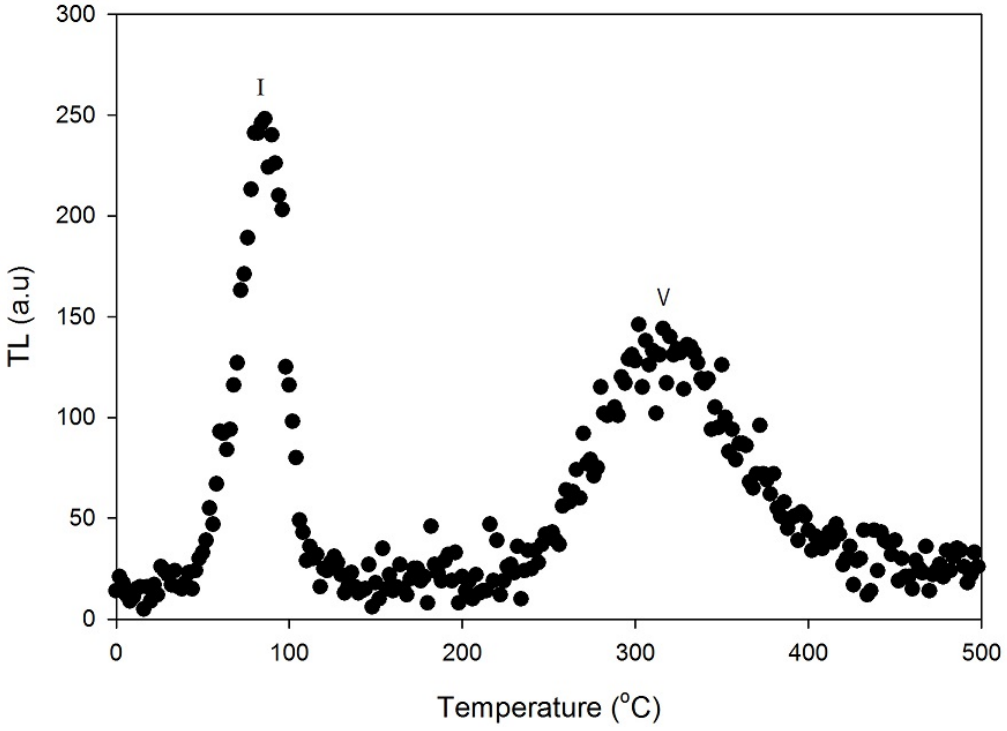

FIGURE 5.76: Glow curve measured from the sample irradiated to 93 Gy, heated at 5.0 °C/s, preheated to 280 °C and illuminated for 3 s. Peak I is due to phototransfer.

The variation in the PTTL peak intensity with illumination time is shown in Figure 5.77. Upon changing the scale of the illumination time axis to a log scale as shown in Figure 5.78, it can be seen that the PTTL peak intensity increases with illumination time from 3 to 8 s and then decreases towards a steady value at longer illumination.

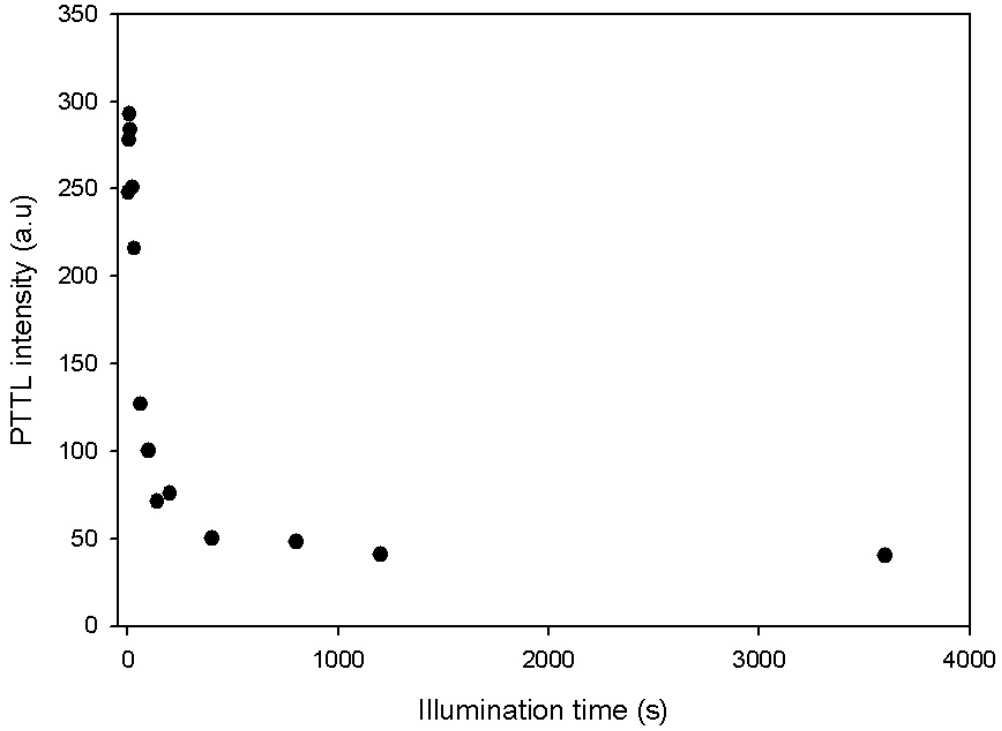

FIGURE 5.77: Intensity of the PTTL peak recorded after a 280 °C preheat on a sample irradiated to 93 Gy and heated at 5.0 °C/s.

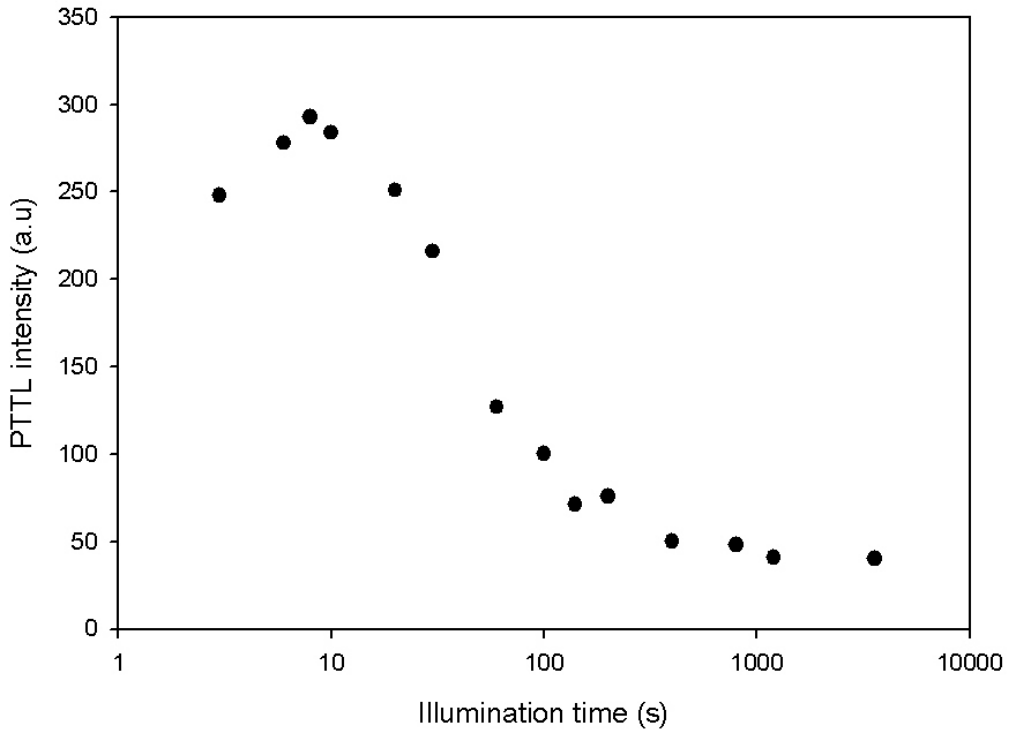

FIGURE 5.78: Intensity of the PTTL peak at 84 °C recorded after 280 °C preheat, shown on a semi-log scale

So far, our results have suggested that for both samples, that is annealed and unannealed, the traps responsible for peak V (at 325 °C) are the main traps from which charges are transferred during the illumination stage of the PTTL procedure. Removing peak V should therefore reduce the concentration of electrons released during illumination significantly. This reduction of the optically released electrons will in turn affect the PTTL. Having preheated the sample to 360 °C, we found that upon illumination and heating, the PTTL intensity recorded for various illumination times were at background level. Therefore any possible contribution from deeper traps (375 °C and beyond) is negligible. Figure 5.79 is an example of a glow curve obtained after preheating the sample to 360 °C and exposing it to light for 3 s.

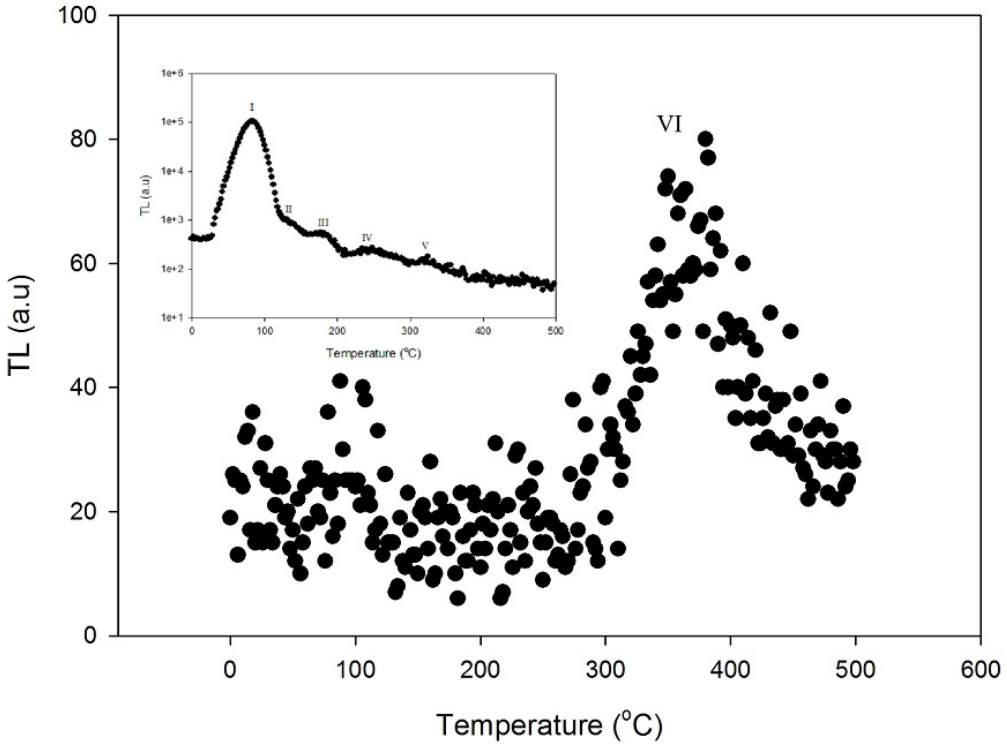

FIGURE 5.79: Example of a PTTL glow curve taken after a preheat to 360 °C. The only "visible" peak is around 390 °C. For comparison, the original TL glow curve from the same sample is shown in the inset.

5.3.4 Pulse annealing: annealed sample

A pulse annealing experiment was also carried out on the sample annealed at 500 °C for 10 minutes. The aim of the experiment was to study the effect of preheating on the PTTL signal. As such, a sequence of PTTL measurements was made with preheat temperatures varying from 90 °C to 600 °C in steps of 20 °C each. The irradiation dose was kept at 93 Gy. For each PTTL measurement, the sample was illuminated with 470 nm blue light for 80 s at room temperature and the heating was done at a rate of 5.0 °C/s. The background signal was recorded and subtracted from each of the PTTL glow curves during analysis. Figure 5.80 shows the effect of preheating on the PTTL peak intensity where the peak intensity is the normalised area under the PTTL peak.

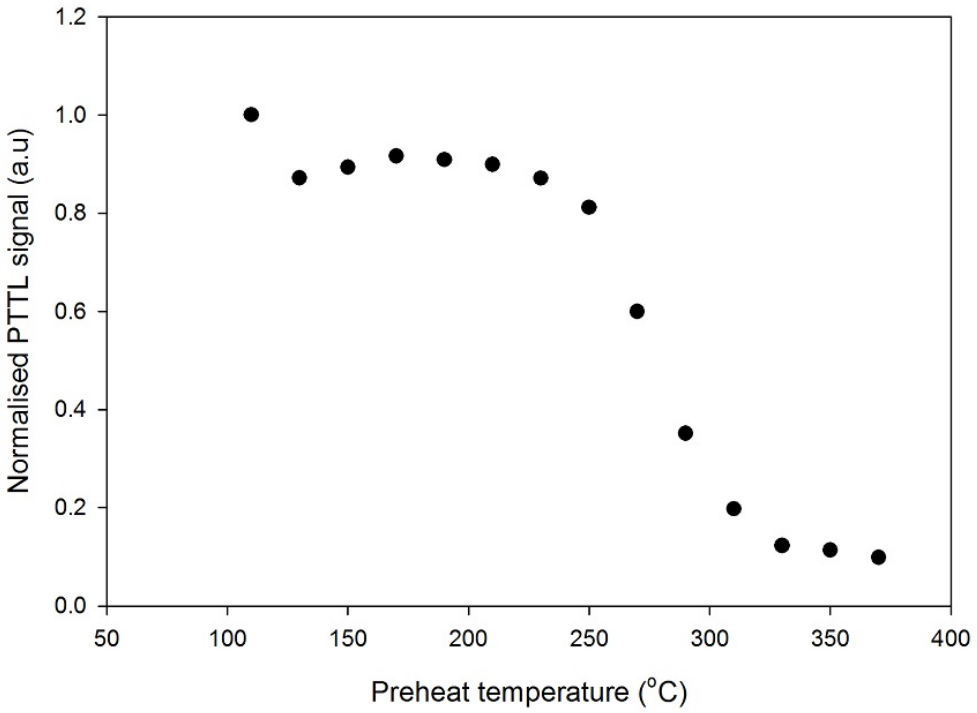

FIGURE 5.80: Effect of preheating on the PTTL peak intensity. The sample was irradiated to 93 Gy for each PTTL measurement and illuminated for 80 s.

The plot shown in Figure 5.80 can be seen as consisting of three regions. In the first region, which ranges from 100 to 200 °C, the intensity of the PTTL peak is nearly constant. The second region, from 220 to 330 °C shows a drastic drop in PTTL intensity. For preheat temperatures beyond 390 °C, the PTTL signal was negligible and indistinguishable from the background signal. This is the reason why the axis showing the preheat temperature only goes up to 400 °C instead of 600 °C, the maximum preheat temperature used. The result presented in Figure 5.80 is consistent with the suggestion that the traps associated with the 325 °C (peak V) are the main contributors to the PTTL. The fact that no PTTL could be measured for preheat temperature greater than 390 °C supports our earlier observation in subsection 5.3.3 (Figure 5.79) about the negligible contribution from deeper traps to the PTTL.

5.3.5 Discussion of PTTL signals

The study of the PTTL of natural quartz (unannealed and annealed) presented here shows that only the main TL peak is regenerated after illumination with 470 nm blue light and heating. The intensities of the intermediate peaks at 140, 178 and 240 °C decrease with the increase in illumination time. The traps responsible for the 325 °C

peak (peak V) are evidently the main source of the optically transferred charges which lead to PTTL. We believe that the contribution of deeper traps (375 °C and above) to the PTTL is negligible. For a preheat to 120 °C, the intensity of the phototransferred peak grows with illumination time up to a maximum and then decreases afterwards. For the annealed sample, the maximum intensity is reached at 40 s of illumination whereas for the unannealed sample, it is reached at 160 s. For higher preheat temperatures, and except for the 280 °C preheat (Figure 5.78), the build up part of the PTTL dependence on illumination time is not observed.

At longer illumination times (e.g., 30 min, 1 h), irrespective of whether the sample is annealed or not, the PTTL signal decreases to a non-zero level. PTTL signals decreasing to a non-zero residual value were also reported by Milanovich-Reichhalter and Vana [20]. Studies of time and wavelength responses of PTTL from several types of quartz, conducted by Alexander et al. [22] also revealed PTTL peaks with intensities increasing with illumination up to a maximum and then decreasing to a non-zero value.

As described in section 2.1, the simple model of PTTL, which consists of a donor trap, a shallow trap and radiative recombination centre can only predict the decreasing part of the PTTL response to illumination if it is assumed that during the PTTL procedure, some of the electrons from the shallow trap are lost due to optical stimulation. However with this assumption, the PTTL signal will eventually decrease to zero and not necessarily to non-zero constant value [22]. With the inclusion of a non-radiative recombination centre, as described in section 2.2, the non-zero steady value of the PTTL signal at longer illumination time can be explained. Hence, the model proposed by Bøtter-Jensen et al. [24] to explain the sensitivity changes in quartz as a result of annealing is a valid PTTL model for the present study.

5.3.6 Kinetic analysis of the PTTL peak

For both samples, annealed and unannealed, the intensity of the PTTL peak was typically 2 to 3 orders of magnitude less than the intensity of the main TL peak in the corresponding samples. Hence, the IR method of analysis failed for the PTTL peak because we could not get data which satisfied the criterion for applying this method.

The PS method too did not yield reliable results. The failure of the PS method was due to the fact that in some instances the approximated values of the temperatures T_1 and T_2 corresponding to the value of the intensity at full width half maximum were very far from the actual values. Table 5.9 shows results obtained from the PS method in the

case of the unnanealed sample for a 200 °C preheat, a heating rate of 5.0 °C/s and a dose of 93 Gy. The illumination time is represented by t. The only reliable values of T_1

TABLE 5.9: Geometric factors and activation energy E computed using Chen's equations [34] for the PTTL glow peak of the unannealed sample.

t(s)	$T_M(K)$	$T_1(K)$	$T_2(K)$	τ	δ	ω	$\mu_g = \tau/\omega$	E_τ(eV)	E_δ(eV)	E_ω(eV)
5	357.15	343.15	369.15	14	12	26	0.46	1.17	1.17	1.24
10	359.15	341.15	369.15	18	10	28	0.36	0.73	0.57	0.74
40	357.15	341.15	367.15	16	10	26	0.38	0.88	0.79	0.91
80	359.15	343.15	367.15	16	8	24	0.33	0.79	0.48	0.76
120	357.15	341.15	369.15	16	12	28	0.43	0.95	0.95	1.02
160	357.15	343.15	367.15	14	10	24	0.42	1.08	1.04	1.14
300	359.15	341.15	369.15	18	10	28	0.36	0.73	0.57	0.74

and T_2 in Table 5.9 were those corresponding to $\mu_g = 0.43$ because in that case, T_1 and T_2 were close to the expected values. The corresponding values of E_τ, E_δ and E_ω are 0.95 , 0.95 and 1.02 eV respectively. In addition the peak shape method could only be tried for preheat temperatures $\geq$ 200 °C since these temperatures gave complete PTTL peaks.

5.3.6.1 Variable heating rate: unannealed sample

The influence of heating rate on the PTTL peak was studied for heating rates between 0.2 and 5.0 °C/s. For this purpose, the unannealed sample was irradiated to 93 Gy, preheated to 120 °C and illuminated for 160 s for each of the measurements. As in the case of the normal TL glow curve, we observed a shift of the PTTL peak towards higher temperature as the heating rate was increased. This shift in peak temperature was associated with a decrease in intensity. The decrease in peak intensity implies that the peak due to phototransfer also suffers from thermal quenching. Figure 5.81 and 5.82 show the effect of heating rate on the temperature and the intensity of the PTTL peak respectively.

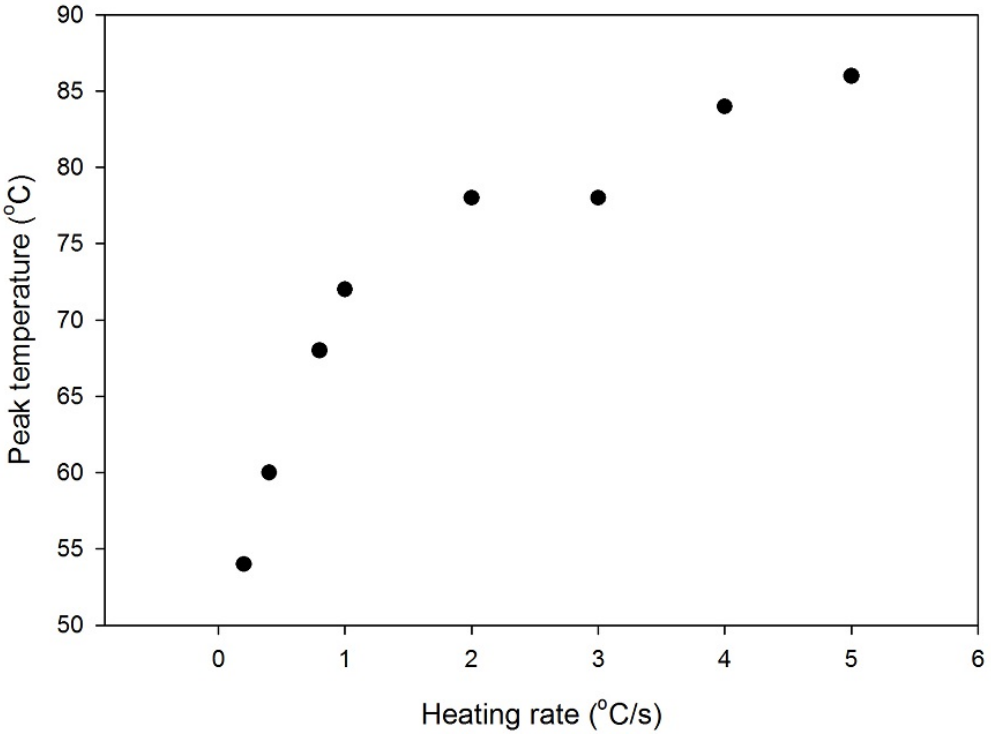

FIGURE 5.81: Influence of heating rate on the temperature of the PTTL peak (i.e., peak I) for an irradiation dose of 93 Gy, a 120 °C preheat and 160 s of illumination.

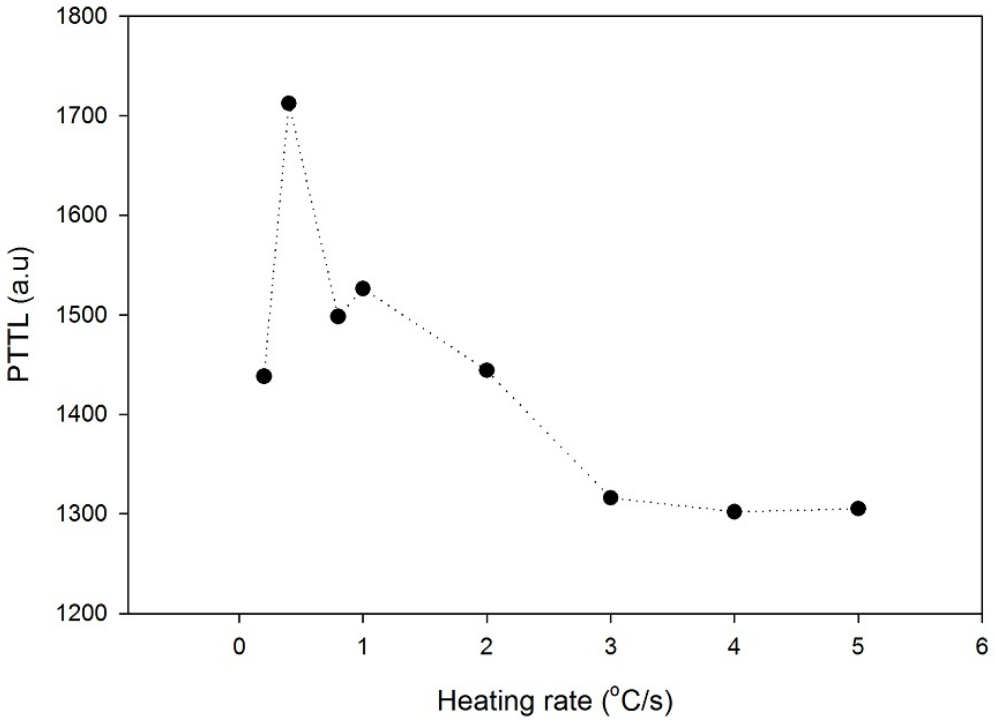

FIGURE 5.82: Influence of heating rate on the intensity of the PTTL peak for an irradiation dose of 93 Gy, a 120 °C preheat and 160 s of illumination.

The Hoogenstraaten [29] method of analysis was then used to derive the activation energy E of the PTTL peak. Figure 5.83 shows the plot of $\ln(T_M^2/\beta)$ against $1/kT_M$. The value of the activation energy E determined from this plot was 0.96 ± 0.06 eV and that of the frequency factor s was 1.2×10^{13} s^{-1}. This value of E is comparable with the various values of E obtained for the main TL peak of the unannealed sample (e.g., 0.92 ± 0.02 eV from the IR method and 0.88 ± 0.02 eV from variable heating rate, and the values of E reported in Table 5.1).

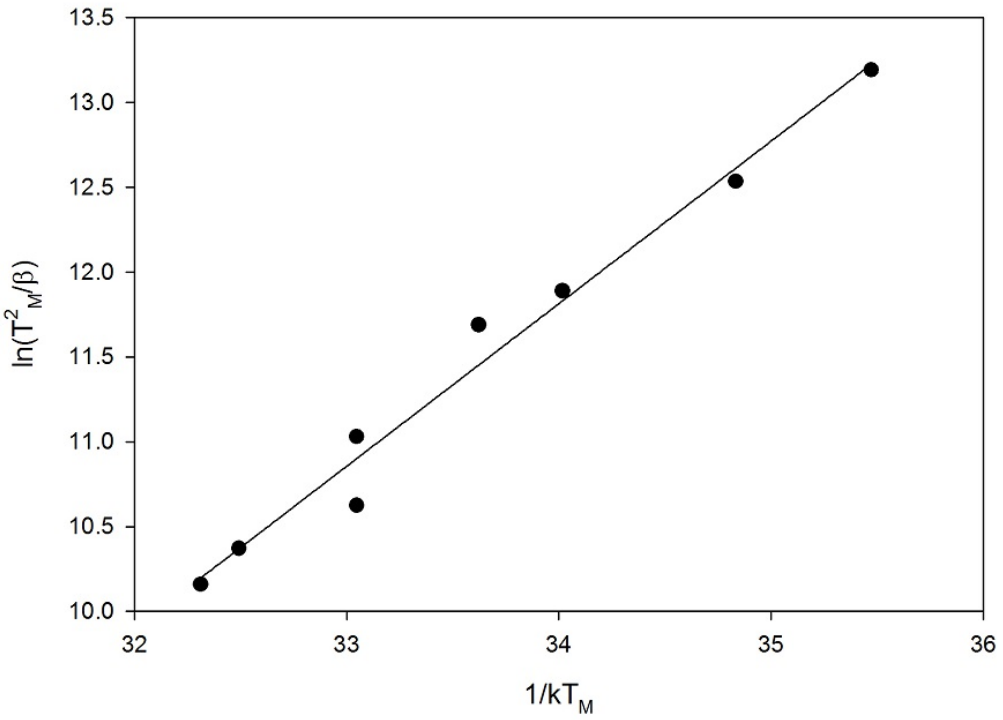

FIGURE 5.83: Plot of $\ln(T_M^2/\beta)$ as a function of $1/kT_M$ used to determine E and s.

5.3.6.2 Variable heating rate: annealed sample

The effect of heating rate was also investigated on the PTTL peak of the annealed sample. A sequence of PTTL measurements were taken on the annealed sample for heating rates ranging from 0.2 to 5.0 °C/s. For each measurement, the sample was irradiated to 93 Gy preheated to 120 °C and illuminated for 40 s. Figure 5.84 shows the shift in the PTTL peak temperature with heating rate.

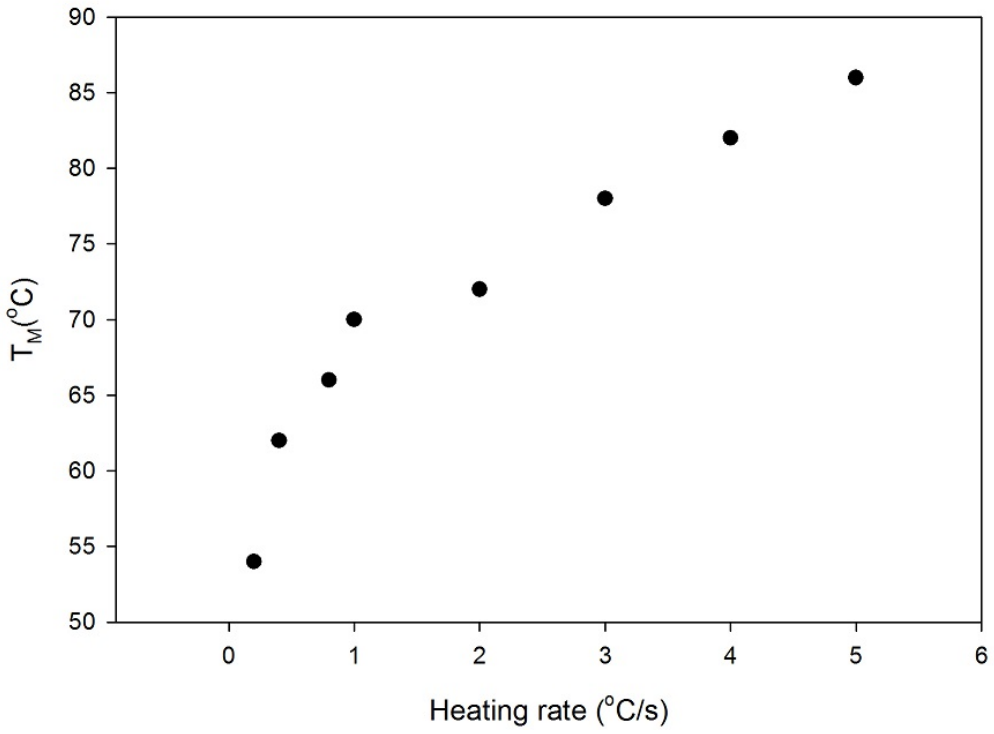

FIGURE 5.84: Influence of heating rate on the temperature of the PTTL peak for an irradiation dose of 93 Gy, a 120 °C preheat and 40 s of illumination.

As in the case of the main TL peak of the annealed sample, the PTTL peak also shifted to higher temperatures with the increase in heating rate. The intensity of the PTTL peak increased after the first measurement at 0.2 °C/s and then decreased with heating rate from 0.4 to 5.0 °C/s as shown in Figure 5.85

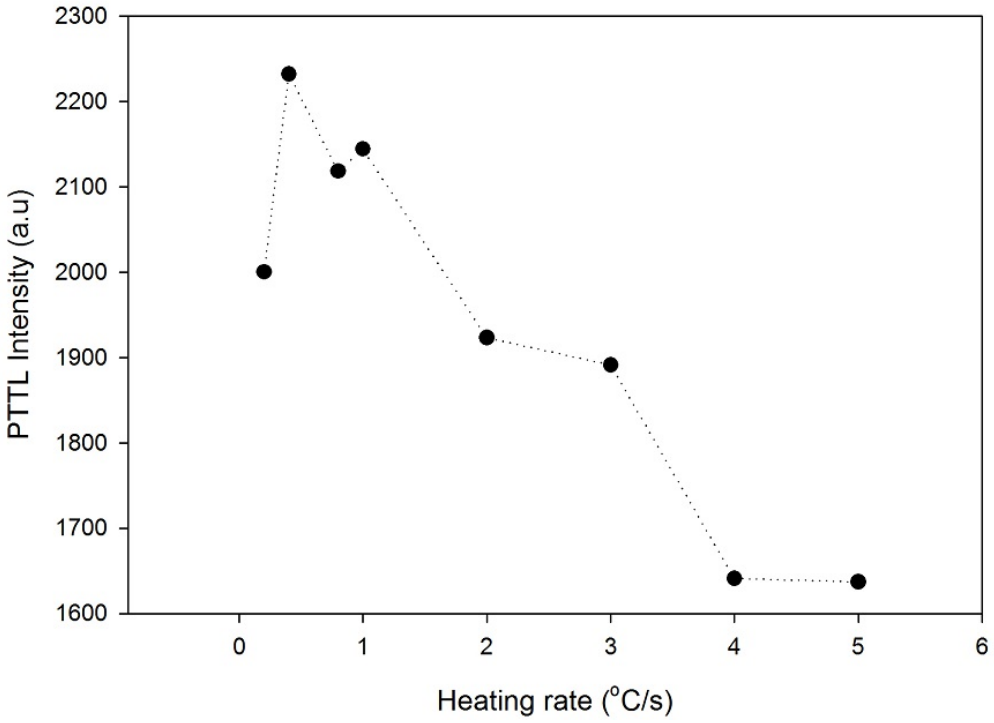

FIGURE 5.85: Influence of heating rate on the intensity of the PTTL peak for an irradiation dose of 93 Gy, a 120 °C preheat and 40 s of illumination. The decrease in intensity is an indication of thermal quenching.

The activation energy E of the PTTL peak and the frequency factor s were then evaluated from the Hoogenstraaten [29] method of analysis. From the plot of $\ln(T_M^2/\beta)$ against $1/kT_M$, shown in Figure 5.86, we found $E = 1.02 \pm 0.07$ eV and $s = 1.11 \times 10^{14}$ s^{-1}. This value of the activation energy is consistent with the values of E obtained for the main TL peak of the annealed sample (e.g., 0.89 ± 0.02 eV from variable heating rate analysis, 0.96 ± 0.03 eV from IR, 1.03 ± 0.04 eV from the influence of repeated measurement on the activation energy, and the values of E reported in Table 5.7)

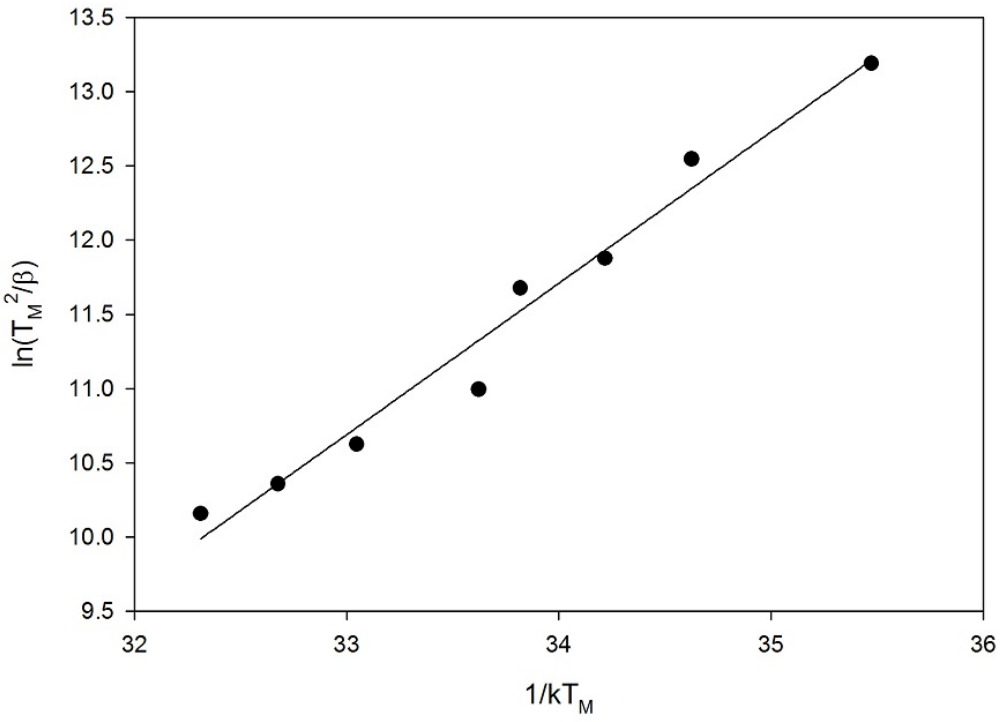

FIGURE 5.86: Plot of $\ln(T_M^2/\beta)$ as a function of $1/kT_M$ used to determine E and s for the PTTL peak of the annealed sample.

5.3.7 Dosimetric features of the PTTL peak: annealed sample

5.3.7.1 Dose dependence of the PTTL peak

The influence of irradiation on the PTTL peak was investigated on the annealed sample. For this purpose, a sequence of PTTL measurements were carried out on the same aliquot of the annealed sample. The experimental procedure was similar to the PTTL procedure described in section 5.3. As for the study of the dose response of the original TL peak, the irradiation dose was varied from 2 to 151 Gy. The sample was illuminated for 40 s during each measurement. Preheat temperatures of 120, 160 and 200 °C were used. These temperature were chosen to progressively remove the intermediate peaks in the original TL glow curve of the sample and to observe their effect if any on the dose response of the PTTL peak. The sequence of PTTL measurements associated with each preheat temperature was repeated three times. A heating rate of 5.0 °C/s was used for all measurements. Figure 5.87 shows the dependence of the PTTL peak temperature on irradiation dose for a preheat of 120 °C.

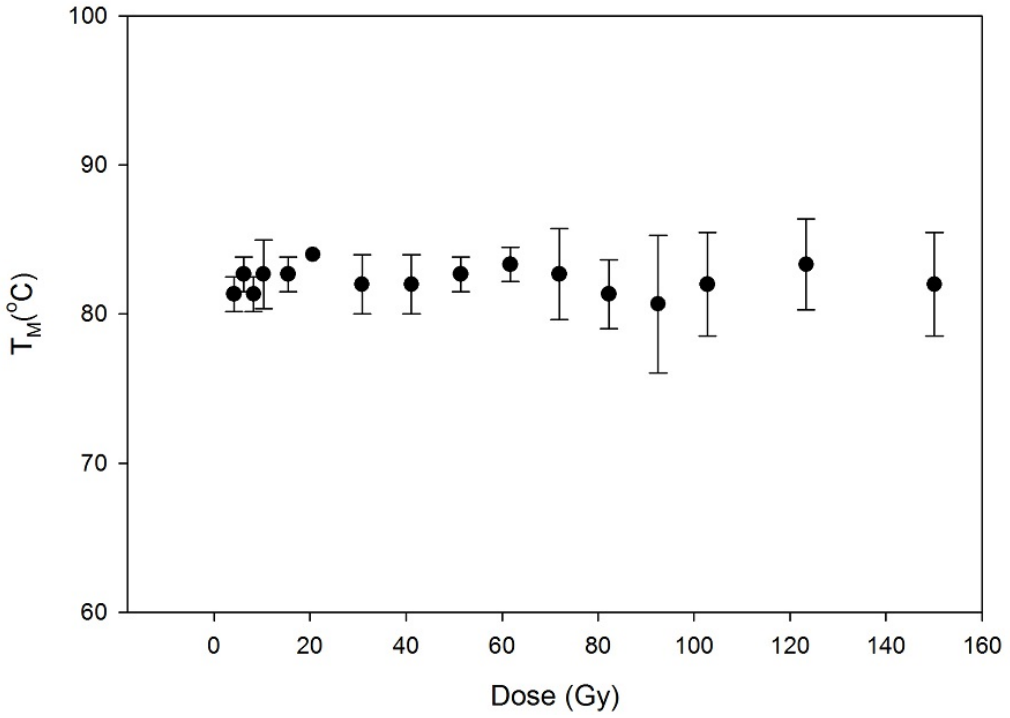

FIGURE 5.87: Dependence of the PTTL peak temperature on the irradiation dose for a preheat of 120 °C and a heating rate of 5.0 °C/s. Each data point corresponds to the average temperature obtained at a given dose for the sequence of measurements repeated three times.

The result, presented in Figure 5.87, shows that the temperature of the PTTL peak is independent of the dose, suggesting that the PTTL peak of the annealed sample follows a first-order behaviour. Therefore, the peak induced by phototransfer and the original main peak follows the same order of kinetics.

The dependence of the peak intensity on the irradiation dose is shown in Figure 5.88.

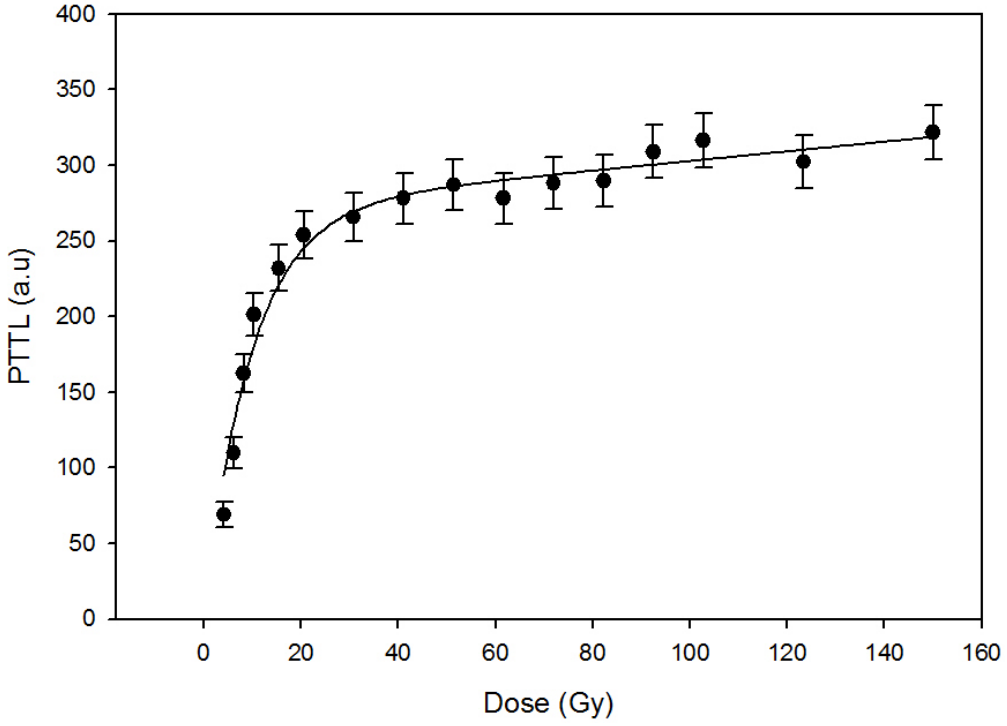

FIGURE 5.88: Dependence of the PTTL peak intensity on dose for a preheat of 120 °C and a heating rate of 5.0 °C/s. Each data point corresponds to the average peak intensity obtained at a given dose for the sequence of measurements repeated three times. The error bar were evaluated using the square root of each value. The solid line is the fit obtained from equation (5.7).

The dose response of the PTTL peak of the annealed sample behaves similarly to that of the main TL peak of the annealed and unannealed sample. In other words, The PTTL grows linearly with doses ranging from 2 to about 10 Gy. For doses in the intermediate range from 10 to 60 Gy, the response is sub-linear and for greater doses, it is linear. As pointed out earlier in subsection 5.1.4.1, for this qualitative description of the dose response, the deviation from linearity is with respect to the initial linear region from 2 to 10 Gy.

Results similar to those presented in Figure 5.87 and 5.88 were found for preheat temperatures of 160 and 200 °C respectively. Figure 5.89 shows the dose responses obtained for each of the preheat temperatures.

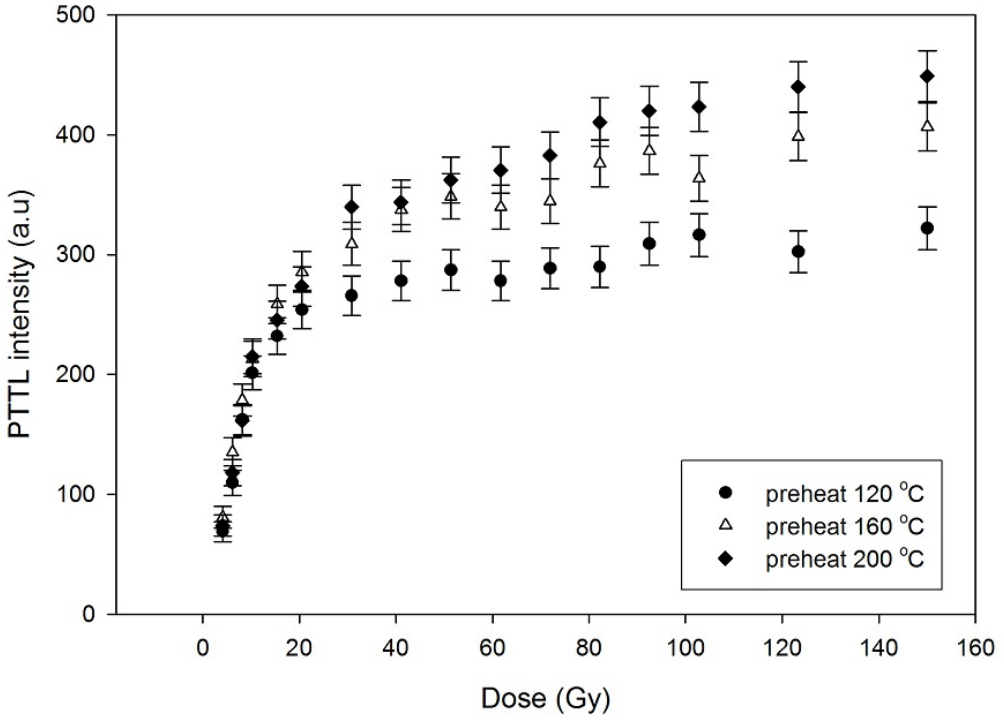

FIGURE 5.89: Dose response of the PTTL peak shown for preheat temperatures of 120, 160 and 200 °C respectively and a heating rate of 5.0 °C/s. Each data point is the average peak intensity obtained at a given dose for the sequence of measurements repeated three times. The error bar were evaluated as the square root of each value.

Figure 5.89 shows that for irradiation doses between 2 and 20 Gy, the intensity of the PTTL peak is the same irrespective of the preheat temperature (at least for preheat temperatures used here). However, for irradiation doses greater than 20 Gy, an increase in the PTTL peak intensity with the preheat temperature is observed. Such an increase can be attributed to the fact that as the preheat temperature increases, the intermediate peaks at 140 and 180 °C are progressively removed. Since PTTL measurements carried out during this work showed that only the main peak is regenerated by phototransfer, the removal of the 140 and 180 °C peaks would therefore imply that there are more electrons available for recombination from the donor traps leading to an increase in PTTL intensity.

5.3.7.2 Influence of delayed stimulation on PTTL peak

The influence of delay between optical exposure and thermal stimulation was investigated on the PTTL peak of the annealed sample. The experimental procedure was similar to the normal PTTL procedure except that after illumination, the heating was delayed. For

each PTTL measurement, the annealed sample was irradiated to 93 Gy and preheated to 200 °C at a rate of 5.0 °C/s. The heating was delayed for 1, 2, 4 or 6 h respectively. Figure 5.90 shows the exponential decrease in the intensity of the PTTL peak as a function of the delay time.

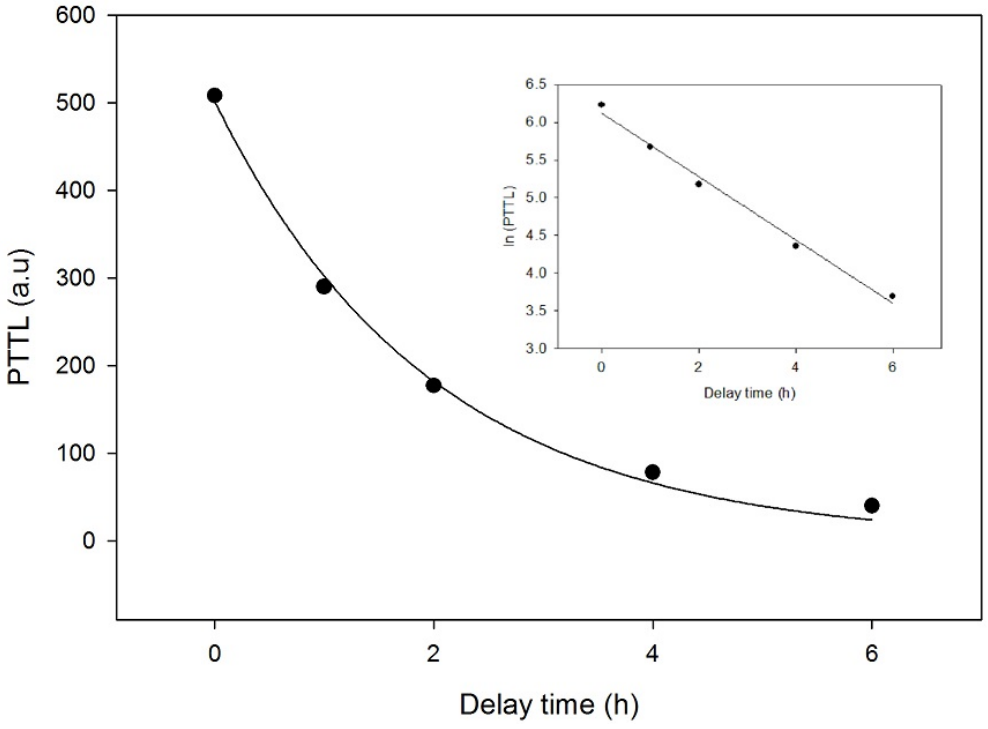

FIGURE 5.90: Effect of delayed stimulation on the intensity of the PTTL peak for an irradiation dose of 93 Gy; a preheat to 200 °C and 40 s of illumination. The solid line is the fit obtained from equation (5.9). The inset shows the $\ln(PTTL)$ versus time, which confirms the exponential feature of the decay.

The decay constant f derived from the fit shown in Figure 5.90 was 0.50 h^{-1}. This decay constant yields a half-life of 1.40 h. The half-life of the PTTL peak from the annealed sample is therefore greater than the half-lifes of the main TL peak in the annealed (1.17 h) and unannealed (1.26 h) sample respectively.

The kinetic analysis shows that the features of the PTTL peak such as the dose response, the order of kinetics and the fading, are similar to those of the original TL peak. In both cases, the order of kinetics f is the same and the half-life of the peaks are comparable.

In order to understand the dynamic of charges which leads to the fading of the PTTL peak, we studied the behaviour of the other peaks during the delay period. For each of the preheat temperatures used, we plotted the ratio between the intensity of each peak and that of peak I (peak due to phototransfer). Figure 5.91 shows the ratio between the intensity of peak V (325 °C) and that of the PTTL peak against delay time.

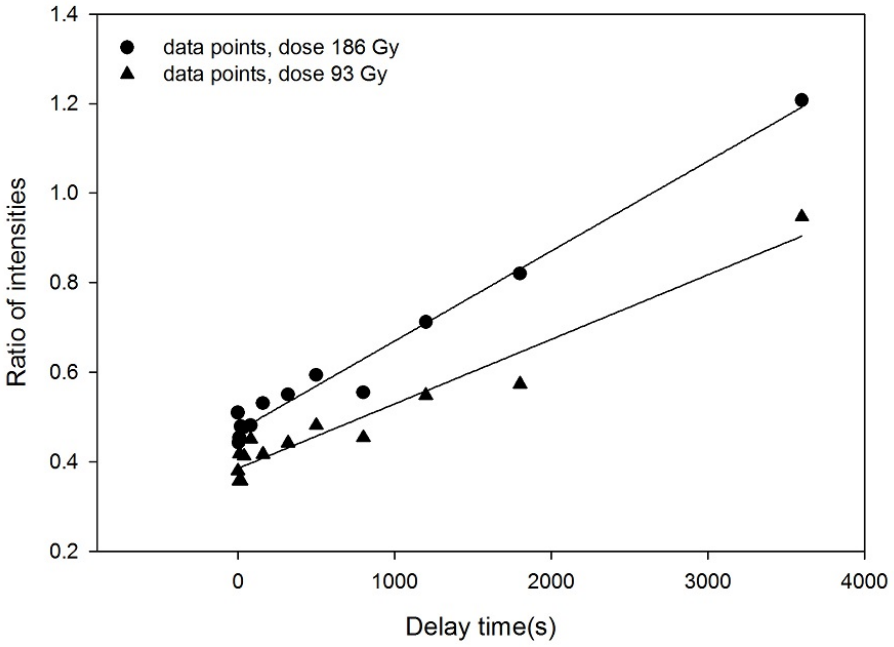

FIGURE 5.91: A plot showing the ratio of intensities (I_5/I_1) between peak V and peak I for a preheat temperature of 280 °C and 160 s of illumination. The sample was heated at a rate of 5.0 °C/s and the measurement was performed for irradiation doses of 93 and 186 Gy respectively. The solid line is the straight line fit through each set of data points.

The important feature in Figure 5.91 is the increase of the ratio between the intensity of the two peaks with delay time. This result implies that some of the electrons lost from the trap responsible for peak I (PTTL peak) are re-trapped at the trap associated with peak V. In addition, we also recorded the signal lost as phosphorescence during a delay period of 5 h. This signal was recorded as an OSL decay but with the LEDS off. In order to measure the phosphorescence, the sample was irradiated to 93 Gy, preheated to 280 °C at the rate of 5.0 °C/s, and illuminated for 160 s. After illumination, the signal which is shown in Figure 5.92 was recorded during the 5 h delay period. At last the PTTL glow curve was then recorded at a rate of 5.0 °C/s.

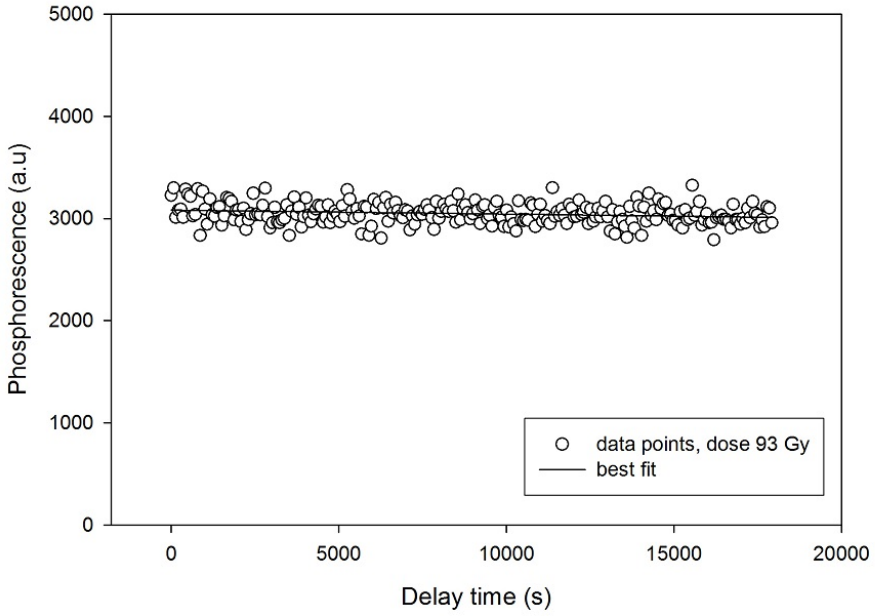

FIGURE 5.92: Signal loss as phosphorescence during a 5 h delay. The sample was irradiated to 93 Gy, preheated to 280 °C, and illuminated for 160 s after which the heating was delayed for 5 h. The signal shown here was recorded with the LEDS off during this delay. A straight line was fitted to the data points.

Figure 5.92 shows that the signal loss as phosphorescence is almost constant as such, this alone cannot account for the fading of the PTTL peak with delay time. As shown in Figure 5.91, re-trapping is also one of the causes of the fading.

5.4 Radioluminescence of natural quartz

Radioluminescence (RL) is one of the techniques used in the study of luminescent materials. RL refers to the light emitted from a sample during exposure to ionising radiation [2]. X-rays are a common irradiation source used in RL measurements. From the study of TL, we gain knowledge about the possible traps in a given materials and from RL, we gain an understanding of the emission bands (recombination centres) [13]. By examining results obtained from various luminescence techniques, we can enhance our understanding of the processes leading to luminescence emission.

Bøtter-Jensen et al. [24] investigated the effect of annealing on the luminescence sensitivity of quartz, and observed a significant increase in luminescence sensitivity for samples annealed between 500 and 800 °C. Bøtter-Jensen et al. [24] attributed the

changes in luminescence sensitivity to the transfer of holes between the recombination centres during annealing. The influence of annealing temperature, measurement temperature and irradiation dose have been investigated on luminescence lifetimes obtained from time-resolved optically stimulated luminescence (TR-OSL) spectra from natural quartz (e.g., Galloway [55], Chithambo [56], Chithambo et al. [42, 57, 58], Ogundare and Chithambo [59] and references therein). A TR-OSL spectrum displays the luminescence recorded from a previously irradiated sample with the aid of a pulsing system that controls the emission of the stimulating light [60]. Luminescence lifetimes measure the delay between stimulation and the emission of light [42]. The luminescence lifetimes reported in the literature are independent of the annealing temperature for quartz annealed below 600 °C. However for quartz annealed at 600 °C and above, a decrease in luminescence lifetimes with annealing temperature is noticed. Galloway [55] proposed a model similar to that of Bøtter-Jensen et al. [24] but consisting of independent luminescent centres L_S, L_L and L_H. The recombination centres L_S, L_L and L_H are associated with luminescence lifetimes τ_S, τ_L and τ_H respectively. Galloway then suggested that the decrease in luminescence lifetimes at higher annealing temperature is due to the fact that at any given annealing temperature, the measured luminescence lifetime is mostly due to the recombination centre with the dominant population of holes. Pagonis et al. [61] recently proposed a model which incorporates the luminescence centres L_L and L_H into their previous model of thermal quenching in quartz [62]. The authors also presented additional RL measurements which revealed a new emission band at 3.73 eV, denoted the M band, for quartz annealed at 600 °C and above.

With the aim of understanding the effect of annealing on recombination centres in quartz and the correlation to luminescence lifetimes reported in the literature, RL emission spectra were measured on natural quartz annealed for 10 minutes at 500, 600, 700, 800, 900 and 1000 °C respectively; as well as on unannealed natural quartz. In our analysis, more attention was given to the sample annealed at 500 °C for 10 minutes since it is one of the two main samples studied in this project.

5.4.1 Sample preparation and RL instrumentation

Natural quartz (BDH Ltd, UK) samples with grain size between 90 - 500 μm were used. These quartz samples are the same samples used previously by Chithambo et al. [42, 57] for the studies of luminescence lifetimes. For each RL measurement, a thin layer of grains of each quartz sample was placed on a stainless steel disc with silicon spray being used to hold the grains in place. The experimental setup consisted of a charge-coupled device, CCD, (Jobin-Yvon Spectrum One 3000) coupled to a monochromator (Jobin-Yvon Triax

180) with a 250 to 1100 nm detection range. The RL excitation was generated by X-ray irradiation through a Be window using a Philips 2274 X-ray tube with a tungsten target operated at 20 kV/20 mA. The sample was irradiated to approximately 10 Gy during each RL measurement. The RL spectra were collected at room temperature and were corrected for the spectral response of the detection system. The experimental setup described here was the same one used by Martini et al. [63] for the study of RL spectra in synthetic and pegmatitic natural quartz.

5.4.2 Emission spectra

5.4.2.1 Unannealed sample

Figure 5.93 shows 2 of the 40 RL spectra collected from the unannealed sample under continuous X-ray irradiation. The first of the two spectra has two apparent emission bands; one centred around 1.9 eV ($\sim$ 649 nm) and a broader band centred around 3 eV ($\sim$ 402 nm). The broader band comprises of at least two bands centred around 2.8 eV ($\sim$ 441 nm) and 3.4 eV ($\sim$ 366 nm) respectively.

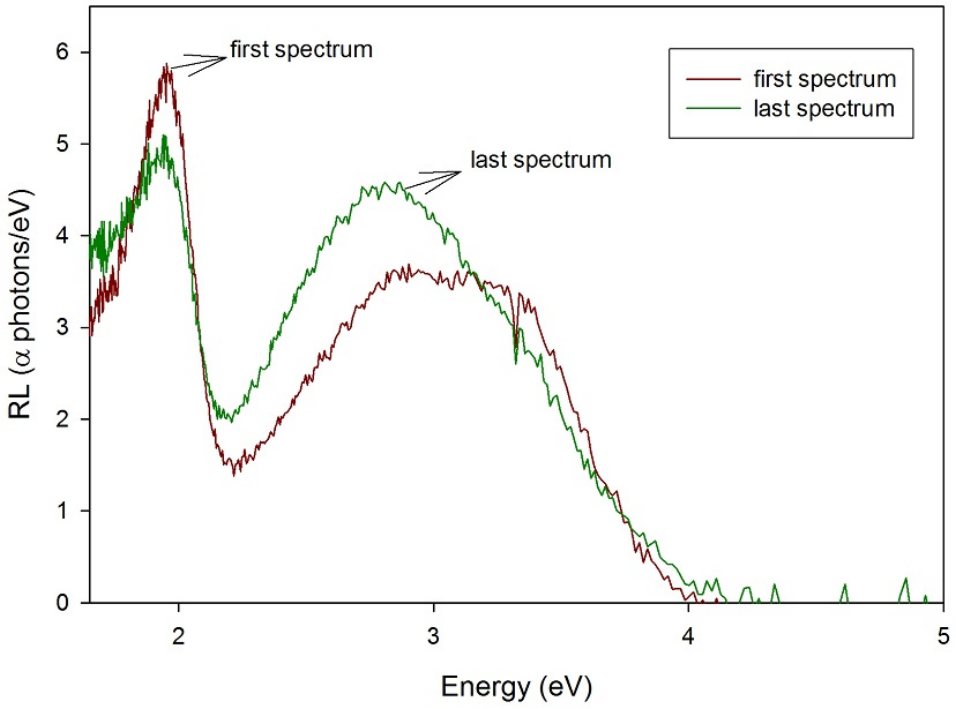

FIGURE 5.93: RL emission spectra of unannealed natural quartz collected under continuous X-ray irradiation. 40 Consecutive spectra were measured only the first and the last spectra of the sequence are shown here.

From Figure 5.93, it can be seen that the 1.9 eV emission band of the unannealed sample is reduced under continuous X-ray irradiation. The behaviour of the broader emission band centred at 3 eV is more complex. This complexity arises from the fact that the band in question is a composite of multiple emission bands. It however appears that the 2.8 eV component of the broader emission band at 3 eV grows faster with irradiation than the 3.4 eV. Such a suggestion explains the apparent shift in the broader band at 3 eV between the first and the last spectrum in Figure 5.93. It is important to point out that the 1.9, 2.8 and 3.4 eV emission bands mentioned so far are not the only possible emission bands. Other emission bands may be present but with very low intensity relative to the ones mentioned. These emission bands are however consistent with the red, blue and ultra-violet (UV) emission bands commonly observed in quartz (e.g., Martini et al. [63] and references therein).

5.4.2.2 Sample annealed at 500 °C for 10 minutes

Figure 5.94 presents the first and the last emission spectra of the sequence of 40 consecutive RL spectra measured on natural quartz annealed at 500 °C for 10 minutes. It is evident from Figure 5.94 that annealing at 500 °C for 10 minutes enhances the 3.4 eV emission band. However, the same 3.4 eV emission band decreases progressively under continuous X-ray irradiation. The other emission bands with low intensity become more evident with the decrease of the 3.4 eV band. A small increase in the intensity of the 1.9 eV emission band under continuous X-ray irradiation is also noticed. This decrease in the 3.4 eV may be due to the reduction of holes from the associated recombination centres during the continuous irradiation. King et al. [64] investigated the effect of irradiation on the emission spectra of quartz samples of different origin using spectroscopic ionoluminescence (IL), and they observed a similar decrease of the UV emission band at 380 nm (~3.3 eV) with irradiation dose. King et al. [64] attributed this decrease of the UV emission band to the reduction in the population of $[AlO_4/M^+]^o$ and $[AlO_4]^o$ luminescent centres.

The enhancement of the 3.4 eV emission band following annealing at 500 °C, observed in the present work, was reported previously by Martini et al. [63]. The work carried out by Martini et al. [63] also showed a correlation between the enhancement of the 3.4 eV RL emission band and the increase in sensitivity of the main TL peak in quartz for a cycle of irradiation and heating to 500 °C. This result led Martini et al. [63] to conclude that the recombination centres involved in the RL and TL emission of the main TL peak in quartz are the same.

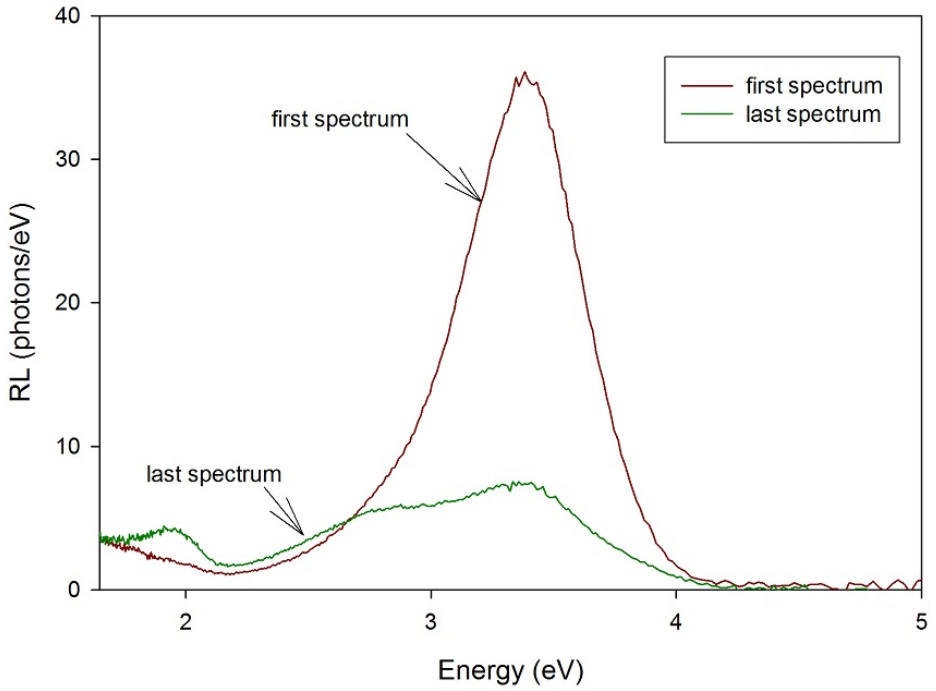

FIGURE 5.94: First and last of the sequence of 40 RL emission spectra of the sample of natural quartz annealed at 500 °C for 10 minutes collected under continuous X-ray irradiation.

5.4.2.3 Influence of annealing on RL

A series of sequences of 40 RL emission spectra were collected for samples annealed for 10 minutes at temperatures between 500 and 1000 °C respectively. The first RL spectrum from each sample is shown in Figure 5.95. The aim of the experiment was to observe the influence of annealing on the various emission bands.

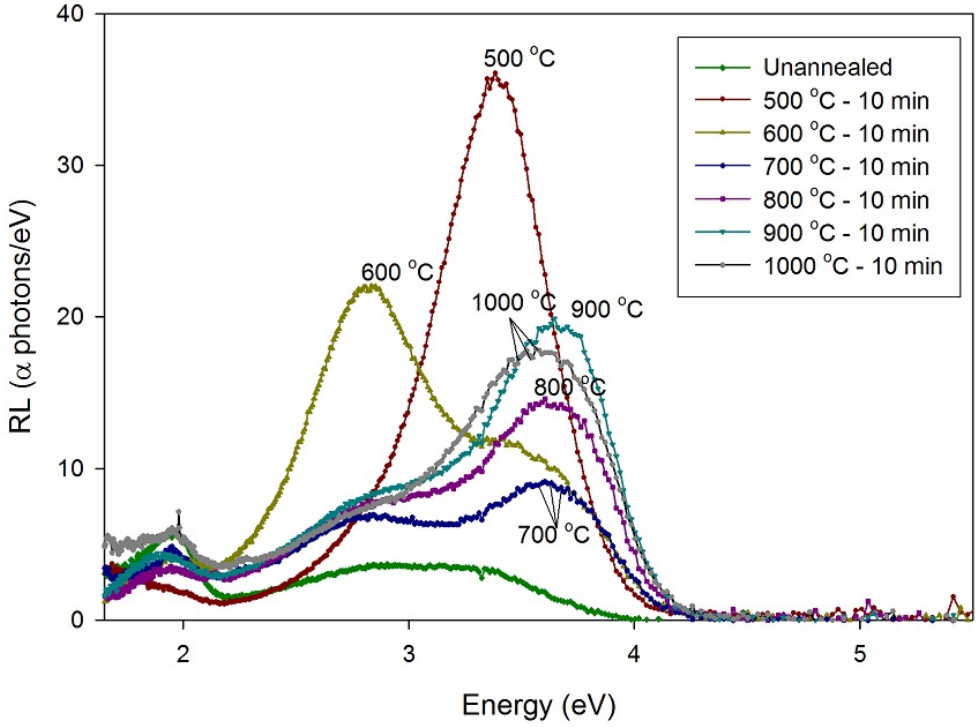

FIGURE 5.95: Effect of annealing on emission centres in natural quartz. A sequence of 40 RL emission spectra was collected under continuous X-ray irradiation for each annealing temperature. Only the first spectrum from each sequence is shown here for comparison. The spectrum of the unannealed sample is also shown.

The spectra in Figure 5.95 show a progressive increase of the 1.9 eV emission band with annealing from 500 to 1000 °C for 10 minutes. It is also evident from the spectra in Figure 5.95 that annealing at 500 °C results in a strong enhancement of the emission band at 3.4 eV. However, as mentioned earlier, the 3.4 eV band decreases continually with annealing temperature from 600 to 1000 °C. Annealing at 600 °C reveals a new emission band at 3.73 eV ($\sim$ 330 nm), which increases with annealing temperature up to 1000 °C. Pagonis et al [61] refer to the 3.73 eV band as the M band. The spectrum of the sample annealed at 600 °C also shows an enhancement of the 2.8 eV band, which reduces to a stable level at higher temperature annealing (700 - 1000 °C). It is important to point out that the 500 - 600 °C region in which the new emission band (M band at 3.73 eV) occurs corresponds to a region of phase change ($\alpha - \beta$ phase transition) in quartz. In addition, the luminescence lifetimes reported in literature are constant with annealing temperature up to 500 °C but decrease for samples annealed at 600 °C and above (e.g., Galloway [55], Chithambo et al. [42, 57, 58] and references therein). It may be that the recombination centres involved in RL and TR-OSL emission are the same. However, as pointed out by Pagonis et al. [61], there is no direct experimental evidence showing that

the recombination centres involved in the two processes are indeed identical. In order to explain the change in luminescence lifetimes with annealing temperatures, Galloway [55] used an expression of the form,

$$\tau(T) = \tau_L + \frac{(\tau_H - \tau_L)}{1 + C\ \exp(-W_R/kT)}, \tag{5.10}$$

where C is a dimensionless constant, k is Boltzmann's constant, T is the annealing temperature and W_R is the thermal activation energy for the transfer of holes into the recombination centre L_L. For annealing temperatures $T < 500$ °C, the measured lifetime is constant and mostly due to τ_H. However for annealing temperature $T \geq 600$ °C. the recombination centre L_L is dominant and the measured lifetime is dominated by τ_L [55, 61]. For samples annealed at 600 °C, the new emission band at 3.73 eV could in principle be due to the transfer of holes from L_H to L_L. The RL measurements presented here show that some of the emission centres in quartz (e.g., the 1.9 eV emission band and the recently observed emission band centred at 3.73 eV) increases with annealing whereas others, such as the 3.4 eV, which is strongly enhanced with annealing at 500 °C, do not. The spectra presented thus far only show the prominent emission bands some of which may be composite. We therefore need to deconvolve a given spectrum into a sum of Gaussian terms to get the contribution of each band to the total spectrum. The deconvolution exercise was only performed for the sample annealed at 500 °C.

5.4.2.4 RL spectra deconvolution

Guided by the previous work on RL spectra of quartzes by Martini et al. [63, 65], the RL spectra collected from the sample annealed at 500 °C for 10 minutes were deconvoluted into six Gaussian components. Following Martini et al. [65], the emission bands associated with these Gaussian components will be referred to as the O, A, B, X, C and D band respectively. The M band at 3.73 eV, which was recently observed by Pagonis et al. [61] for a sample annealed at 600 °C and above, was not used in the deconvolution of the RL spectra of the sample annealed at 500 °C. Figure 5.96 shows the first RL spectrum of the sample annealed at 500 °C for 10 minutes deconvoluted into the six Gaussian components mentioned here.

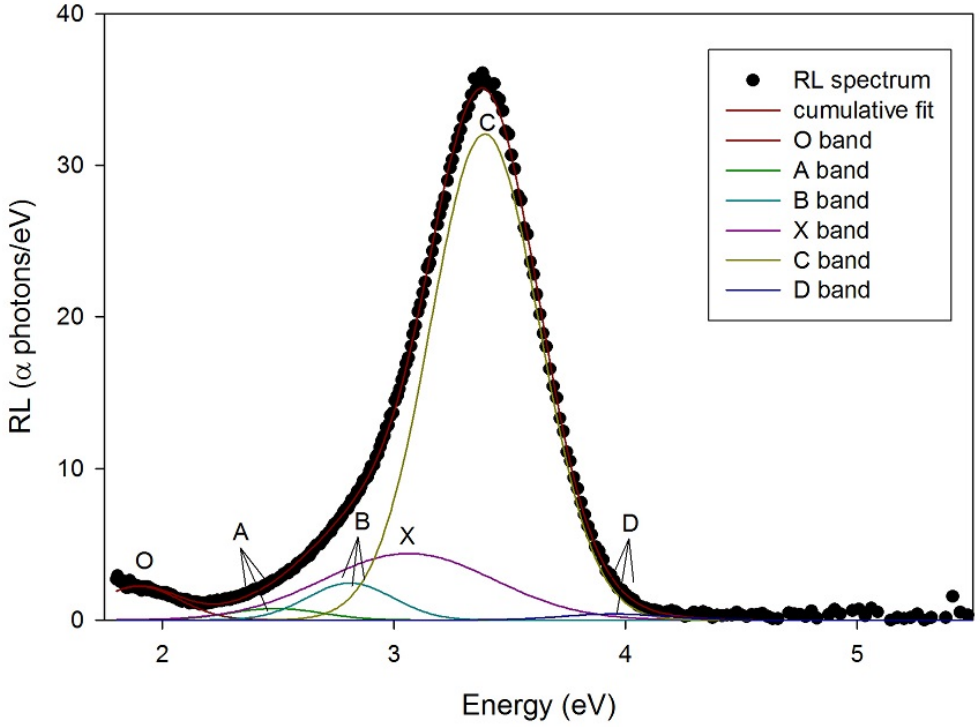

FIGURE 5.96: Deconvolution of the first RL spectrum of the sample annealed at 500 °C for 10 minutes into a sum of six Gaussian components. Each of these Gaussian component is associated with a given emission band.

The parameters obtained from the deconvolution are shown in Table 5.10 which gives

TABLE 5.10: Deconvolution of the RL spectrum of quartz annealed at 500 °C for 10 minutes into six Gaussian components. The spectra were measured at room temperature.

Band	Energy (± 0.02 eV)	Wavelength (nm)	w (± 0.02 eV)
O	1.91	649	0.31
A	2.49	498	0.41
B	2.81	441	0.37
X	3.08	402	0.78
C	3.39	366	0.51
D	3.91	317	0.39

the energy of each emission band and the corresponding wavelength of emission. The parameter w is proportional to the FWHM of the Gaussian. The parameters shown in this table compare well with those reported by Martini et al. [63, 65]. The last RL spectrum of the same quartz sample was also deconvoluted in a similar way. The aim was to observed the effect of continuous irradiation on each emission band. Figure 5.97 shows the last spectrum of the sample annealed at 500 °C for 10 minutes deconvoluted into the same set of six Gaussian components.

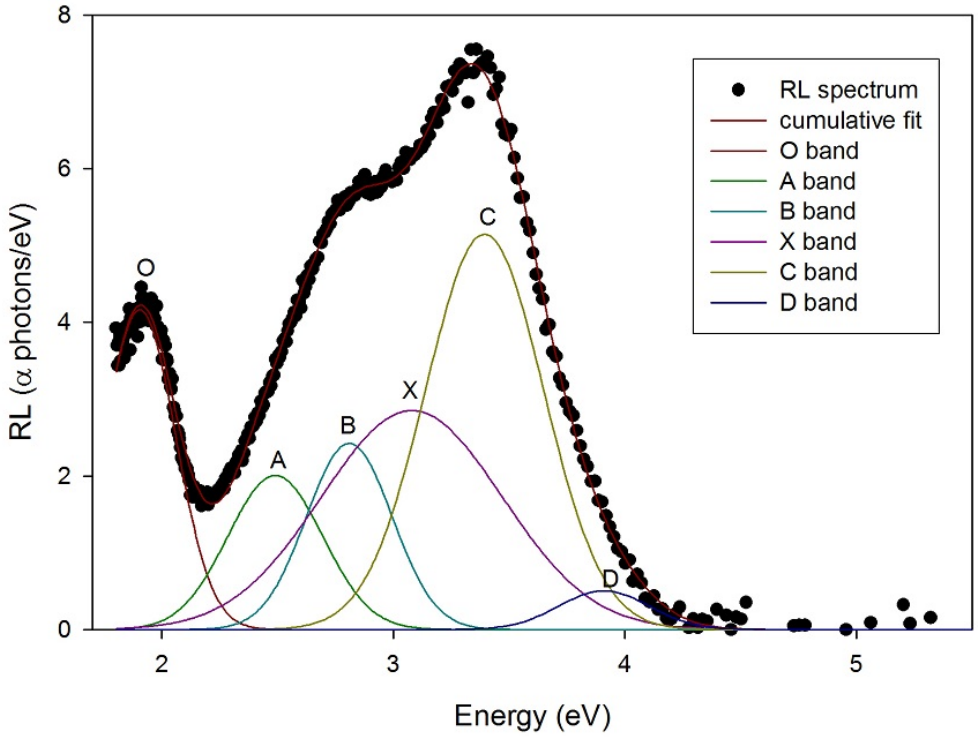

FIGURE 5.97: Deconvolution of the last (40 th) RL spectrum of the sample annealed at 500 °C for 10 minutes into a set of six Gaussian components. Each of these Gaussian component is associated with a given emission band.

It is worth noting the decrease of the 3.4 eV emission band (i.e., band C) and the increase of the other bands. In the RL spectrum of Figure 5.96, the 3.4 eV emission band which is very intense dominates the other bands but in Figure 5.97, all the bands are clearly seen.

From this study, it is evident that the emission bands and hence the associated recombination centres are affected by annealing and irradiation. The 3.4 eV ($\sim$ 366 nm) emission band is strongly enhanced in samples annealing at 500 °C but decreases with higher annealing temperatures. Annealing can also result in the creation of new emission bands. This is the case of the 3.73 eV ($\sim$ 330 nm) emission band. Continuous irradiation may result in the increase or decrease of an emission band. For example, the 3.4 eV band is decreased under continuous irradiation.

Chapter 6

Conclusion

The goal of this thesis was threefold. The first objective was to investigate the kinetic and dosimetric features of the main TL peak for samples of natural quartz annealed for 10 minutes at 500 °C and unannealed. The natural TL glow curve measured at 5.0 °C/s from the unannealed sample consists of peaks near 280 and 325 °C. In contrast, the annealed sample yields no TL prior to laboratory irradiation as expected. TL glow curves recorded from both samples at a heating rate of 5.0 °C/s have a dominant peak around 90 °C and subsidiary peaks at higher temperatures. The activation energy of the main peak for each of the sample is about 0.93 eV.

For the two samples, the values of the activation energy E are in good agreement and there is no evidence suggesting that the value of E is affected by annealing at 500 °C. The main peak of each sample can be approximated to a first-order glow peak with a value of b between 1.0 and 1.2. For low doses, typically between 2 and 10 Gy, the dose response of the main peak of each sample is linear. In the intermediate dose range from 10 to 60 Gy, the growth of the main peak is sub-linear and for doses greater than 60 Gy, the peak has a linear dose response. The influence of delayed stimulation between irradiation and TL readout was investigated for the main peak of each sample. The fading of the main peak of each sample can be described with a single exponential function. Such a behaviour is consistent with first-order kinetics. The half-life of the main peak for the unannealed sample is 1.26 h whereas that of the annealed sample is 1.17 h.

The main peak of each sample suffers from thermal quenching when the heating rate is progressively increased during measurements.

The second objective of this work was to study the kinetic and dosimetric features of the phototransferred peaks as well as their dependence on illumination time for each of the sample. The study revealed that only the main TL peak in each of the samples is regenerated by phototransfer. Irrespective of annealing, the peak due to phototransfer appears at the same position as the original TL peak and its activation energy is similar to that of the original TL peak. The dose response, which was studied only for the annealed sample, is sub-linear for doses ranging from 2 to 151 Gy. For preheat temperatures of 120, 160 and 200 °C, the dose response is independent of the preheat temperature up to 20 Gy, but increases with preheat temperature at higher doses. We suggested that this increase in the dose response with preheat temperature at higher doses was due to the progressive removal of electrons from traps associated with the intermediate peaks which are not regenerated by phototransfer. The traps associated with the 325 °C peak are the main source of the electrons transferred to the shallow traps during optical stimulation. As for the original main peak from the annealed sample, the phototransferred peak fades exponentially with a half-life of 1.40 h. It also obeys the same order of kinetics as the original TL peak and has a similar activation energy (about 0.95 eV). For both sample, the intensity of the phototransferred peak decreases to a non-zero constant level. Hence, a model such as the one proposed by Bøtter-Jensen et al. [24] which includes a non radiative recombination centre is required to describe the behaviour of the intensity of the phototransferred peak with illumination time. The initial increase of the phototransferred intensity with illumination time is only observed for some combination of preheat temperature and initial illumination time.

The final objective of this thesis was to investigate the influence of annealing on radioluminescence (RL) emission spectra in quartz. The RL emission spectra of quartz consists of red, blue and ultra-violet emission bands; some of which are composite. There is a strong enhancement of the 3.4 eV emission band (C band) with annealing at 500 °C. However, the intensity of this C band decreases under continuous irradiation. A new emission band, namely the M band, is observed at 3.73 eV for samples annealed at 600 °C and grows with annealing up to 1000 °C. An attempt was made to correlate the changes in RL emission spectra with annealing to those observed in luminescence lifetimes measured in TR-OSL for various annealing temperatures. It is well known from TR-OSL measurements that luminescence lifetimes of quartz are independent of annealing temperature up to 500 °C but decrease with higher annealing temperatures. So the changes in the RL spectrum with annealing temperature could in principle be related to the changes in luminescence lifetimes since, such changes imply the dominance of a particular recombination centre at a given annealing temperature.

As a consequence of its predose effect, the main peak of quartz has been studied intensively and some of the features observed in this work are already known. However much is still not known about the mechanisms leading to TL and phototransferred TL in quartz. A future study could focus on the features of phototransferred peaks in quartz; namely, the influence of annealing on phototransfer or the dependence of the illumination wavelength on phototransfer. Further investigation of the dependence of illumination on the phototransfer is also needed.

References

[1] C. Kittel. *Introduction to Solid State Physics*. John Wiley & Sons, Inc, 2005.

[2] S. W. S. McKeever. *Thermoluminescence of solids*. Cambridge University Press, 1985.

[3] S. W. S. McKeever, M. Moscovitch, and P. D. Townsend. *Thermoluminescence Dosimetry Materials: Properties and Uses*. Nuclear Technology, 1995.

[4] R. Chen and S. W. S. McKeever. *Theory of Thermoluminescence and Related Phenomena*. World Scientific, 1997.

[5] R. B. Laughlin. The optical absorption edge of silicon dioxide. *Phys. Rev. B*, 22 : 3021 – 3029, 1980.

[6] A. J. J. Bos. Theory of thermoluminescence. *Radiat. Meas.*, 41 : 45 – 56, 2006.

[7] A. H. Carter. *Classical and statistical thermodynamics*. Prentice Hall, 2000.

[8] J. T. Randall and M. H. F. Wilkins. Phosphorescence and electrons traps: I. the study of trap distributions. *Proc. R. Soc. London*, A 184 : 366 – 389, 1945.

[9] J. T. Randall and M. H. F. Wilkins. Phosphorescence and electrons traps: II. the interpretation of long-period phosphorescence. *Proc. R. Soc. London*, A 184 : 390 – 407, 1945.

[10] V. Pagonis, G. Kitis, and C. Furetta. *Numerical and Pratical Exercises in Thermoluminescence*. Springer, 2006.

[11] G. F. J. Garlick and A. F. Gibson. The electron trap mechanism of luminescence in sulphide and silicate phosphors. *Proc. Phys. Soc.*, 60 : 574 – 589, 1948.

[12] C. E. May and J. A. Partridge. Thermoluminescence kinetics of alpha irradiated alkali halides. *J. Chem. Phys.*, 40 : 1401 – 1415, 1964.

[13] F. Preusser, M. L. Chithambo, T. Götte, M. Martini, K. Ramseyer, E. J. Sendezera, G. J. Susino, and A. G. Wintle. Quartz as a natural luminescence dosimeter. *Earth Sci. Rev.*, 97 : 184 – 214, 2009.

[14] X. H. Yang and S. W. S. McKeever. The pre-dose effect in crystalline quartz. *J. Phys. D: Appl. Phys.*, 23 : 237 – 244, 1990.

[15] M. Martini, M. Fasoli, and A. Galli. Quartz OSL emission spectra and the role of $[AlO_4]^o$ recombination centres. *Radiat. Meas.*, 44 : 458 – 461, 2009.

[16] J. F. de Lima, M. S. Navarro, and M. E. G. Valerio. Effects of thermal treatment on the tl emission of natural quartz. *Radiat. Meas.*, 35 : 155 – 159, 2002.

[17] A. J. J. Santos, J. F. de Lima, and M. E. G. Valerio. Phototransferred thermoluminescence of quartz. *Radiat. Meas.*, 33 : 427 – 430, 2001.

[18] M. Bertucci, I. Veronese, and M. C. Cantone. Photo-transferred thermoluminescence from deep traps in quartz. *Radiat. Meas.*, 46 : 588 – 590, 2011.

[19] R. Chen and V. Pagonis. *Thermally and Optically Stimulated Luminescence A Stimulation Approach.* John Wiley, 2011.

[20] Milanovich-Reichhalter and N. Vana. Phototransferred thermoluminescence in quartz. *Radiat. Prot. Dosim.*, 33 : 211 – 213, 1990.

[21] F.D. Walker, L.E. Colyott, N. Agersnap Larsen, and S.W.S. McKeever. The wavelength dependence of light-induced fading of thermoluminescence from $\alpha-Al_2O_3$:C. *Radiat. Meas.*, 26 : 711 – 718, 1996.

[22] C. S. Alexander, M. F. Morris, and S.W.S. McKeever. The time and wavelength response of phototransferrred thermoluminescence in natural and synthetic quartz. *Radiat. Meas.*, 27 : 153 – 159, 1997.

[23] C. S. Alexander and S.W.S. McKeever. Phototransferred thermoluminescence. *J. Phys. D: Appl. Phys.*, 31 : 2908 – 2920, 1998.

[24] L. Bøtter-Jensen, N. Agersnap Larsen, V. Mejdahl, N. R. J. Poolton, M. F. Morris, and S. W. S. McKeever. Luminescence sensitvity changes in quartz as a result of annealing. *Radiat. Meas.*, 24 : 535 – 541, 1995.

[25] J. Zimmerman. The radiation-induced increase of the 100 °C thermoluminescence sensitivity of fired quartz. *J. Phys. C: Solid. State. Phys.*, 4, 1971.

[26] J. Nahum and A Halperin. Thermoluminescence and the relation between thermal and optical activation energies in diamond. *J. Phys. Chem. Solids.*, 24 : 823 – 834, 1963.

[27] C. H. Haake. Critical comment on a method for determining electron trap depths. *JOSA*, 47 : 649 – 652, 1957.

[28] A. H. Booth. Calculation of electron trap depths from thermoluminescence maxima. *Can. J. Chem*, 32 : 214 – 215, 1954.

[29] W. Hoogenstraaten. *Philips. Res. Rep.*, 13, 1958.

[30] R. Chen and S. A. A. Winer. Effects of various heating rates on glow curves. *J. Appl. Phys*, 41 : 5227 – 5232, 1970.

[31] S. W. S. McKeever. On the analysis of complex thermoluminescence. glow-curves: Resolution into individual peaks. *Physica Status Solidi (a)*, 62 : 331 – 340, 1980.

[32] C. Furetta. *Handbook of Termoluminescence*. World Scientific, 2003.

[33] A. Halperin and A. A. Braner. Evaluation of thermal activation energies from glow curves. *Phys. Rev.*, 117 : 408 – 415, 1960.

[34] R. Chen. On the calculation of activation energies and frequency factors from glow curves. *J. Appl. Phys.*, 40 : 570 – 585, 1969.

[35] N. S. Mohan and R. Chen. Numerical curve fitting for calculating glow parameters. *J. Phys. D: Appl. Phys.*, 3 : 243 – 247, 1970.

[36] D. Shenker and R. Chen. Numerical curve fitting of general order kinetics glow peaks. *J. Phys. D: Appl. Phys.*, 4 : 287 – 291, 1971.

[37] G. Kitis, J. M. Gomez-Ros, and J. W. N. Tuyn. Thermoluminescence glow-curve deconvolution functions for first, second and general orders of kinetics. *J. Phys. D: Appl. Phys*, 31 : 2636 – 2641, 1998.

[38] D. W. Marquardt. An algorithm for least-square estimation of nonlinear parameters. *J. Soc. Indust. Math.*, 11 : 431 – 441, 1963.

[39] Y. S. Horowitz and D. Yossian. Computerised glow curve deconvolution: application to thermoluminescence dosimetry. *Radiat. Prot. Dosim.*, 60 : 3 – 3, 1995.

[40] Technical University of Denmark. *Guide to "The Risø TL/OSL Reader "*, 2011.

[41] D. S. Betts, L. Couturier, A. H. Khayrat, B. J. Luff, and P. D. Townsend. Temperature distribution in thermoluminescence experiments. i. experimental results. *J. Phys. D: Appl. Phys.*, 26 : 843 – 848, 1993.

[42] M. L. Chithambo and R. B. Galloway. On the slow component of luminescence stimulated from quartz by pulsed blue light-emitting diodes. *Nucl. Instrum. Meth. B.*, 183 : 358 – 368, 2001.

[43] D. K. Koul. 110 °C thermoluminescence glow peak of quartz - A brief review. *Pramana - J. Phys.*, 71 : 1209 – 1229, 2008.

[44] K. Ankama Rao, Sk. Parvin Nuyaz, N.V. Poornachandra Rao, and K. V. R Murthy. Thermally stimulated luminescence studies of silicate minerals. *Arch. Phys. Res.*, 2 : 89 – 93, 2011.

[45] R. Nanjundaswamy, K. Lepper, and S. W. S. McKeever. Thermal quenching of thermoluminescence in natural quartz. *Radiat. Prot. Dosim.*, 100 : 305 – 308, 2002.

[46] A. G. Wintle. Thermal quenching of thermoluminescence in quartz. *Geophys. J. R. Astron. Soc.*, 41 : 107 – 113, 1975.

[47] A. Mandowski. Semi-localized transitions model for thermoluminescence. *J. Phys. D: Appl. Phys.*, 38 : 17 – 21, 2005.

[48] V. Pagonis, L. Blohm, M. Brengle, G. Mayonado, and P. Woglam. Anomalous heating rate effect in thermolumiescence intensity using a simplified semi-localized transition (SLT) model. *Radiat. Meas.*, 51 : 40 – 47, 2013.

[49] M L Chithambo. The analysis of time-resolved optically stimulated luminescence: II. computer simulations and experimental results. *J. Phys. D: Appl. Phys.*, 40 : 1880, 2007.

[50] M. J. Aitken. *Thermoluminescence dating.* Academic Press, 1985.

[51] D. Mebhah, D. Imatoukene, F.Z. Abdelazziz, and Z. Lounis-Mokrani. Evaluation of trap parameters associated with thermoluminescence peaks in fired quartz. *Radiat. Meas.*, 41 : 813 – 818, 2006.

[52] G. Kitis, V. Pagonis, H. Carty, and E. Tatsis. Detailed kinetic study of the thermoluminescence glow curve of synthetic quartz. *Radiat. Prot. Dosim.*, 100 : 225 – 228, 2002.

[53] R. M. Bailey. Towards a general kinetic model for optically and thermally stimulated luminescence of quartz. *Radiat. Meas.*, 33 : 17 – 45, 2001.

[54] A. G Wintle and A. S. Murray. The relationship of quartz thermoluminescence, photo-transferred thermoluminescence, and optically stimulated luminescence. *Radiat. Meas.*, 27 : 611 – 624, 1997.

[55] R. B. Galloway. Luminescence lifetime in quartz: dependence on annealing temperature prior to beta irradiation. *Radiat. Meas.*, 35 : 67 – 77, 2002.

[56] M. L. Chithambo. Time-resolved luminescence from annealed quartz. *Radiat. Prot. Dosim.*, 100 : 273 – 276, 2002.

[57] M. L. Chithambo and F. O. Ogundare. Luminescence lifetime components in quartz: influence of irradiation and annealing. *Radiat. Meas.*, 44 : 453 – 457, 2009.

[58] M. L. Chithambo, F. O. Ogundare, and J. Feathers. Principal and secondary luminescence lifetime component in annealed natural quartz. *Radiat. Meas.*, 43 : 1 – 4, 2008.

[59] F. O. Ogundare and M. L. Chithambo. Characteristics of luminescence lifetimes in natural quartz from Brazil and South Korea. *Radiat. Eff. Defect. S*, 168 : 460 – 467, 2013.

[60] L. Bøtter-Jensen, S. W. S. McKeever, and A. G. Wintle. *Optically Stimulated Luminescence Dosimetry.* Elsevier, 2003.

[61] V. Pagonis, M.L. Chithambo, R. Chen, A. Chruścińska, M. Fasoli, S. H. Li, M. Martini, and K. Ramseyer. Thermal dependence of luminescence llifetime and radioluminescence. *J. Lumin*, 145 : 38 – 48, 2014.

[62] V. Pagonis, C. Ankjærgaard, A. S. Murray, M. Jain, R. Chen, J. Lawless, and S. Greilich. Modelling the thermal quecnhing mechanism in quartz based on time-resolved optically stimulated luminescence. *J. Lumin*, 130 : 902 – 909, 2010.

[63] M. Martini, M. Fasoli, I. Villa, and P. Guibert. Radioluminescence of synthetic and natural quartz. *Radiat. Meas.*, 47 : 846 – 850, 2012.

[64] G. E. King, A. A. Finch, R. A. J. Robinson, and D. E. Hole. The problem of dating quartz 1: Spectroscopic ionoluminescence of dose dependence. *Radiat. Meas.*, 46 : 1 – 9, 2011.

[65] M. Martini, M. Fasoli, A. Galli, I. Villa, and P. Guibert. Radioluminescence of synthetic quartz related to alkali ions. *J. Lumin*, 132 : 1030 – 1036, 2012.